Charles University

Faculty of Sciences

Study programme: Organic Chemistry

Branch of study: D-ORGCH

Miguel Alexandre Gomes Mateus, Msc.

Synthesis and Application of Transition Metal Complexes Bearing *N*-Heterocyclic Carbene Ligands

Type of thesis:

Doctoral thesis

Supervisor: Dr. Lukáš Rýček, M.Sc.

Prague, 2024

Univerzita Karlova v Praze

Přírodovědecká fakulta

Studijní program: Organická chemie

Studijní obor: D-ORGCH

Miguel Alexandre Gomes Mateus, Msc.

Syntéza a Využití Komplexů Transitních Kovů s Ligandy na Bázi N-Heterocyklických Karbenů

Typ závěrečné práce:

Disertační práce

Vedoucí závěrečné práce/Školitel: Dr. Lukáš Rýček, M.Sc.

Praha, 2024

Prohlášení:

Prohlašuji, že jsem závěrečnou práci zpracoval samostatně a že jsem uvedl všechnypoužité informační zdroje a literaturu. Tato práce ani její podstatná část nebylapředložena k získání jiného nebo stejného akademického titulu.

V Praze, 07/06/2024

Miguel Mateus

ACKNOWLEDGEMENT

First and foremost, I would like to thank my supervisor Dr. Lukáš Rýček for the opportunity and the interesting project provided. My heartfelt gratitude for your exceptional guidance and unwavering support throughout my doctoral journey. Your insightful feedback, patience, and encouragement have been invaluable, pushing me to achieve my best. Thank you for believing in me and for your dedication to my success.

I would like to thank all the past and present people from the Group of Organometallic and Synthetic Chemistry with special gratitude to Dr. Sundaravelu Nallappan, Dr Anita Kiss and Dominik Kunak.

Appreciation to Dr. Martin Štícha for the HRMS measurements, Dr. Michal Urban for IR measurements, Dr. Ivana Císařová for the X-ray crystallography, Dr. Tomasz M. Karpiński for the MIC measurements and Dr. Róbert Gyepes for the DFT calculations.

Gratitude to all my upbringing friends and the ones made during my doctoral studies, for sharing and supporting this journey. Thank you to all the personnel from the Department of Organic Chemistry for making the journey simpler and pleasant.

Lastly, I dedicate this thesis to my mother and father. I am deeply grateful for your unwavering support, boundless patience, and constant encouragement throughout my journey. Your belief in me has been my strongest pillar of strength, pushing me to persevere even when the path seemed overwhelming. The sacrifices you made and the understanding you showed have been instrumental in my success. Thank you for always being there, for listening, and for believing in my potential. This achievement is as much yours as it is mine. I am forever indebted to you both.

“To be great, be whole; don't exaggerate
Or leave out any part of you,
Be complete in each thing. Put all you are
Into the least of your acts.
So too in each lake, with its lofty life,
The whole moon shines."
Fernando Pessoa, Lisboa: Ática, 1946

ABSTRACT

In recent years, there has been a notable increase in interest in *N*-heterocyclic carbenes (NHC), which have emerged as a subject of considerable significance due to their strong σ-donating ability and steric features. These characteristics make them attractive ligands in transition metal complexes, with some NHC-metal complexes proving superior to their metal-phosphine counterparts. Among the transition metals where NHCs have been applied, NHCs-silver complexes have gained significant attention due to their simple synthesis, stability, fascinating structural diversity, and wide range of applications. Herein, a novel chelate mononuclear NHC-silver(I) was accomplished bearing a bisamide moiety in its backbone. Such mononuclear complex is synthesised using an equimolar ratio of the silver source and ligand precursor. Conversely, if an excess of the silver source was used, the reaction led to the formation of an unprecedented tetranuclear silver complex. Additionally, NHC-silver complexes have been recognised as effective carbene group transfer agents, enabling the synthesis of NHC complexes with other metals, such as nickel and palladium. These complexes exhibited chirality due to the coordination of the ligand to the metal centre in a helical manner. Both complexes were analysed in solid and liquid states, and DFT calculations were performed to understand the transition state and energy barrier of the configurational flip. The scope was extended with the synthesis of nickel and palladium complexes containing a larger side chain on the imidazole moiety, which proved to be more configurationally stable than their previous analogues**.** Furthermore, the synthesised NHC-silver complexes were also tested as antimicrobial agents, in which they demonstrated extraordinary properties. The minimum inhibitory concentration (MIC) values were as low as 1 μg/ml and were active against Gram-positive bacteria, Gram-negative bacteria and Fungi. The silver complexes were also tested as catalysts in A^3 (aldehyde, amine, alkyne) and KA^2 (ketone, amine, alkyne) coupling reactions. The catalysts proved to be very reactive towards both coupling reactions with great overall yields and a wide tolerance for the substrate scope. Since A^3 coupling is a multicomponent reaction and with the good results presented by the complex, a small library of compounds was synthesised and was further used in data storage. Storage of data using small molecules remains a rather unexplored field. The use of the synthesised compounds proved to be suitable and efficient with a new cheaper and user-friendly approach being employed.

ABSTRAKT

V posledních letech došlo k významnému nárůstu zájmu o N-heterocyklické karbeny (NHC), které se ukázaly jako klíčové díky své silné schopnosti σ-donování a výrazným sterickým vlastnostem. Tyto vlastnosti z nich činí atraktivní ligandy v komplexech přechodných kovů, přičemž některé komplexy NHC-kov v mnoha aspektech předčí jejich kov-fosfinové protějšky. Mezi přechodnými kovy, kde byly NHC použity, získaly zvláštní pozornost komplexy NHC-stříbro, a to díky jejich jednoduché syntéze, stabilitě, fascinující strukturní rozmanitosti a široké škále aplikací. V rámci této disertační práce byl připraven nový mononukleární NHC-stříbrný (I) komplex s chelatujícím ligandem, obsahujícím bisamidovou skupinou v hlavním řetězci. Tento mononukleární komplex byl syntetizován použitím ekvimolárního poměru zdroje stříbra a prekurzoru ligandu. Naopak při použití přebytku zdroje stříbra vedla reakce k vytvoření bezprecedentního tetranukleárního stříbrného komplexu. Připravené stříbrné komplexy byly využity jako účinná činidla pro přenos karbenových skupin, což umožňuje syntézu NHC komplexů s jinými kovy, jako je nikl a palladium. Tyto komplexy vykazovaly topologickou chiralitu díky koordinaci ligandu s kovovým centrem v helikálním uspořádání. Oba komplexy byly analyzovány jak v pevném, tak kapalném stavu, a byly provedeny DFT výpočty pro pochopení přechodového stavu a energetické bariéry konfiguračního zvratu. Rozsah výzkumu byl rozšířen o syntézu komplexů niklu a palladia s většími postranními řetězci na imidazolové části, které se ukázaly být konfiguračně stabilnější než jejich předchozí analogy. Syntetizované komplexy NHC-stříbro byly dále testovány pro jejich antimikrobiální účinky. V tomto směru se látky jevily jako mimořádně účinné. Hodnoty minimální inhibiční koncentrace (MIC) dosahovaly až 1 μg/ml a byly účinné jak proti grampozitivním bakteriím, tak i gramnegativním bakteriím a plísním.

Komplexy stříbra byly také testovány jako katalyzátory při kaplingových reakcích typu A^3 (aldehyd, amin, alkyn) a KA^2 (keton, amin, alkyn). Tyto katalyzátory se v obou případech ukázaly být velmi účinnými s celkově vysokými výtěžky a širokou tolerancí pro různorodé substráty. S využitím těchto metod byla syntetizována malá knihovna sloučenin, která byla dále využita pro ukládání dat. Ukládání dat pomocí malých molekul je stále poměrně neprozkoumanou oblastí, ale použití syntetizovaných sloučenin se ukázalo jako vhodné a efektivní, díky novému levnějšímu a uživatelsky přívětivému přístupu.

TABLE OF CONTENTS

1. Structure of the thesis

Due to the broad scope of the thesis, a scheme is presented for guidance and clarification of the thesis structure. The thesis consists of three major sections: Introduction, Results and Discussion, and Experimental section. The results and discussion sections were merged for convenience and coherence. All the sections of the thesis will respect the following order: Firstly, *N*-heterocyclic carbenes (NHC) precursors followed by the NHC-silver(I) complexes will be introduced and discussed. From this point onwards, such silver complexes will be discussed in three different paths. The first application introduced and discussed will be the usage of silver complexes for NHC carbene transfer, meaning transmetalation from silver to other transition metals. Interestingly, some of the NHC-transition metal complexes isolated proved to be *chiral-at-metal* complexes, leading to a profound study of said chirality. Then, the silver complexes were tested as antimicrobial agents. Lastly, the silver complexes were used as catalysts for A^3 and KA^2 coupling for the formation of propargyl amines. The synthesised propargyl amines proved to be suitable for application in data storage, a new topic that will be comprehensively introduced and discussed. By respecting this order in all the sections, the coherence and course of the thesis should be maintained.

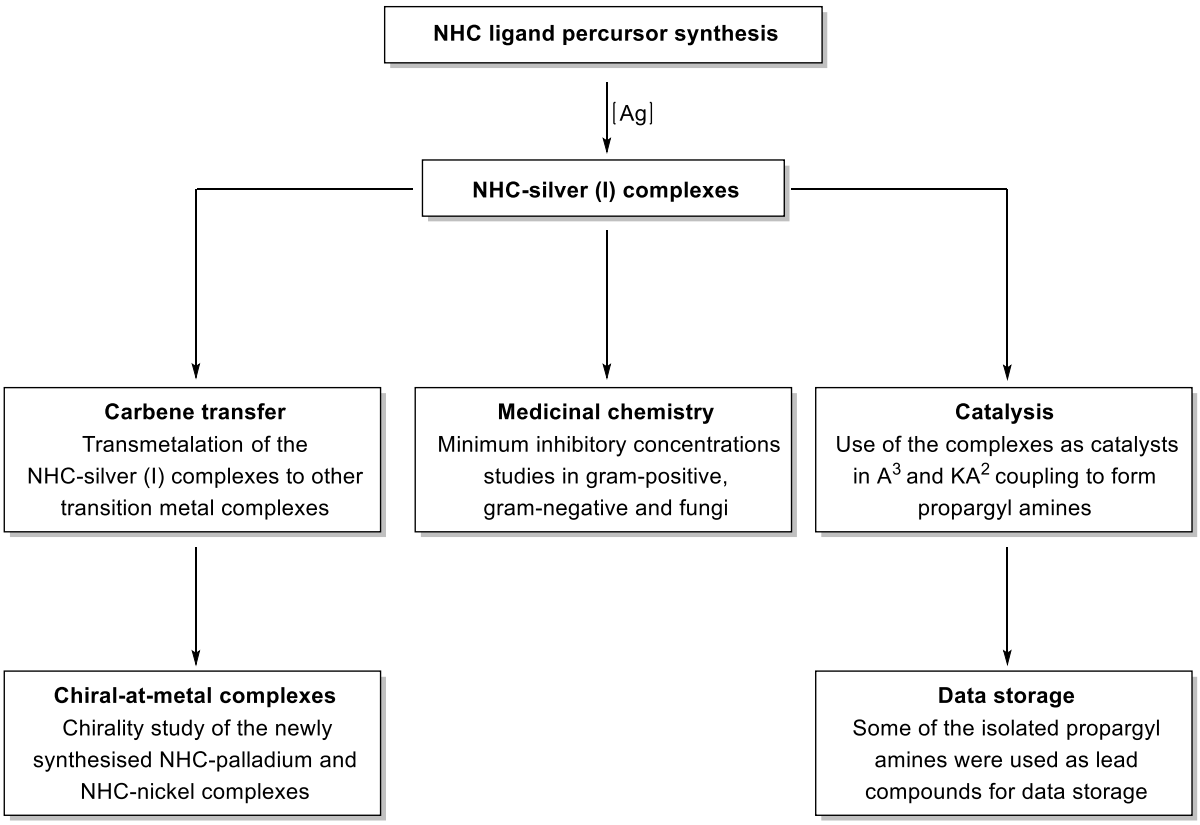

2. State of the art

2.1. *N*-Heterocyclic carbenes

2.1.1. General considerations

The story of NHC carbenes can be traced back to 1925 by Chugaev *et al.* with the attempted synthesis of platinum complexes with coordinated isocyanates. However, only years later, the structure was elucidated and proved to be the first example of an NHC-metal complex **1**.[1] In 1968 Öfele made the groundbreaking discovery of the inaugural monodentate NHC-transition metal complex.[2]

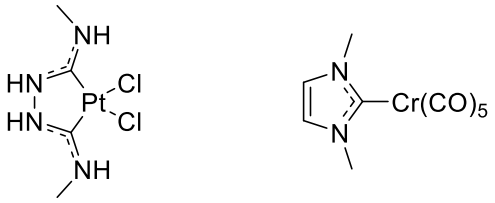

1 **2**

Figure 1. Platinum complex isolated by Chugaev (**1**) and first isolated NHC-metal complex (**2**).

In 1962, H. W. Wanzlick hypothesised that electron-rich imidazole moiety should stabilise the carbene centre bonded between two nitrogen atoms, indicating that the carbene in this instance would be nucleophilic.[3] Indeed, years later he proved that imidazolium salt **3** could be deprotonated by potassium *tert*-butoxide. This was proved by trapping the corresponding carbene **4** with phenyl isothiocyanates, forming **5**. Furthermore, in the same paper, the authors also reported an NHC-mercury complex, where they were able to isolate both the monomeric and dimeric versions **7** and **8**, respectively. Interestingly, for the dimeric complex, the authors

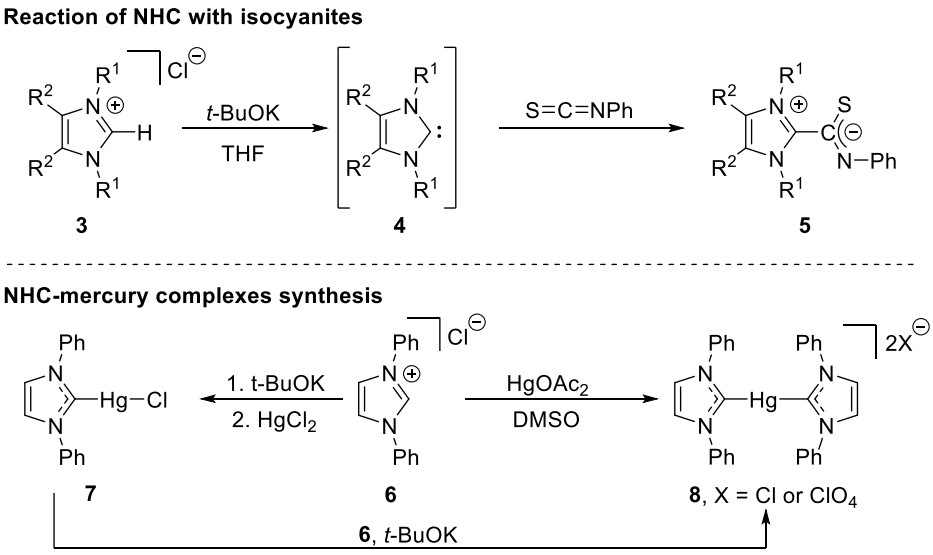

Scheme 1. Reported work by H. W. Wanzlick *et al* using NHCs.

could access it without the need to use any additional base, since the acetate group coordinated to mercury is basic enough to deprotonate the imidazolium salt **6**, as demonstrated in Scheme 1.[4,5]

Nearly two decades later, A. J. Arduengo successfully achieved the pioneering isolation of electronically stabilised, nucleophilic carbenes for the first time.[6] When A. J. Arduengo subjected bis-(1-adamantyl)imidazolium chloride **9** to deprotonation with sodium hydride, employing a catalytic amount of dimethyl sulfoxide, the resulting carbene **10** precipitated. This carbene compound exhibited a colourless, crystalline, and more importantly, thermally stable nature (with a melting point of 240-241 °C) without undergoing decomposition, as elucidated in Scheme 2. This outcome was further corroborated through crystal structure analysis. Notably, the ^{13}C NMR spectrum displayed a characteristic feature: a low field signal for the carbene carbon atom (δ = 211.4). This remarkable achievement triggered a surge in investigations into NHCs and their involvement in metal complexes.

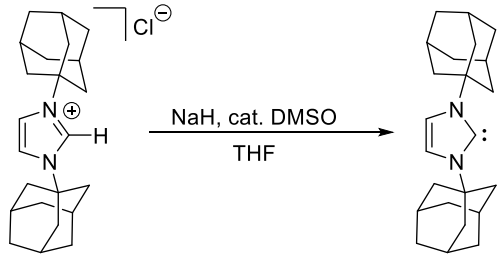

9 **10**

Scheme 2. First stable imidazol-2-ylidene **10** isolated by A. J. Arduengo.

NHCs incorporated into five-membered rings such as imidazolylidenes, imidazolinylidenes thiazolylidenes, and triazolylidenes, are the most widely employed (Figure 2, type B). Additionally, NHCs featuring modified backbones, such as phenyl (Figure 2, type C) are also well established. The latter variant, pyrrolylidene[7] (Figure 2, type D) exhibits distinct reactivity and selectivity patterns due to variations in their electronic and steric properties. Carbenes can also be categorised based on their electronic configurations. Singlet carbenes are characterised by paired unshared electrons within the same σ or π orbitals (Figure 2, type B, C and D). Triplet carbenes feature two unshared electrons in distinct orbitals with parallel spins. This is the case of diarylcarbenes (Figure 2, type A).[8] Since the beginning of the 21st century, new NHCs with modified backbones, such as diboron backbone[9] or a carbonyl group[10,11] as well as expanded rings[12], have been studied.

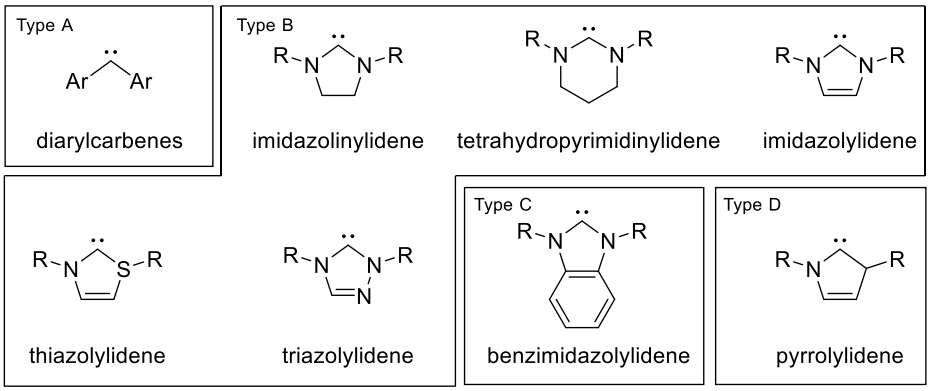

Figure 2. A variety of NHC structures.

2.1.2. Steric and electronic considerations of carbene metal complexes

Carbene metal complexes can be classified into two groups, namely Fischer and Schrock metal carbene complexes, depending on the nature of the formal metal-carbon bond. Fischer-type carbenes result in the interaction of a singlet carbene with a low-valent late-transition metal. These carbenes act predominantly act as L-type σ-donors through the lone pair due to π-donor substituents such as alkoxy and alkylamine and usually favour low oxidation state metals containing strong π-acceptor ligands (e.g. CO, CN^{-}, NO ligands). The π-backbonding from the filled metal *d*-orbital to the empty *p*-orbital on the carbene leads to a double bond. Notably, late transition metals exhibit greater electronegativity when compared to the early transition metal counterparts, resulting in more stable M(d_π) orbitals. Besides, the presence of π-acceptor ligands serves to increase the stability of the M(d_π) levels.[13,14]

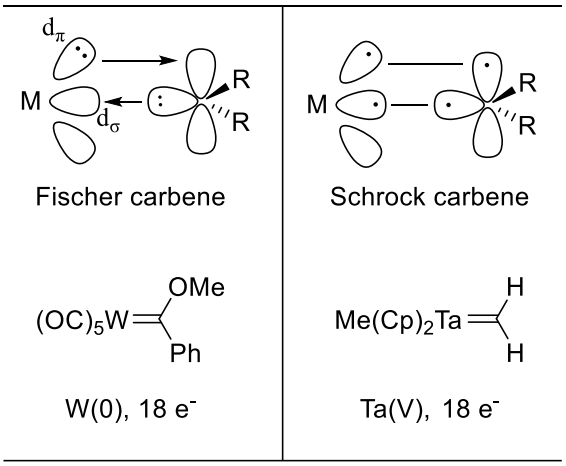

Figure 3. Representation of Fischer (left) and Schrock(right) type metal carbene complexes.

In opposition, Schrock-type carbenes involve the interaction between a triplet carbene and an early transition metal in a high oxidation state. In this scenario, the metal complex lacks any π-acceptor ligands, and the carbene substituents are not π-donors, normally hydrogen or alkyl substituents. Two covalent bonds are established between the triplet carbene and the metal fragment, which possesses two unpaired electrons. Schrock carbenes function as X type ligands.[15,16] In Figure 3 can be found the representation of Fischer- and Schrock-type metal carbene complexes as well as some respective examples.

Through the years NHCs have been employed in a wide range of application, reaching from transition metal catalysis,[17–19] to metallopharmaceuticals[20,21] and supramolecular chemistry[22], among others. The reason for this achievement can be ascribed to the simple tune of steric and electronic properties, high σ-donor character, stability, and accessibility through many well-established synthetic routes.[23] One of the key factors for the electronic stabilisation is due to the adjacent nitrogen atoms, giving the NHC a singlet ground state, with the HOMO and LUMO frontier orbitals best described as a formally sp^2 hybridised lone pair and an unoccupied *p* orbital on the C_2 carbon. NHCs have sometimes been categorised as a sub-class of Fischer carbenes since both exist in the singlet state. However, NHCs can be differentiated from Fischer and Schrock carbenes since NHCs predominantly serve as spectator ligands. The stabilisation of the NHC is contributed by the electronic donation from the lone pair of π-donating substituents to the unoccupied *p*-orbital of the carbenic carbon atom, as depicted in Figure 4. Furthermore, NHCs only establish a single *σ*-bond with the metal centre, in contrast to the double bond made by Fischer- and Schrock-type carbenes.[24]

The robust *σ*-donor capabilities and relatively modest *π*-acceptor traits exhibited by NHCs share resemblances with the coordination properties of phosphines. However, distinctions between the two ligand classes exist. NHCs, especially those derived from imidazolylidene and imidazolinylidene (structure in Figure **2**) that have been extensively studied, demonstrate a higher degree of donation when compared to even the most Lewis basic phosphines. This

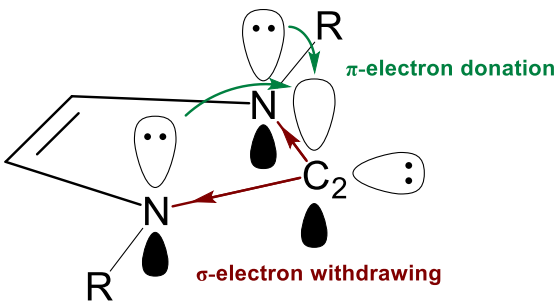

Figure 4. Demonstration of the NHC stabilisation by electron donation and electron withdrawing.

comparison is possible from studying the Tolman Electronic Parameters (TEP) by measuring the CO stretching of carbonyl metal complexes frequencies using IR spectroscopy.[25] A higher electron-donating capacity in the ligand corresponds to an electron-rich metal centre, intensifying π-backbonding into the carbonyl ligands and consequently weakening their bond and infrared stretching frequency. Due to the stronger electron donating properties of NHCs relative to phosphines the bond formed between the metal and NHC ligand tend to be thermodynamically more stable. This reflects on the high bond dissociation energies and shorter bond lengths of metal-NHC ligand when compared with their phosphine's counterparts. In consequence, this stronger metal-ligand interaction makes the metal-NHC ligand coordination less labile than metal-phosphine binding and the complexes are more thermally stable.[26,27]

Another important point where NHCs and phosphines have notable distinctions is the steric properties. While the sp^3-hybridisation of phosphines results in a cone-shaped spatial arrangement of steric bulk, most classes of NHCs, including widely used imidazole-derived types, exhibit an umbrella-shaped configuration, demonstrated in Figure 5. In these NHCs, the nitrogen-substituents adjacent to the carbene carbon are oriented more towards the metal centre. Quantifying the steric properties of NHCs is conveniently achieved through the 'buried volume' parameter (*% V_{bur}*), as established by Steven P. Nolan and his collaborators.[28–30] In simple words, *% V_{bur}* stands for the percentage of a sphere occupied or 'buried' by the ligand upon coordination with the metal at the centre of the sphere. Typically, a higher *% V_{bur}* stands for a more substantial steric impact of the ligand on the metal centre. The buried volume is normally determined by crystallographic data or theoretical calculations using various sources such as free NHCs, different NHC-metal complexes, or the imidazolium salt precursor.

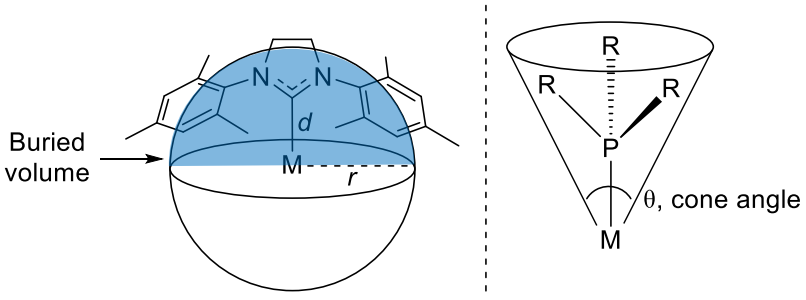

Figure 5. Diagram of the buried volume of NHCs ligands (left) and cone angle of phosphine ligands (right).

2.2. Silver(I)-NHC complexes

2.2.1. Synthesis and structural diversity

A variety of metals have been employed bearing NHCs as ligands and among these metals, silver is one of the most interesting ones. The first successful synthesis of silver(I)-NHC complex was reported by Arduengo *et al*. in 1993.[31] The synthesis utilised a free carbene route, as explained in Scheme 3. The free carbene was then treated with silver(I) triflate in THF to give **13**. Nonetheless, due to the difficulty of generating free carbenes, as well as their sensitivity to various environmental factors, such as moisture and heat,[32] this methodology can be only found in a reduced number of NHC-silver(I) complexes synthesis.[33,34]

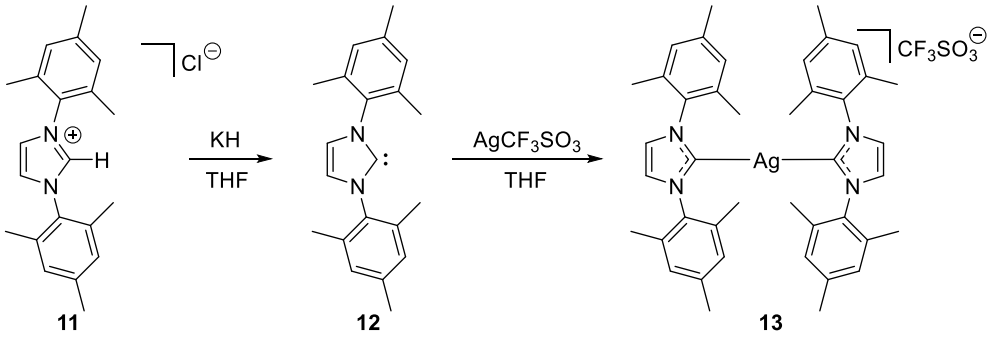

Scheme 3. Synthesis of the first NHC-silver(I) complex by Arduengo *et al.*

The most widely employed method for synthesising NHC-silver complexes involves the *in-situ* deprotonation of imidazolium salts using basic silver precursors. Silver(I) oxide is the most utilised base for this reaction, although alternatives such as silver(I) acetate and silver(I) carbonate have also been employed. The pioneering instance of this approach was demonstrated by Bertrand and colleagues in 1997, who reacted a triazolium salt **14** with silver acetate, resulting in the formation of the inaugural polymeric NHC-silver(I) complex **15**.[35,36] Subsequently, in 1998, Lin *et al*. introduced a method employing an imidazolium salt and silver oxide to synthesise NHC-silver(I) complexes. The treatment of the corresponding imidazolium salts (**16a** and **16b**) with Ag_2O in dichloromethane yielded silver(I) complexes **17a** and **17b**.[37] The use of silver oxide in this synthesis provides several advantages, since it simplifies the reaction procedure, permits operation at ambient conditions, and accommodates various organic solvents. Consequently, silver oxide stands out as the preferred base for the generation of NHC-silver complexes.[38] Both synthesis are described in Scheme 4.

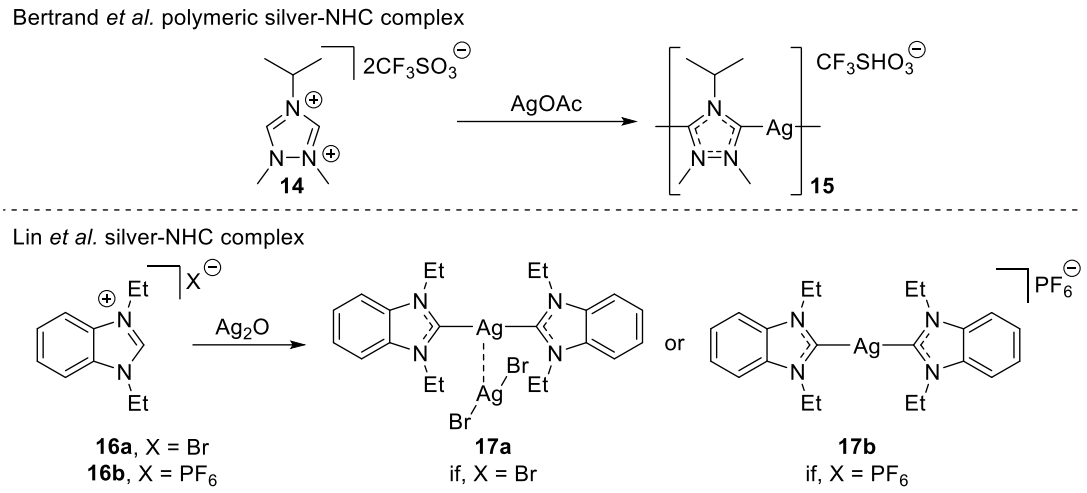

Scheme 4. Synthesis of NHC-silver complex **15**, **17a** and **17b.**

The structural diversity of silver(I) complexes comprehends various binding motifs observed in NHC-silver(I) complexes. Crucial factors influencing the formation and structural diversity of these complexes include the nature of the NHC ligand, the silver source, and the ratio of the silver reagent to the NHC ligand. Additionally, solvent characteristics and reaction temperature play pivotal roles in determining the binding motifs.[39,40] Numerous studies emphasise the substantial influence of the substituents in the imidazolium salts. For instance, the presence of short alkyl chains tends to favour the formation of dimeric NHC-silver(I) complex **18**.[41] On the opposite direction, bulky groups often result in monomeric silver(I) complexes, such as **19**.[42,43] Notably, imidazolium salts with long alkyl chains as substituents may lead to the formation of bimetallic complexes where each silver is coordinated to one NHC ligand and two halides, as shown in structure **20** in Figure 6.[44]

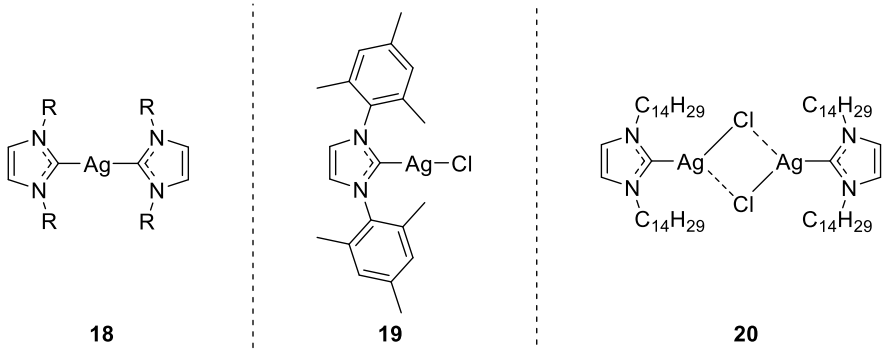

Figure 6. The effect of the NHC substituent on the structural properties of NHC-silver(I) complexes.

Most of the NHC-silver(I) complexes found in the literature are either mono- or binuclear complexes, indicating that the complex contains either one or two silver atoms in the structure. In most instances is even possible to achieve the dimeric version from the respective monomeric

complex. [45,46,47,48] Nonetheless, other interesting modes of coordination have also been reported, such as tri-[49,50] and tetranuclear[51,52] NHC-silver where it was mostly studied their physical properties and cytotoxicity. A more interesting and rare mode of coordination was achieved by F. Ekkehardt Hahn *et al*.[53] where the authors accomplished a novel hexanuclear NHC-silver(I) complex, by using a lutidine-bridged tetraimidazolium salt. The X-ray analysis of the complex shows an interesting and unique sandwich-like hexanuclear silver(I) complex. This proves the versatility and opportunity to explore novel modes of coordination with silver. The X-ray structure of the hexanuclear complex is shown in Figure 7.

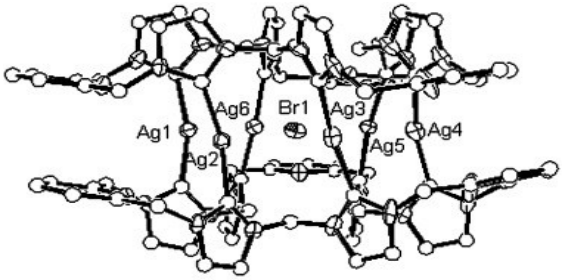

Figure 7. X-ray of the hexanuclear NHC-silver complex isolated by F. Ekkehardt Hahn *et al.* Picture retrieved from the article.[53]

Although silver (I) complexes have a substantial number of binding motifs, it is infrequent to find monomeric chelate silver (I) complexes. In 2012, Amin M.S. Abdul Majid *et al.* reported the synthesis of a monomeric bidentate NHC-silver(I) complex linked through a benzene ring.[54] To the best of my knowledge this is the only example of a monomeric bidentate chelate silver (I) complex. Another chelating NHC-silver(I) complex was reported recently by Eduardo Peris and co-workers and interestingly the author relied on the formation of the NHC-silver(I) complex to then proceed with the synthesis of macrocycles and removal of the silver metal.[55] However, in this case, the authors used a polydentate ligand. The lack of literature on monomeric chelate silver complexes reinforces the difficulty of accessing such complexes, since silver tends to adopt other binding motifs.

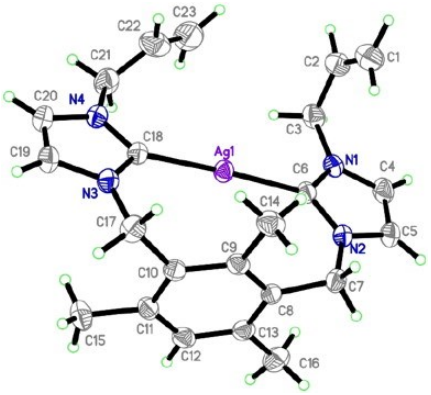

Figure 8. X-ray of the monomeric bidentate chelating NHC-silver(I) complex isolated by Amin M.S. Abdul Majid *et al*. Picture retrieved from the article.[54]

2.3. Other transition metal complexes bearing NHC ligands

2.3.1. Transmetalation of NHC-silver(I) complexes

Transmetalation stands as a foundational technique within the field of organometallic chemistry, valued for its pivotal role in the synthesis of NHC-metal complexes. This method, characterised by its versatility and efficacy, consists of a series of chemical manoeuvres that culminate in the creation of intricate molecular architectures with tailored metal-ligand interactions. At the heart of transmetalation lies the strategic utilisation of basic metals to catalyse the deprotonation of imidazolium salts, a crucial step in the creation of metal NHC complexes. Following the deprotonation process, transmetalation takes place, allowing for the smooth transfer of the NHC ligand onto a different metal centre. This elegant technique not only expands the collection of available metal-NHC complexes but also enables the tailored design of molecular structures with desired metal compositions. Silver bases, including silver oxide, silver carbonate, and silver acetate, have emerged as vital reagents for transmetalation purposes, owing to their remarkable efficiency in facilitating the synthesis of NHC-silver complexes. These NHC-silver complexes serve as versatile intermediates, acting as molecular scaffolds upon which diverse metal compositions can be constructed. This is due to the remarkable lability and fluxional behaviour exhibited by NHC-silver(I) complexes, a characteristic that has sparked significant interest within the scientific community. Capitalising on this inherent lability, researchers have leveraged NHC-silver(I) complexes as ligand transfer agents. The broad applicability of transmetalation comprehends a variety of metals, including but not limited to Au(I), Pd(I), Cu(I), Cu(II), Ni(II), Pt(II), Ru(II), and Ru(III).[56] This expansive scope underscores the profound impact of transmetalation in shaping the landscape of modern organometallic chemistry.

The method pioneered by Wang and Lin[37] involves the deprotonation of the imidazolium with the basic metal that leads to the initial binding of the NHC ligand with silver. Subsequently, the NHC ligand can be transferred to a metal of choice. Notably, the silver complexation method demonstrates remarkable versatility, succeeding in various environmental conditions including exposure to air or moisture. Its ability to tolerate a wide range of solvents, including water[57], has positioned it as the method of choice for numerous researchers seeking robust and reliable synthetic routes in organometallic chemistry. Lin and co-workers showcased the efficacy of NHC-silver(I) complexes **17**, synthesised through the reaction of imidazolium salts **16** with silver oxide, as transfer agents for generating palladium **21** and gold complexes **22** and **23**, as depicted in Scheme 5. Interestingly, the authors achieved different transmetalation results when

the NHC-silver(I) possess different counter anion. It was to be expected that the treatment of **17a** with excess of chloro(dimethyl sulfide)gold(I) should lead to the chelating NHC-gold complex **23**. Instead, the reaction promoted only the formation of the gold monomer **22**.[37]

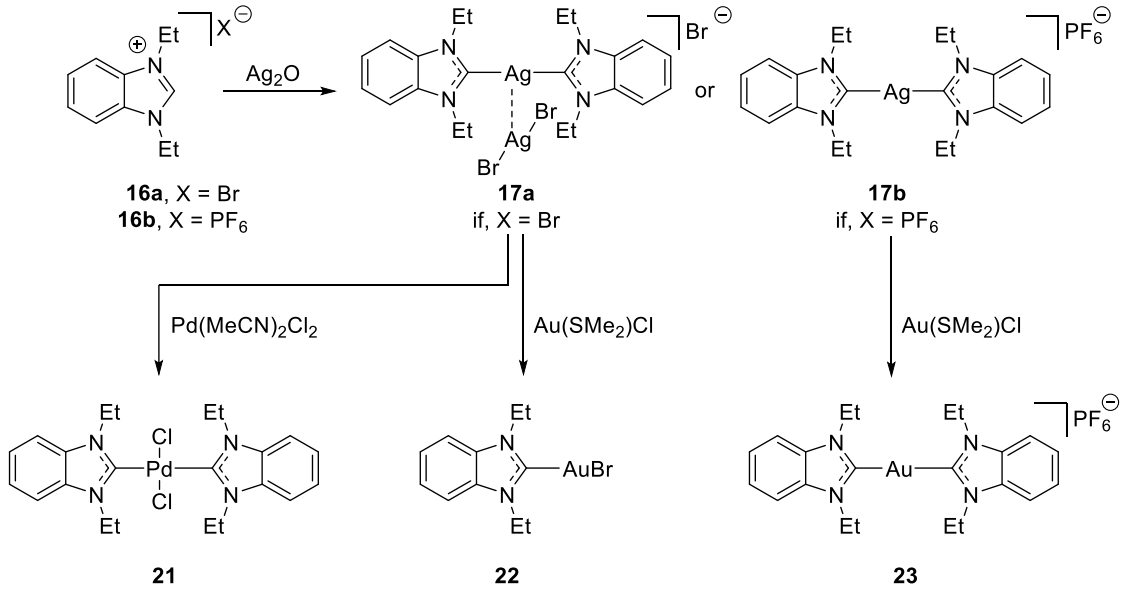

Scheme 5. Synthesis of NHC-Pd **21** and NHC-Au **22** and **23** by Wang and Lin.

Meanwhile, Coleman and collaborators extended the utility of this method by utilising it to synthesise a variety of NHC-palladium and NHC-rhodium complexes. The imine functionalised imidazolium salt **24** was treated with silver oxide to afford NHC-silver(I) complex **25**. Complex **25** proved to be sensitive to air but could be readily characterised by elemental analysis, mass spectrometry and NMR. Although it was impossible to obtain structural data, the complexation of two carbene ligands to one silver atom was confirmed in this case by mass spectrometry. The silver complex was promptly used to form palladium complex **26** and rhodium complex **27**, as shown in Scheme 6. Interestingly, there was also the tautomerisation of imines to enamines. The work was particularly useful since it proved that the use of transfer agents is particularly important when the imidazolium precursors contain functional groups that are sensitive to strong bases, necessary to form the free carbene.[58] With its broad applicability and demonstrated success, the silver complexation method has become a cornerstone in the arsenal of modern organometallic synthesis techniques, offering researchers invaluable tools for the tailored design and synthesis of metal-NHC complexes.

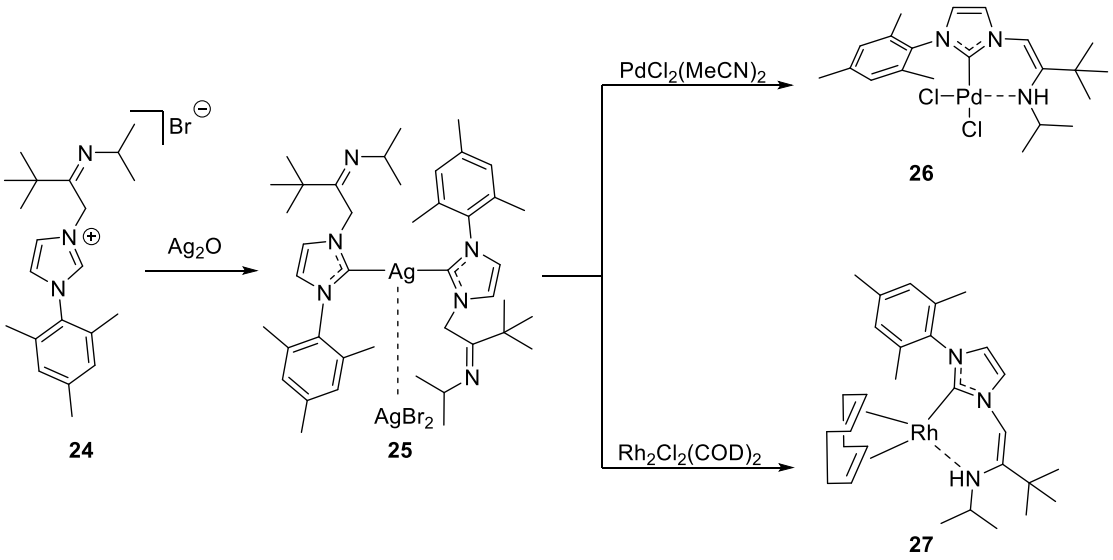

Scheme 6. Synthesis of palladium complex **26** and rhodium complex **27**.

The carbene transfer method offers the advantage of preventing the formation of free carbenes and thus avoids potential issues such as NHC decomposition. However, challenges have arisen with this method, including reports of low yields and difficulties in transmetalation when chelating NHC ligands are used. A very elucidative work showing this limitation was published in the beginning of the century by Brian W. Skelton *et al*. in which attempts to form chelate palladium complexes using the carbene transfer technique were performed. The formation of monodentate NHC-palladium complexes starting with the respective imidazolium salt and silver oxide was achieved smoothly and with high yields. On the opposite direction, when using the pincer-type bidentate imidazolium salts **28**, **29** and **30**, to achieve the respective chelate palladium complexes, the yields dropped to 10% and the purification procedure proved to be tedious and complex. This led to avoiding using silver oxide and the need to adopt a different synthetic route.[41]

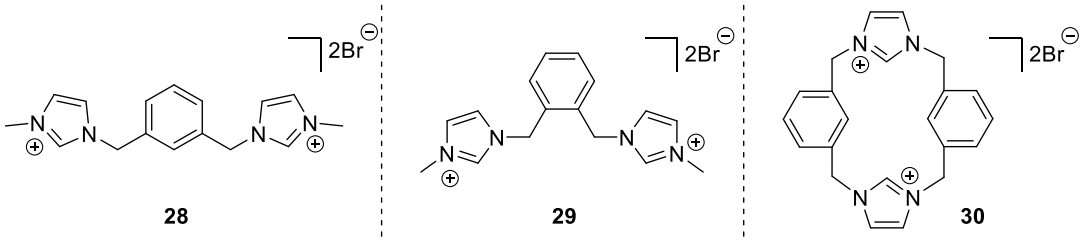

Figure 9. Bidentate NHC ligands used by Brian W. Skelton *et al.*

Years later, Robert H. Crabtree faced a similar issue when attempting to synthesize a chelating NHC-rhodium complex. When the imidazolium salt **31**, with either propyl or butyl chain, the isolated rhodium complex **32** is isolated instead of the respective chelate rhodium complex. The solution found by the author for this problem was the synthesis of the chelate rhodium complex *via* deprotonation and generation of the free carbene *in situ*.[59]

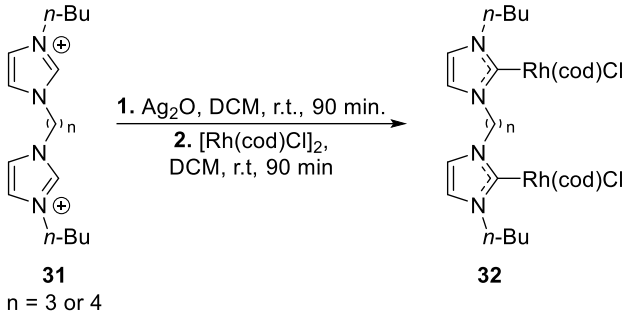

Scheme 7. Synthesis of non-chelating binuclear rhodium complex **32**.

Interestingly, on rare occasions it is possible to achieve the desired chelate metal complex using the carbene transfer technique. It was recently reported by Diego Martinez-Otero and co-workers the synthesis of a chelate nickel complex with a 2,6-lutidine as backbone. As seen previously, the use of lutidine as backbone and bulky substituent in the NHC moiety, in this instance the mesityl and 2,6-diisopropylphenyl group, led to the formation of the binuclear NHC-silver(I) complex **34** as expected. However, surprisingly when the silver complex **34** was treated with nickel (II) chloride ethylene glycol dimethyl ether complex, the authors isolated the chelate complex **35** with relatively high yields.[60] The synthesis of the chelate transition metal from the chelate silver complexes is an unexplored area since the access to chelate silver complexes is difficult.

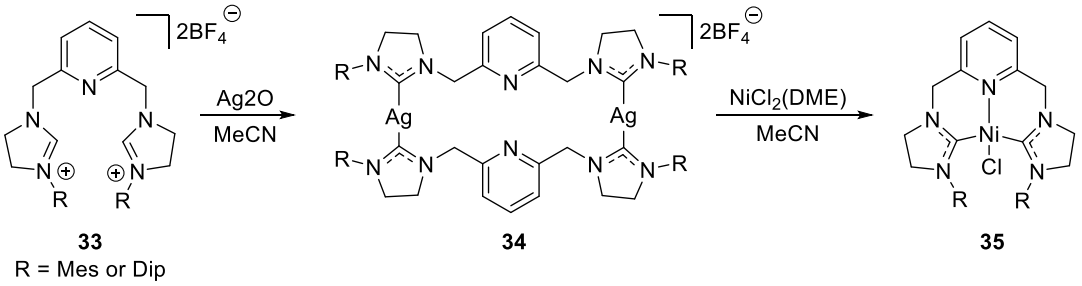

Scheme 8. Synthesis of chelating pincer complex **35** from binuclear silver complex **34**.

2.3.2. *Chiral-at-metal* complexes

Despite the numerous amounts of chiral catalysts developed in recent years, a universal solution for all asymmetric transformations remains elusive. High turnover numbers (<1 mol% loading) in organocatalysis present a particularly daunting challenge. Metal-based asymmetric catalysts heavily rely on intricate chiral organic ligands, which pose synthetic challenges compared to their achiral counterparts due to the difficulty of installing multiple functional groups around the metal centre. The chemistry of *chiral-at-metal* complexes for asymmetric catalysis has been largely neglected in recent decades, as evidenced by the shortage of publications in this area. *chiral-at-metal* complexes comprehend the synthesis of chiral metal complexes using achiral ligands. The chirality is only presented once the ligand precursor is coordinated with the metal centre. Developing an efficient *chiral-at-metal* catalyst typically requires interdisciplinary research in chemistry fields.

Although still rather unexplored nowadays, in the 19th century Alfred Werner introduced the concept of chiral coordination compounds, initially termed "Spiegelbildisomer," which translates to mirror image isomerism. His work distinguished between asymmetric carbon atoms and chirality induced by chelate ligands. Werner accurately anticipated the presence of two enantiomers in coordination compounds,[61] a prediction later confirmed through experimental evidence. This evidence was derived from the resolution of enantiomers in cobalt complexes like $[CoCl(NH_3)(ethylenediamine)_2]Cl_2$, depicted in Figure 10.[62] This work by Werner led him to be recognised with the Nobel prize in 1913.

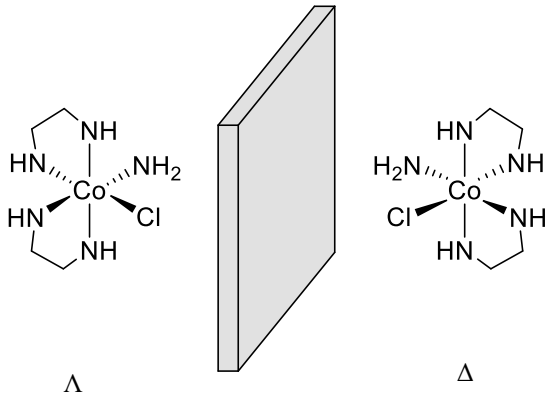

Figure 10. The two enantiomers of Werner's $[CoCl(NH_3)(ethylenediamine)_2]Cl_2$ enantiomers. Charges are omitted from the structures for clarity.

Gladysz and co-workers introduced a straightforward synthesis of *chiral-at-metal* Werner complexes capable of functioning as hydrogen bond catalysts. Firstly, the author had to enhance the solubility of the enantiopure Δ-Werner complex in dichloromethane. This was achieved with the use of the bulky tetrakis[3,5-bis(trifluoromethyl)phenyl]borate anion to form complex **39**. At the beginning, the Werner cobalt salt is solubilised in the aqueous phase which, as the reaction proceeds and the counterion changes, is then transferred to the organic phase. This innovation allowed for the Michael addition of dimethyl malonate **37** to cyclopentenone **36**, as showed in scheme 9, with a reasonable yield of 78% but modest enantiomeric excess (ee), only 33%. Notably, due to the catalyst's substitutional inertness, the authors proposed that asymmetric induction occurs via the N-H bonds acting as hydrogen-bonding donors around the metal centre, which may be a reason for the low enantiomeric excess.[63]

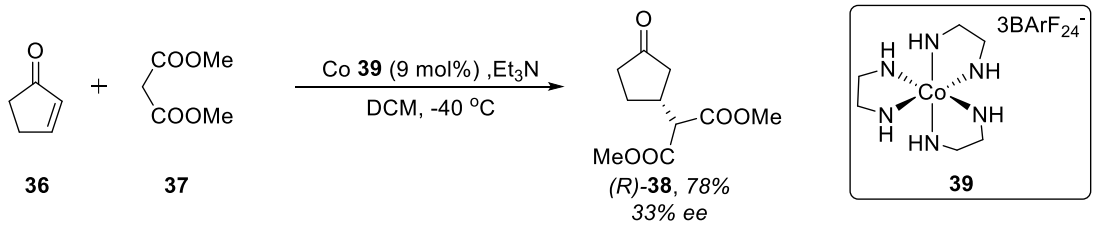

Scheme 9. Reaction of dimethyl malonate to cyclopentenone catalysed by Co **39** complex.

In 2003, Fontecave and colleagues introduced one of the earliest ruthenium *chiral-at-metal* complexes. Although impressive, the complex proved relatively ineffective as catalysts in oxidation reactions that aimed to produce sulfoxides, yielding a modest 18% ee at best. However, this marked a significant breakthrough.[64] In 2007, the same research group developed a novel catalyst featuring an enantiopure octahedral metal centre. This catalyst was applied in the enantioselective reduction of ketones, with the yields being slightly better than the previous reported catalyst, achieving a maximum enantioselectivity of 26%. Specifically, the reaction was conducted at 80°C using acetonaphtone **40**, sodium formate and 0.5 mol% of Ru complex **42** in H_2O (6 mL), resulting in the formation of methyl-2-naphthtalenemethanol **42**.[65]

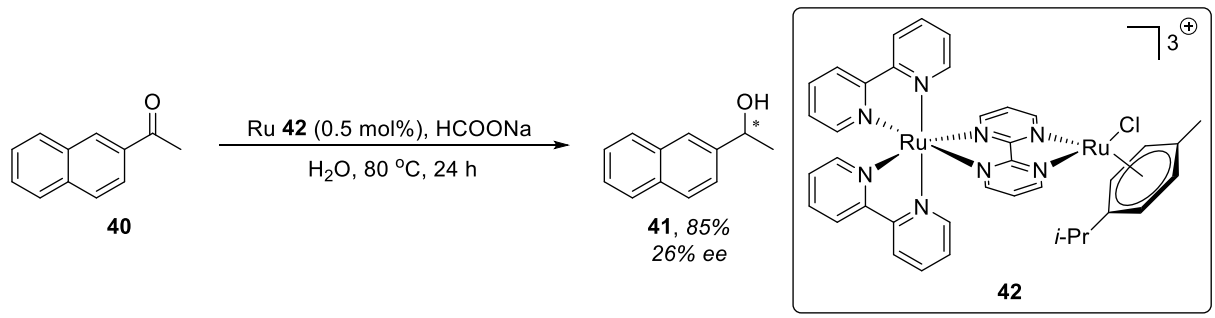

Scheme 10. Enantioselective transfer hydrogenation of ketones with complex **42** as a catalyst.

The Meggers research group has significantly advanced *chiral-at-metal* chemistry through their extensive studies on various complexes. One notable contribution was the development of a highly sophisticated iridium complex **45**, aimed at catalysing the hydrogen transfer reaction of nitroalkene **43** with Hantzsch ester. By incorporating 5-amino-3-(2-pyridyl)-1H-pyrazole as the catalytically active ligand, complex **45** possesses dual hydrogen bond donor functionality, facilitated by both NH groups. This feature allows the catalyst to effectively immobilise and activate nitroalkene **43** simultaneously. Furthermore, the hydroxyl group on the benzoxazole ligand plays a crucial role in activating Hantzsch ester as a hydrogen acceptor, while also directing attack from a single prochiral face. The presence of the 3,5-dimethylphenyl substituents ligands enhances stereoselectivity by obstructing the alternate prochiral face, thereby minimising undesired reactions. Additionally, these substituents accelerate the reaction by stabilising the hydrogen bond adduct formed between catalyst **45** and nitroalkene **43**.[66]

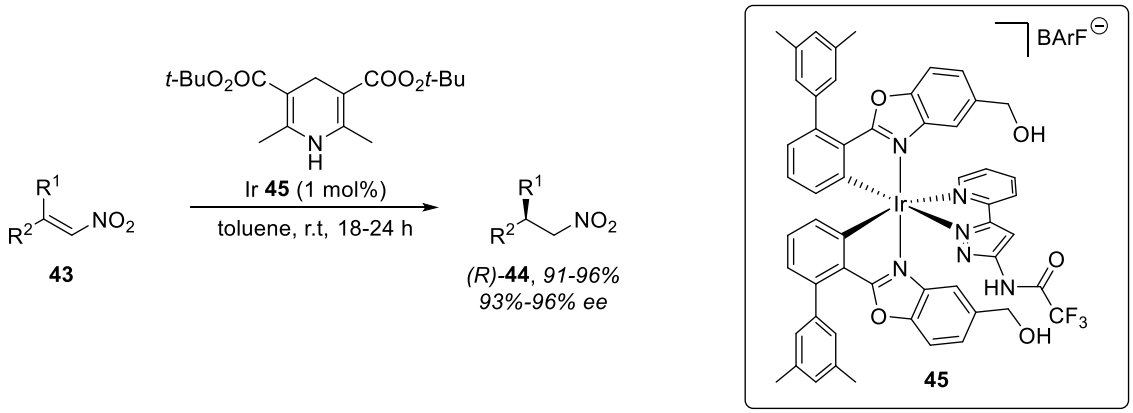

Scheme 11. Asymmetric hydrogen transfer reaction between nitroalkene **43** and Hantzsch ester using the *chiral-at-metal* iridium (III) complex **45**.

The previous examples contemplate octahedral metal complexes. On the other hand, only one example in literature can be found regarding square planar *chiral-at-metal* complex. This was the work of Guido H. Clever and co-workers, where a new kind of *cis*- and *trans*-cyclometalated square-planar platinum(II) complex was synthesised and characterised.[67]

In conclusion, the utilisation of the chirality inherent in *chiral-at-metal* complexes for asymmetric organic catalysis remains an area with significant room for improvement. The primary challenge involves effectively transferring the chiral information from the catalytic metal to carbon or other stereocentres within the substrate molecules. This task presents a formidable obstacle that researchers continue to grapple with in their efforts to advance the field of asymmetric catalysis.

2.4. NHC-silver(I) complexes in medicinal chemistry

The historical use of silver as an antimicrobial can be traced back to ancient civilisations, where silver metal was employed to purify and store drinking water.[68] The antimicrobial properties of silver nitrate were recognised well before the 1800s, making it an antiseptic in wound care for over two centuries.[69] The use of 2% silver nitrate solution to prevent eye infections in newborns began in 1881, initiated by Créde.[70] Colloidal silver solutions, introduced in the early twentieth century to escape irritation associated with silver nitrate, remained popular until the 1940s.[71] However, with the arrival of penicillin and new antibiotics, silver compounds fell out of favour. The interest was revived in the 1960s with Moyer's use of a 0.5% silver nitrate solution for burn wound treatment.[72] The true resurgence occurred in 1968 with the discovery of silver sulfadiazine by Fox, combining the antibiotic sulfadiazine with silver for a broad-spectrum antibiotic. Silver sulfadiazine, effective against various bacteria, is marketed as Silvadene® cream 1%, a water-soluble cream widely used for burning infections.[73] Silver has further been incorporated into wound dressings in various forms, including organic and inorganic compounds and nanocrystalline silver metal. These dressings aim to provide sustained silver release, creating a barrier against infection, facilitating ease of use, managing wound exudates, and supplying optimal moisture for wound healing. Silver-containing dressings have been successfully applied in the treatment of acute and chronic wounds, leg ulcers, and different degrees of burn wounds.[74]

Silver shows efficacy against a diverse spectrum of gram-positive and gram-negative bacteria, fungi, and yeast.[75,76] While the pure metal is inactive, the presence of moisture induces ionisation, transforming silver into silver cations that exhibit antimicrobial activity. The mechanism of action of silver cations remains incompletely understood. These cations bind to the surfaces of bacterial cells and engage with enzymes and proteins crucial for cell wall synthesis. Additionally, silver can impact cell respiration, transport, and metabolism, as well as influence DNA, RNA, and the structure of subcellular organelles.[77] Nevertheless, the effectiveness of silver cations is dependent on their bioavailability. Recent research indicates that in the presence of elevated concentrations of chloride anions, silver becomes more bioavailable, forming soluble anionic $AgCl_2$ compounds instead of precipitating as AgCl. Both sensitive and resistant bacteria exhibit increased sensitivity to silver in the presence of chloride anions, likely stemming from increased access of the silver cation to the cell membrane.[78] Factors such as delivery methods, solubility, and ionisation of the silver sources can further influence bioavailability.[79]

Common topical antimicrobials like silver sulfadiazine and silver nitrate have been noted for their rapid bacteria-killing action. However, they tend to lose their effectiveness rapidly, leading to the re-infection of the wound site. Furthermore, issues such as skin discoloration, known as Argyria, and the development of resistance in certain organisms to sulfonamides constrain the utilisation of traditional silver antibiotics.[80] The gradual release of silver at wound sites is crucial for expediting healing and preventing infections. The strong binding capacity of NHCs to silver can yield more stable complexes capable of slowly releasing silver ions. This property ensures the sustained antimicrobial effect over an extended duration.[81]

The first use of silver NHCs as antimicrobial agents was reported by Youngs *et al*. in 2004.[82] The NHC-silver(I) complexes **47a** and **47b** were synthesised from the pincer ligands **46a** and **46b** that are substituted with hydroxyethyl and hydroxypropyl groups respectively. The reaction was carried out in methanol or water with the use of silver oxide. Interestingly, in the solid state, comprehended by X-ray, the complex **47a** exists as an one-dimensional linear polymer while in the liquid and gas states the complex exists as a monomer, as reported by the authors. Moreover, in both cases, **47a** and **47b**, the complex counter-anion was found to be hydroxyl instead of iodine in the case of **47a**, or bromine in the case of **47b**. The complexes were then tested against clinically relevant bacteria: *E. coli, S. aureus,* and *P. aeruginosa*, to assess their efficacy by determining the minimum inhibitory concentration (MIC). The MIC represents the lowest concentration at which visible growth of the microorganism is inhibited after overnight incubation. Remarkably, **47a** and **47b** showed better bacteriostatic effect (lower MIC value) due to the increased amount of silver cations in the solution, when compared with the standard silver nitrate. The silver cations from silver nitrate precipitated as silver chloride, losing their activity. Moreover, the growth of organisms treated with **47a** and **47b** was delayed for a longer time than the growth of organisms treated with silver nitrate. The obtained results can be explained by the slow decomposition of the complexes in the aqueous culture medium to imidazolium cation and biologically active silver species.

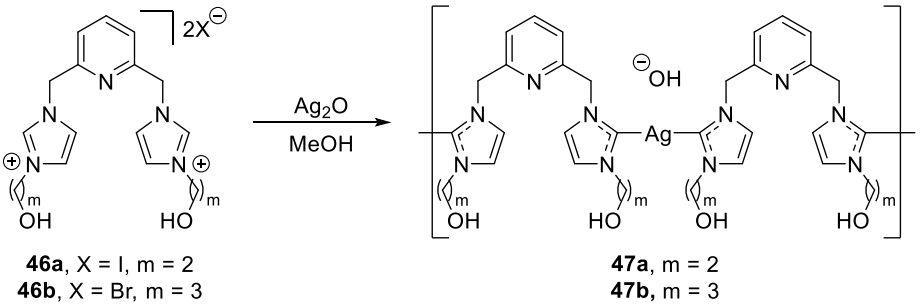

46a, X = I, m = 2
46b, X = Br, m = 3

47a, m = 2
47b, m = 3

Scheme 12. Synthesis of the pincer NHC-silver(I) complex **47a** and **47b.**

One year later, Youngs *et al.*[83] reported the first electrospun fibre encapsulation of an NHC-silver(I) complex. The NHC precursor was achieved by reaction of 2,6- bis(imidazolemethyl) pyridine **48** with 1,3-dichloroacetone **49**. Unexpectedly, the authors obtained the imidazolium salt **50** as a geminal diol instead of carbonyl-linked cyclophane. The imidazolium salt was then treated with silver oxide leading to the binuclear NHC-silver(I) complex **51**. The silver complex **51** was then used for the encapsulation and both free-form and capsulated complex **51** were used for MIC studies. The free silver complex showed poorer results than silver nitrate after a 2 day-incubation, due to its low solubility and fast decomposition in water. To no surprise, when encapsulated, the results were remarkable even when compared to the conventionally used 0.5% silver nitrate and 1% silver sulfadiazine cream. Encapsulation of the silver complex increased the antimicrobial activity by enabling a slower release of active silver species.

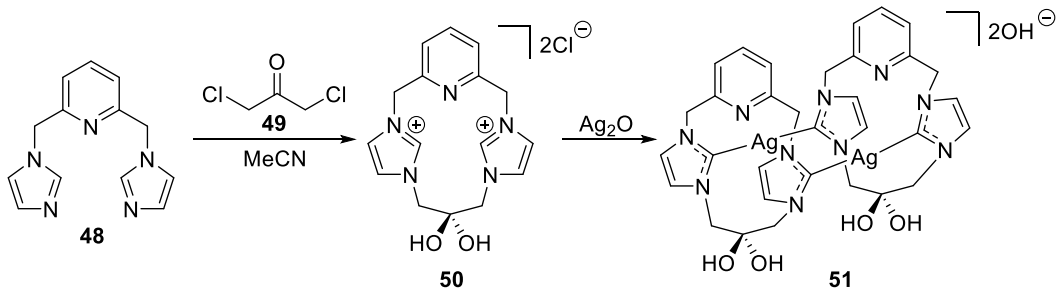

Scheme 13. Synthesis of the binuclear NHC-silver(I) complex.

Nearly 20 years later from the discoveries made by Youngs, an array of NHC-silver(I) complexes has been reported with a range of applications in the medicinal chemistry field. The focus of NHC-silver complexes is still predominantly on the discovery of new antimicrobial agents but, in addition, the paradigm has shifted for their use as promising anticancer agents.[84] Figure 11 depicts some examples of NHC-silver(I) complexes and it is possible to reckon the variety of structures utilised. Sylvain Roland *et al.*[85] reported an extensive study of antimicrobial properties of symmetrical, such as **52**, or unsymmetric, such as **53**, monodentate NHC-silver(I) complex. The authors conclude that slight differences in the NHC ligand structure induce dramatic changes in the activity. The benzimidazole moiety **54** has also been explored in the work of Rosenani A. Haque[86] in which the authors made a series of unsymmetrical NHC-silver(I) complexes. Structural analysis indicates that in the absence of any potential hydrogen bond donor or acceptor, various supramolecular interactions play an important role in stabilising the entire structure. Another approach is the use of bidentate-monoanionic NHC ligands forming complexes as complex **55**. The antimicrobial activity studies performed showed interesting results, with MIC values of 5 mg/ml against *E. coli* and

B. subtilis. The authors hypothesised it was due to the stability of the silver complex to hydrolysis leading to the slow release of the silver.[87] The use of binuclear NHC-silver(I) complexes in medicinal chemistry can also be found in the literature with a variety of NHC ligands. For instance, in complex **56,** each silver metal is coordinated to a benzoxazole and an NHC moiety. On the other hand, complex **57** adopts the dimeric version to avoid steric hindrance of the bulky NHC substituents. Overall, the dimeric versions tend to perform worse in antimicrobial studies when compared to their monomeric versions or similar monomeric versions.

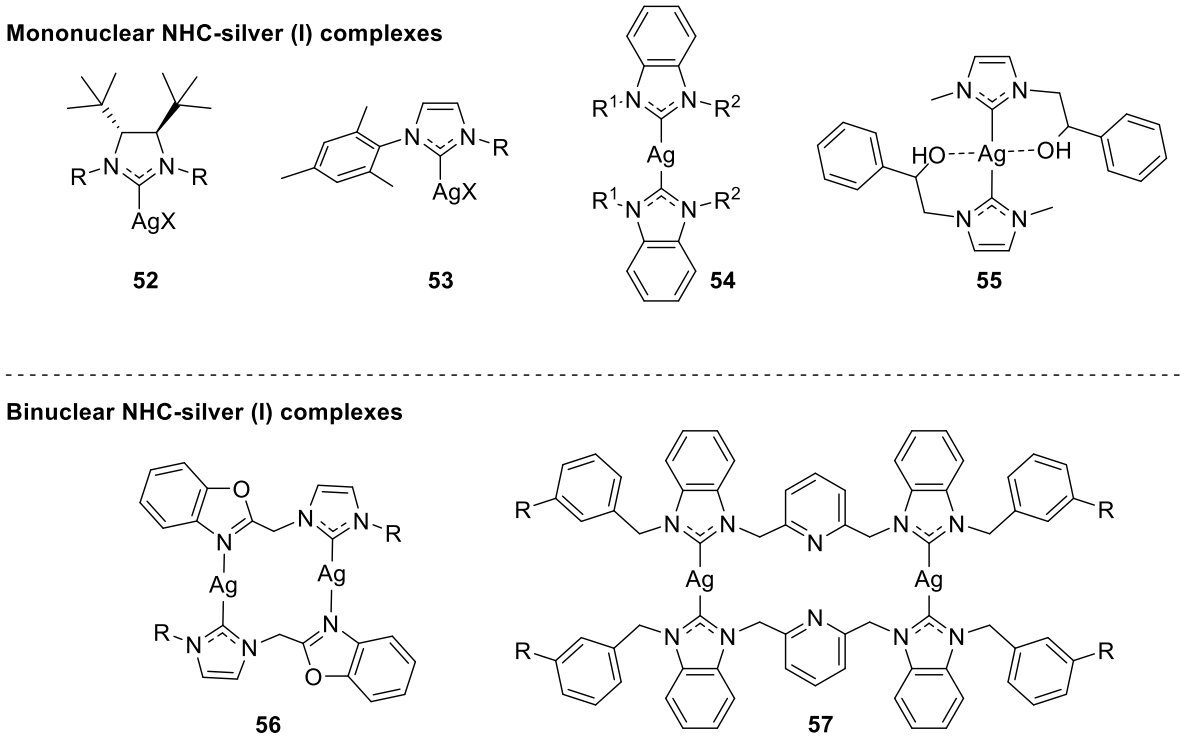

Figure 11. A variety of NHC-silver(I) complexes tested for antimicrobial.

2.5. Silver in catalysis

Silver is categorised as one of the "coinage metals," and it is relatively inexpensive in contrast to gold or other commonly used transition metals, such as palladium, ruthenium, or rhodium. Silver possesses the electronic configuration [Kr] $4d^{10}5s^1$ and its outer orbital $5s^1$ electronic configuration enables the formation of a series of silver (I) salts, either independently or in conjunction with other transition metals, bearing various counter anions. Silver (I) salts can act as σ and/or π-Lewis acids.[88] The d^{10} electronic configuration of silver imparts unique properties for alkyne activation, displaying a preference for interactions with the carbon-carbon π-bond of alkynes. Thus, silver stands out as one of the most potent activators of a carbon-carbon triple bond. As depicted in Scheme 14 the mechanism of interaction of silver with an alkyne depends on the type of alkyne used in the reaction. If an internal alkyne is used, then the silver coordinates with the alkyne forming a silver-π -complex. This complex facilitates the creation of C–Nu bonds through a nucleophilic attack on the activated bond. On the other hand, if a terminal or silylated alkyne is used then the pathway proceeds with the formation of a silver alkynide through deprotonation/desiliconisation. This silver alkynide can then act as a nucleophile, participating in reactions with electrophiles or engaging in cross-coupling reactions *via* the transmetalation process.[89] Furthermore, other functional groups like imines and carbonyls are also activated through coordination with silver, these are less common and will not be further discussed in this thesis.[90]

Additionally, silver can activate substrates such as alkenes, phosphonates,[91] benzylic groups,[92] or other reactive C-H bonds through radical-forming processes, involving one-electron redox cycles, where Ag(0)/Ag(I) and Ag(I)/Ag(II) states have been proposed. These activation processes facilitate various chemical transformations by forming reactive intermediates. The involvement of silver in these redox cycles highlights its versatility and importance in catalytic reactions.

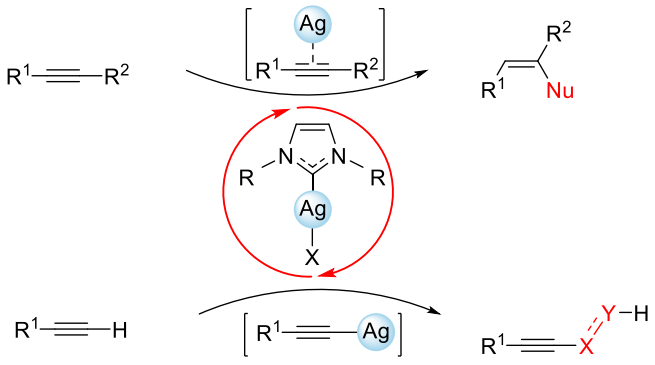

Scheme 14. Mode of action of silver(I) complexes with alkynes.

2.5.1. A^3 coupling reaction

Recently, propargylamine has been considered a convenient starting material and a widely observed intermediate for the construction of various heterocyclic frameworks, biologically active compounds and natural products.[93] The conventional approach for synthesising propargylamine involves the addition of a metal acetylide to an imine. This process typically employs strong bases, such as butyllithium, to generate metal acetylides.[94,95] The stoichiometric amounts of the organometallic reagent, coupled with its increased sensitivity to moisture, make such processes relatively unattractive. Consequently, a more convenient and atom-economic approach has been developed by employing a transition-metal catalyst. This method avoids the drawbacks of stoichiometric quantities and moisture sensitivity. The concept of forming the imine or iminium ion *in situ* from an aldehyde and an amine led to the discovery of a straightforward transition-metal catalysed three-component coupling involving an aldehyde, an amine, and an alkyne, commonly known as A^3 coupling.

In 1998, Dax and co-workers reported the solid-phase synthesis of propargylamine using a three-component coupling involving an aldehyde, an alkyne, and a secondary amine. This reaction was facilitated by using two equivalents of CuCl, and either the amine or the aldehyde component could be attached to the resin.[96] The method represents an interesting example of solid-phase synthesis applying the same principle, yet it derives from the A^3 coupling process as it utilises a stoichiometric amount of CuCl. Subsequently, Alexey Dyatkin and Ralph Rivero, introduced a complementary protocol involving polymer-supported aryl alkynes, variously substituted aldehydes, and secondary amines in the same year. This protocol successfully formed propargylamides **61** with the assistance of a catalytic amount (10 mol%) of CuCl (Scheme 15).[97] Notably, this approach stands out as the first example of an A^3 coupling. Although intuitive, the A^3 coupling has only emerged in recent years.

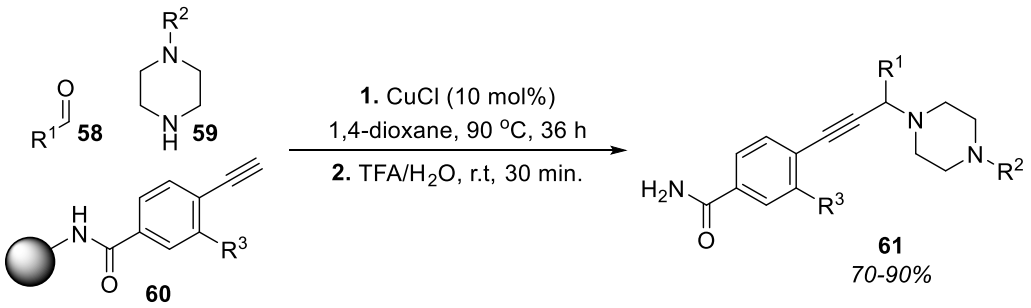

Scheme 15. Synthesis of propargylamine **61** using catalytic amount of CuCl.

Min Wang and co-workers reported in 2008 the first catalytic A^3 coupling reaction employing an NHC-silver(I) as catalyst. They have demonstrated that NHC-silver(I) complexes and polystyrene-supported NHC-silver(I) complexes are efficient catalysts for the reaction. In both polystyrene-supported and non-polystyrene supported complexes, the substitution on the NHC ligand **62** was found to influence the catalytic efficiency. The most reactive was **62b** bearing the benzyl group as substituent. The order of reactivity was then phenyl **62c**, *t*ert-butyl **62d** and methyl **62a**, which approximately correlates with the size of the substituents. The polystyrene supported complexes also showed slightly higher activities compared to the non-polystyrene supported complexes (69-90% vs. 61-80% yield of **66**) and can be recycled for over 12 cycles without significant leaching.[98]

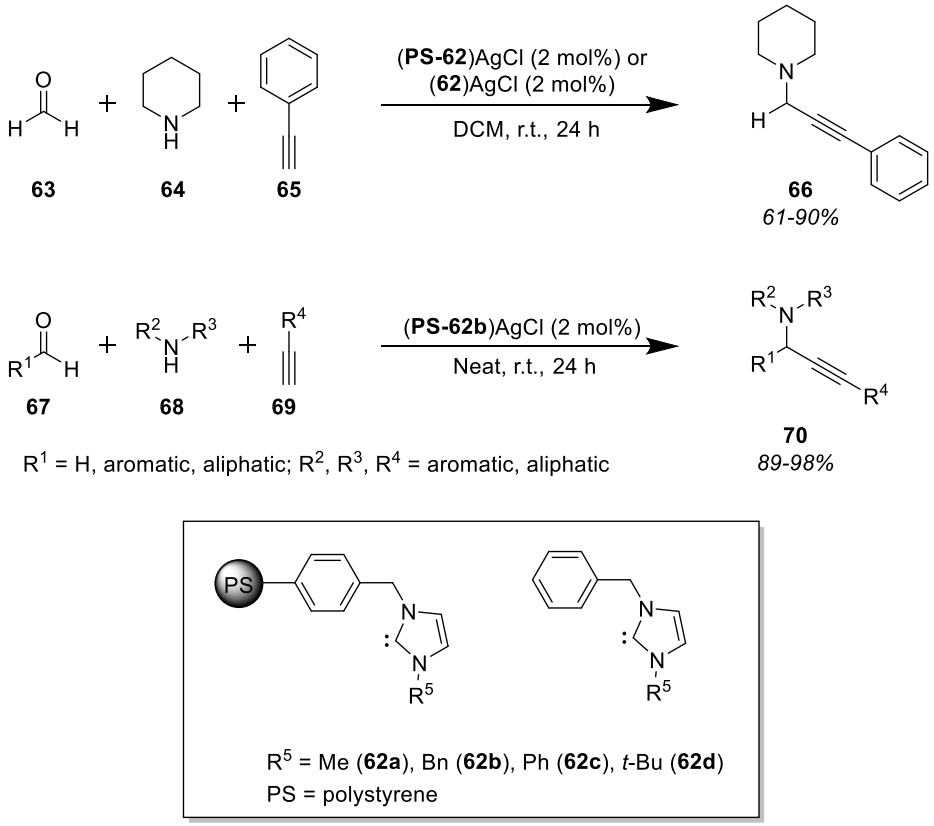

Scheme 16. First A^3 coupling using an NHC-siler(I) catalyst.

Gang Zou and collaborators synthesised the chloro-, bromo-, and bis(NHC)-silver(I) complexes of the NHC ligands **71** and **72**. The structure of all complexes was confirmed through single crystal X-ray crystallography. During the screening of their catalytic activity for the A^3 coupling reaction, it was observed that complexes featuring the more sterically hindered ligand **72** revealed better results. Notably, the chloride complexes demonstrated higher yields when compared to their bromide and bis(NHC) counterparts. The authors proposed that due to the steric hindrance of ligand **72** more stable complexes are formed. The observation that chloride complexes outperformed their bromide counterparts suggests that the initial step of the catalytic cycle involves the coordination of the alkyne to the complex, a process favoured by a smaller anion. The complexes proved to be less reactive than the polystyrene-supported catalysts reported by Wang *et al*. When adopting the same reaction conditions (DCM, r.t) the reaction of 3-phenylpropionaldehyde **73**, piperidine **64** and phenylacetylene **65** only furnished trace amounts of the product **74**. It was necessary the use of harsher conditions to promote the reaction, leading to the formation of the desired product **74** with respectable yields of 61 to 99%, depending on the catalyst employed. Surprisingly, it was found that silver chloride also resulted in 80% yield under the same reaction conditions, being complex (**72**)AgCl the only one with better reactivity yielding 99% of product **74**, surpassing the silver chloride. The complex was then further used for subsequent investigation of the substrate scope with yields ranging from 49% to 99%.[99]

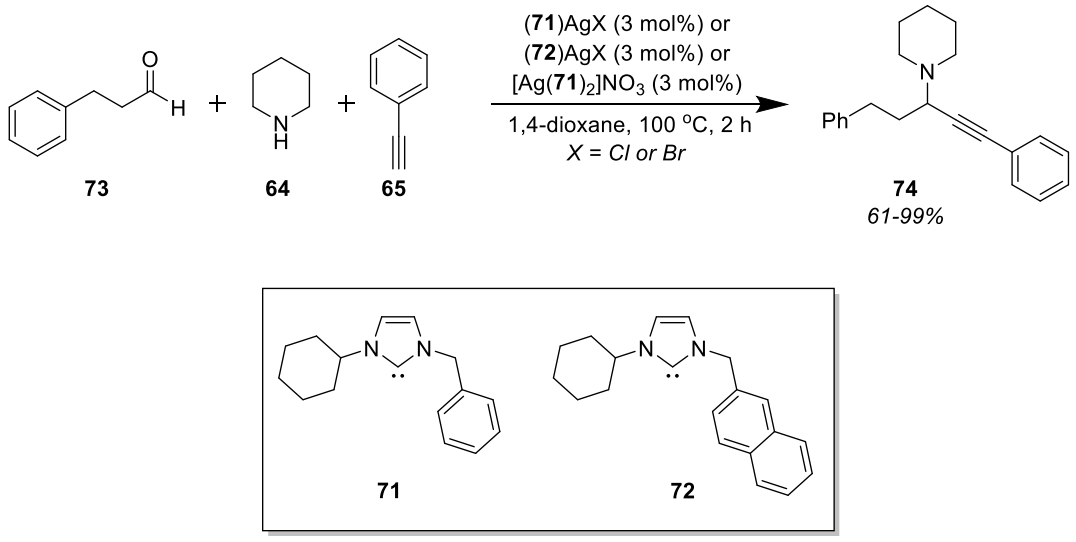

Scheme 17. Catalytic activities of well-defined silver(I) NHC complexes.

Navarro and colleagues observed a similar influence of the size of the anionic ligand on silver. In their comparative study of NHC-silver(I) complexes containing either halide or acetate as contueranion with IPr and SIPr ligands, the catalytic activity was higher with acetate, followed by chloride and lastly with similar when using bromide or iodide as counteranions. Interestingly, minimal differences in activity between the IPr and SIPr ligands were noted. The results support Zou's proposal that the initiating step of the reaction involves the displacement of the halide ligand by the alkyne, resulting in the formation of a silver acetylide intermediate.[100]

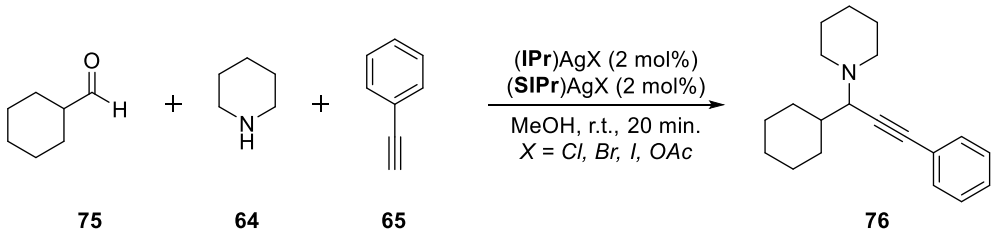

Scheme 18. NHC-silver(I) halide and acetate complexes as catalysts for theA^3 coupling reaction.

The mechanism of the A^3 coupling reaction is described in Scheme **19**. Briefly, the catalyst (NHC)AgX reacts with alkyne and amine to form the silver alkynide and the amine hydrogen halide salt at first. The salt then condenses with aldehyde to generate iminium halide, which reacts with the previously generated silver alkynide to afford the desired product and regenerate the catalyst (NHC)AgX. From the proposed mechanism is fair to conclude that the structural stability and the accessibility of the silver ion play a crucial role in the catalysis. Based on this, it is logic that chloride has a high catalytic activity since it forms stable silver complexes yet with open coordination environment around the silver ion.[99]

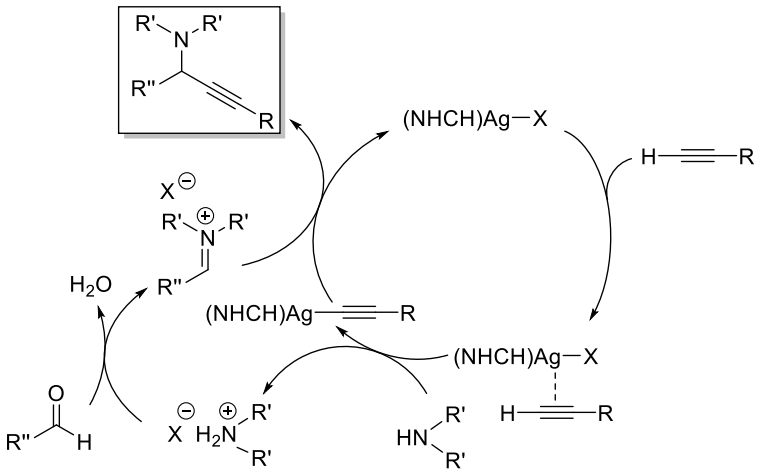

Scheme 19. Plausible mechanism for the A^3-coupling reaction catalysed by (NHC)AgX.

2.5.2. KA^2 coupling reaction

Aldehydes have been utilised in the synthesis to generate propargylamines with tertiary carbons approximately for the past twenty years. However, the analogue method involving ketones to create propargylamines with quaternary carbon centres was only uncovered a decade ago. This signifies a decade-long oversight in employing ketones in one-pot propargylamine synthesis, with a valid explanation: Ketones, along with their ketimine/ketiminium cation counterparts, exhibit significantly lower reactivity compared to aldehydes and their corresponding aldimine/aldiminium cations.

In 2010, Van der Eycken and colleagues published the first instance of a reaction involving ketones, amines, and alkynes in a one-pot synthesis of tetrasubstituted propargylamines. The optimisation of the reaction conditions involved the use of cyclohexanone, 4-methoxybenzylamine (PMB), phenylacetylene **65**, and CuI as the catalyst. Their protocol exclusively employed aliphatic cyclic ketones, except for acetone, which yielded only 30% of the desired product. Aromatic alkynes resulted in good to high yields of the corresponding propargylamines, whereas aliphatic alkynes were less efficiently incorporated. Although most substrate scope studies utilised p-methoxybenzylamine, other primary amines exhibited good reactivity (ranging from 46% to 82%). Moderate to very good yields were obtained with cyclic ketones (31–82%) and *N*-protected piperidinones (61–82%). However, *N*-benzyl-cyclohexanone showed moderate results (38%). Notably, the use of 3-methylcyclohexanone and 2-methylcyclohexanone shed light on the impact of steric hindrance on reaction outcomes: 2-Methylcyclohexanone yielded the product at 33%, while 3-methylcyclohexanone provided a significant higher yield of 75%, indicating that increased steric bulk near the carbonyl group substantially reduces reactivity.[101]

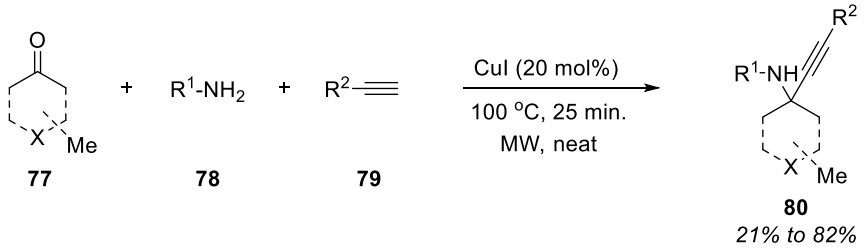

Scheme 20. KA^2 coupling reaction catalysed by CuI.

Recently, Savvas G. Chalkidis and Georgios C. Vougioukalakis reported a KA^2 coupling reaction employing NHC-copper (I) complexes.[102] The authors used cyclohexanone, pyrrolidine and phenylacetylene for the optimisation of the method. When using the complex (SIPr)CuCl the reaction yielded only 19% of the desired propargyl amine. The corresponding copper complex analogue (SIPr)CuBr containing bromine instead of chlorine only led to trace amounts of the product. Another important factor in the outcome of the reaction is the bulkiness of the ligand. When using the complex (SIMes)CuCl the author isolated the final product with a 74% yield. Not satisfied with the results, titanium ethoxide was used as an additive. With the optimised conditions in hand, the authors proceed with the scope. A variety of ketones were tolerated with good yields, cyclohexenone being the only limitation. Regarding the alkyne component, all gave excellent yields except 1-ethynyl-4-nitrobenzene. On the other hand, the amine aspect had some drawbacks. In general, cyclic amines such as pyrrolidine, and piperidine produced good yields. With morpholine a drop of yield was observed to 63% and when using acyclic amine dibutylamine the yield further dropped to 47%. Primary amines were not tolerated, leading to traces amount or even no reaction at all.

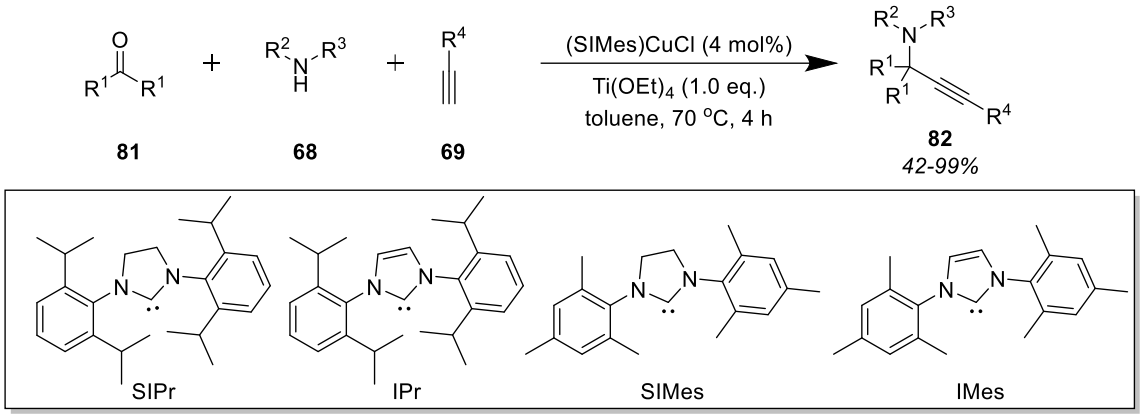

Scheme 21. NHC-copper(I) halide complexes as catalysts for theKA^2 coupling reaction.

It was demonstrated, that such transformation can be catalysed by different inorganic materials, such as Cu-doped zeolites[103], CuO/Fe_2O_3 nanoparticules[104], Cu_2O/ZnO[105], Cd-doped gold nanocluster[106] or zinc[107]. However, in most cases, either high catalytic loadings are required for the reaction to proceed (10-20 mol%), or stoichiometric amount of an additional additive, such as titanium oxide, is required. To the best of my knowledge, no report of KA^2 coupling reaction using well defined silver complexes can be found in the literature.

2.6. The use of small molecules in data storage

In an ever-evolving society, technology has emerged as an indispensable cornerstone of civilisation, reshaping our interactions and modes of operation. An evident manifestation of this evolution is the gradual transition from traditional paper documentation to its digital counterparts, generating large amounts of data in need to be stored. The exponential surge in human-generated data is evident: what was once a mere 5 Zettabytes (ZB) in 2015 has grown to a staggering 173 ZB in 2023, with projections soaring to an estimated double by 2025.[108] Conventionally, data repositories rely on hard drives (HD) or the more contemporary solid-state drives (SSDs), leveraging semiconductor technology to encode information *via* electron density and conductivity. However, the increasing demands for data storage have set the limitations of HD and SSDs, notably their finite storage capacities and susceptibility to degradation with each rewriting cycle. Additionally, the speculation of data loss in scenarios of prolonged disconnection from power sources raises the concern of storing sensitive information in such disks. Furthermore, the ever-increasing costs and the limited supply of rare earth metals essential for SSD and HD fabrication[109] emphasise the urgency for pioneering alternatives ensuring secure, long-term data preservation.

A very elegant approach is the use of DNA for data storage. The use of DNA for data storage offers a density of up to 10^{18} bytes per microlitre, approximately six orders of magnitude denser than the densest media available today.[110] Furthermore, DNA has stood the test of time, with sequences retrieved from fossils dating back centuries. When preserved under optimal conditions, shielded from light, humidity, and kept at moderate temperatures, DNA can remain viable for centuries. Unlike traditional storage media, where copying time is proportional to the data volume and the number of duplicates needed, DNA storage enables the efficient replication of numerous copies with a fixed time process such as PCR.[111] Although sophisticated, a major drawback to the use of DNA storage is the necessity of a very controlled synthesis and the expensive machinery required for such production. For comparison, DNA storage is estimated to cost 800 million USD per terabyte of data (by contrast, tape storage costs approximately 15 USD per terabyte). Due to the complexity of the method and falling outside the scope of the thesis, no more discussion on the topic will be presented. For more specifics, the review by Denis Garoli *et al*[112] on the subject is advised.

As we continue to push the boundaries of technology, we must find innovative and sustainable solutions for storing our ever-growing volume of data. An emerging and innovative

concept is the use of small molecules to store data. While this approach is still in its early stages, it shows great promise for advancing technology. In the context of using mixtures of small molecules for data storage, the binary code is segmented into subsequences, with each position of the subsequence corresponding to a specific molecule. These binary subsequences are then encoded as a mixture of molecules, where the presence of a molecule represents a binary one, and the absence of a particular molecule signifies a binary zero.

The current state of the art contemplates only a handful of examples. The first example of data storage using small molecules was introduced very recently by George M. Whitesides and co-workers. The authors used a small set of molecules, in this instance 32 oligopeptides, to write the binary information. In Figure 12 is possible to denotate the method developed by the authors. As stated previously, this method is based on the premise that the presence of the oligopeptide represents the binary one and the absence of the respective binary zero. The authors first designed each of the 32 oligopeptides consisting of one to five amino acids where the binary information was contained, a charged residue (trimethyl lysine), and lastly an anchor residue (a). The immobilisation of the oligopeptides proceeded *via* thiol-Michael addition (b). The decoding of the binary information was obtained with the use of the SAMDI-MS technique. This is depicted in (c) as the 32 oligomers are observable in the SAMDI spectrum. The usefulness of the method was then proved when the authors encoded, stored, and decoded three different sets of data representing a text and two pictures. Since 32 oligomers were used, and considering each oligomer represents 1 bite of information, it is possible to encode 32 bits of information, in order words 4 bytes, for each SAMDI plate. The recovery rate was near 100% for all the data encoded with the use of a MALDI-TOF spectrometer. The biggest set of data

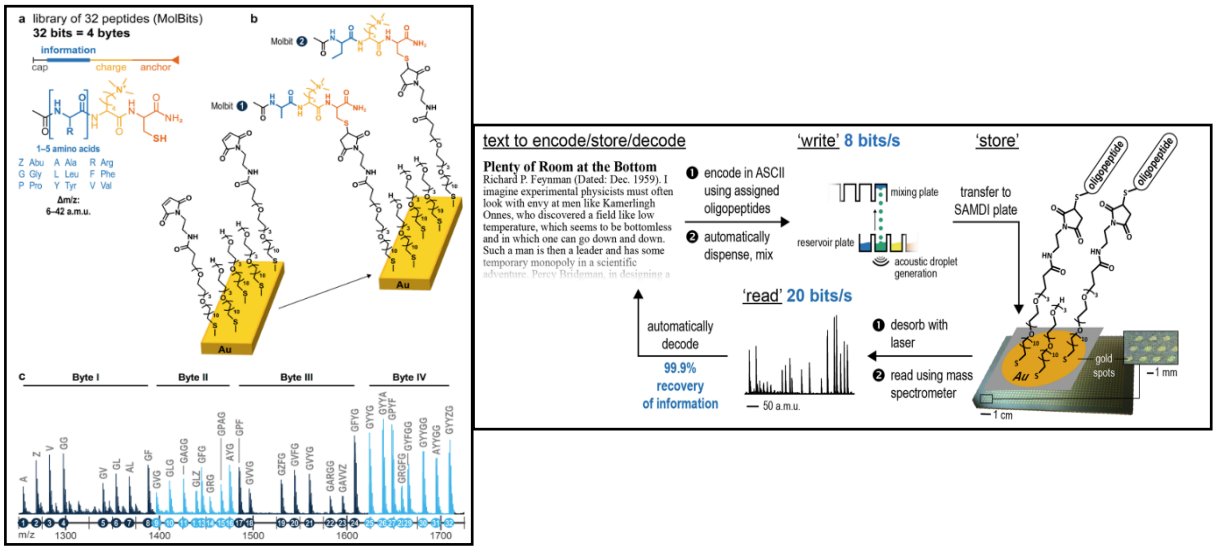

Figure 12. Synthesis, immobilization, and analysis of the oligomers (left). Workflow of the data storage process using the oligopeptides developed by the authors (right). Pictures retrieved from the original publication.

encoded was a picture with 6094 bytes.[113] Altogether, this work was the proof of concept that small molecules can be an interesting and innovative solution.

Only two years later, George M. Whitesides and co-workers reported another fine example of data storage using small molecules. This time, the authors used fluorescent molecules to store the information. Seven commercially available fluorescent dye molecules with different emission maxima were chosen to showcase their strategy. The detection technique employed a multichannel fluorescence detector, utilising a linear array of detection channels to resolve multiple emission bands simultaneously. This allowed for spatially resolved information on the presence or absence of the dye molecules to be obtained in a single scan across the substrate. In principle, the technique could have been expanded to incorporate more dyes and encode more information within the same area. The dyes were dissolved in dimethyl sulfoxide (DMSO) and injected into the inkjet printer cartridge. Once again, the data underwent conversion into a binary bit string, subsequently encoded into printable patterns, and printed using an inkjet printer. The decoding involved imaging the printed substrate using a multichannel fluorescence detector. This detector was capable of simultaneously and independently detecting the presence or absence of dye molecules at specific locations. A notable feature of this approach was that the proximity of the dyes did not affect the decoding process.[114]

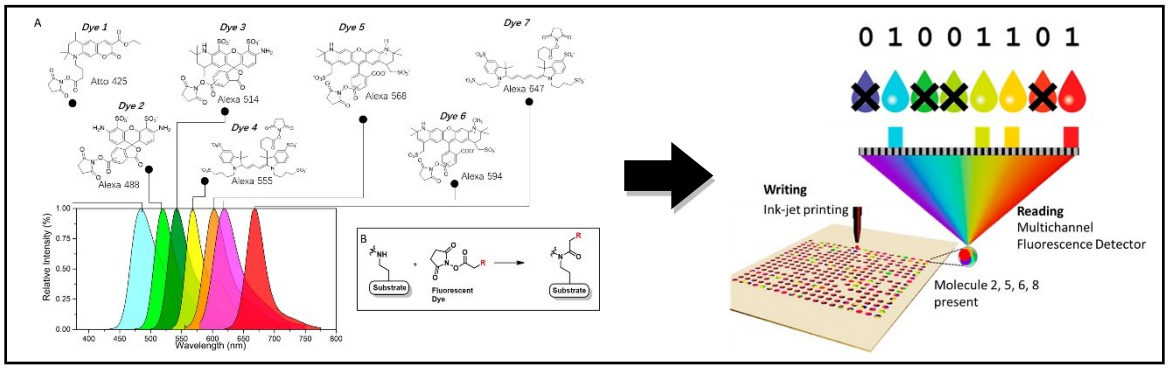

Figure 13. Dyes employed as well as their respective emission spectra in dimethyl sulfoxide, followed by the schematic representation of the "writing" and "reading" process. Pictures retrieved from the original publication.

In 2022, Michael A. R. Meier *et al.* was able to perform, and citing the author, *"Molecular data storage with zero synthetic effort and simple read-out"*. The authors present a rapid and effective technique for storing information using molecular mixtures. This was achieved through the direct application of commercially available chemicals. For the proof of concept, the authors used a mixture of 8 commercial solvents: benzene, dichloromethane, dimethyl carbonate, 1,4-dioxane, dimethyl sulfoxide, acetone, acetonitrile, and cyclohexane. The reason for the choice of such solvents is that each solvent holds one specific singlet ^{1}H NMR signal, making the "decoding" simple and straightforward. Through this method, the names "Felix Bloch" and "Edward Mills Purcell" were effectively encoded into 31 molecular mixtures, and subsequently decoded manually using NMR spectroscopy. Not completely fulfilled with the results and intending to increase the number of molecules in each mixture, the authors turned their attention to the GC-FID system. With this change, the authors were able to increase from 8 to 24 molecules mixture. This means an increment of 2 bytes per mixture. On a first stage the authors were decoding manually the GC-MS mixtures, however, this proved to be awfully time-consuming. To streamline this process, a decoding software was developed, enabling automatic arrangement of the datasets in the correct order. This ensured a faster read-out of the original information with fully recovery of the data stored.[115]

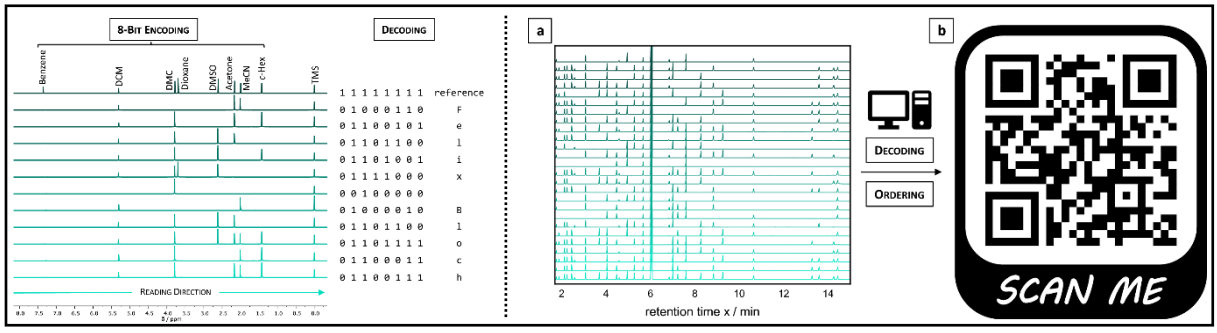

Figure 14. 8-bit encoding using ^{1}H NMR (left) and 24-bit encoding using GC (right). Pictures retrieved from the original publication

Taking into consideration the examples illustrated, it becomes apparent that the limitation of using small molecules is the need to use a large number of molecules and each molecule is stranded to a position in the substring. Furthermore, the decoding process still presents a challenge since it requires time and the use of reasonably expensive machinery. The A^3 coupling reaction is a three-component reaction (involving aldehyde, amine and alkyne as stated previously), therefore it facilitates the synthesis of a small library of compounds with the opportunity to fine-tune the outcome. Among the many applications this small library can employ, their use in data storage emerges as a compelling application due to the opportunity to explore other decoding methods.

3. Aims of the project

The outlook presented in Chapter 2 demonstrates the versatility and diversity of NHC-silver(I) complexes that can be found in the literature. Furthermore, silver complexes have found a wide range of applications, while still being underestimated and overshadowed by other transition metals, such as gold or platinum. To further contribute, the following aims were set:

I. The synthesis of a set of symmetrical bidentate NHC precursors.

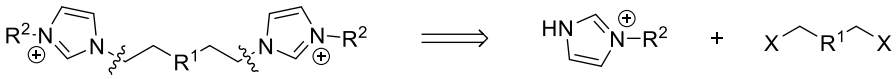

II. The usage of the synthesised ligand precursors to produce monomeric chelating NHC-silver(I) complexes. Chelate silver complexes are quite rare and difficult to access, as stated in chapter **2.2.1**. The goal is to find a straightforward and simple approach to form chelating NHC-silver(I) complexes.

III. Investigate the ligand effect, with a special focus on the imidazole portion, on the NHC-silver(I) complexes, since as shown in Chapter 2, small modifications can lead to different modes of coordination.

IV. Application of the carbene transfer method since it offers advantages over other procedures. The method should provide an approach to either bi- or tetradentate transition metal complexes, that would otherwise be difficult or impossible to achieve. Once again, the ligand effect will be investigated.

V. Test the synthesised silver complexes as antimicrobial agents. As stated previously, silver complexes can and are used for therapeutic purposes, however, the rapid loss of activity remains a challenge. We aim to study if the chelating aspect of the NHC, which forms strong bonds with metal centres, aligning with the chelate aspect of the silver complex can impact the release of the silver cations.

VI. The NHC-silver(I) complexes will also be tested as catalysts in the A^3 and KA^2 coupling reactions. A special focus will be given to the KA^2 reaction since no reaction has been reported with the use of silver.

VII. Lastly, use the propargyl amines synthesised with the silver complexes for data storage. Since A^3 and KA^2 are multicomponent reactions, access to a small library of compounds should be achieved. There is also the appeal to find a new way to decode the data stored in order to make the process economical and simpler.

4. Results and Discussion

4.1. Synthesis of the ligand and silver complexes

We envisioned that a bidentate ligand would be the preferred choice to synthesise the desired chelate silver complexes. As depicted in Figure 15, such silver complexes can be divided into three main parts, that can undergo separate modification, namely, the ligand backbone, (depicted in blue), linker moiety (in green), and the NHC part (in red). Numerous backbones can be considered since a variety of diamines are commercially available. From aliphatic amines such as 1,2-diaminopropane (**85**) to cyclic aliphatic amines such as 1,2-diaminocyclohexane (**86**). Regarding aromatic amines, a broad study could be done with the introduction of different functional groups in the four free positions of the aromatic ring. Commercially available aromatic diamines vary from electron donating groups such as 4-methoxy-o-phenylenediamine hydrochloride, to electron withdrawing groups such as 4,5-dibromobenzene-1,2 diamine. No less important, the linker moiety, can also be changed. A simple alkane linker, such as methane or ethane can be considered **83**. However, to the best of our knowledge, a ligand such as an amide ligand can be employed for such purposes for the first time **84**. This gives the freedom to for instance increase the length of the chain. This will permit understand the importance of the carbonyl group. Regarding the NHC part, an interesting group to study would be the benzimidazole group (**89**). Lastly, the modest methyl group can be switched to bulkier groups such as isopropyl or the introduction of some aryl moieties.

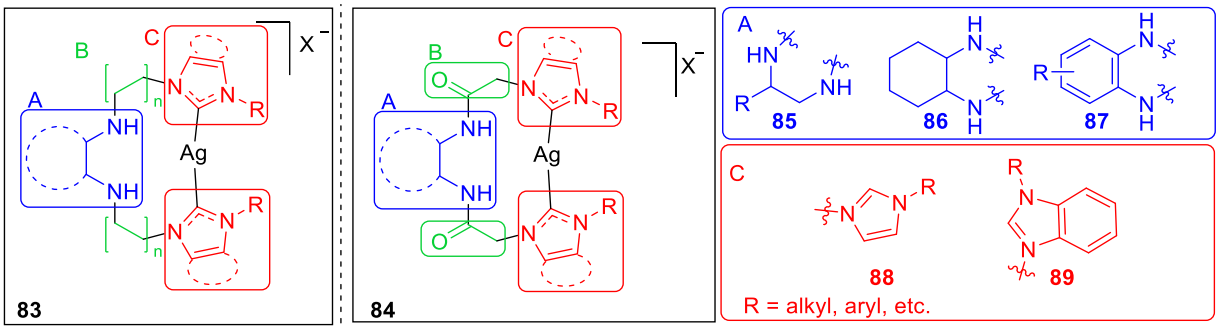

Figure 15. Proposed chelating NHC-silver(I) complexes.

With that in mind, we started the synthesis of the ligands with a simple Mannich reaction between 1,2-dimethylethylenediamine **90**, imidazole **91** and formaldehyde to achieve ligand precursors **92** (Scheme 22). Attempts to improve the yield, by using different acids, as well as bases, and acetone instead of formaldehyde, were unsuccessful. Nevertheless, the synthesis of the ligand precursors proceeded with the attempt to form the necessary imidazolium salt. Various electrophiles, such as methyl iodide or benzyl chloride were used but none provided

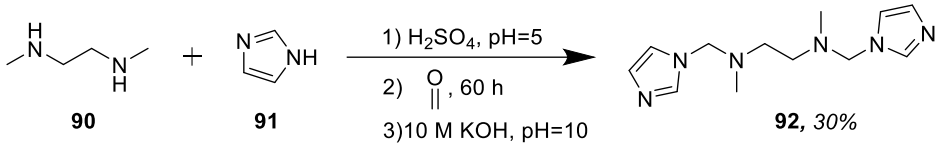

Scheme 22. Synthesis of ligand precursors **92**.

the desired ligands. The only suitable electrophile was benzoyl chloride forming imidazolium **95** due to the precipitation of the product from the reaction mixture. Unfortunately, this product proved to be highly sensitive to moisture and so it decomposed upon isolation. For this reason, the counter anion was changed from chloride to hexafluorophosphate. Hexafluorophosphate is known to stabilise imidazolium salts preventing their decomposition.[116] However, the outcome was equal to chloride, with the decomposition of the compound.

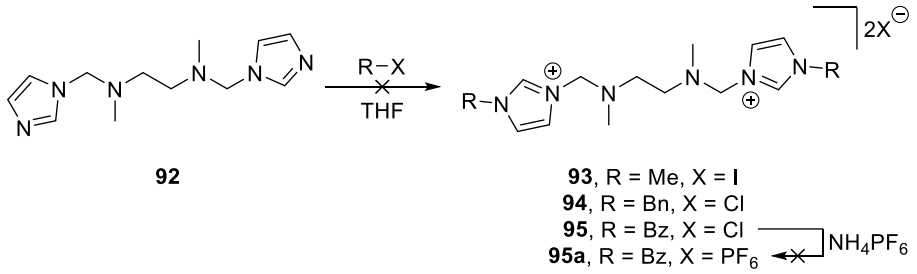

Scheme 23. Attempted synthesis of imidazolium **93, 94** and **95.**

These unsuccessful attempts to generate the imidazolium salts using a simple alkane in the backbone led to a change in the strategy. Instead of an alkane linker, a bisamide linker would be employed as proposed beforehand. The synthesis of the ligand precursors was accomplished in two steps, as outlined in Scheme 24. Initially, 2-chloroacetylchloride **96** reacted with ethylene-1,2-diamine **97** to yield bisamide **98** in 43%, which was then alkylated with 1-methylimidazole and 1-isopropylimidazole **99**. The resulting bisimidazolium salts **100a** and **100b** were obtained in 83% and 98% yields, respectively. Treating 2-chloroacetylchloride **96** with o-phenylenediamine **101** produced bisamide **102** in 66% yield. Subsequent reactions with various imidazoles **99** and 1-methylbenzimidazole **103** yielded bisimidazolium salts **104a-104d**

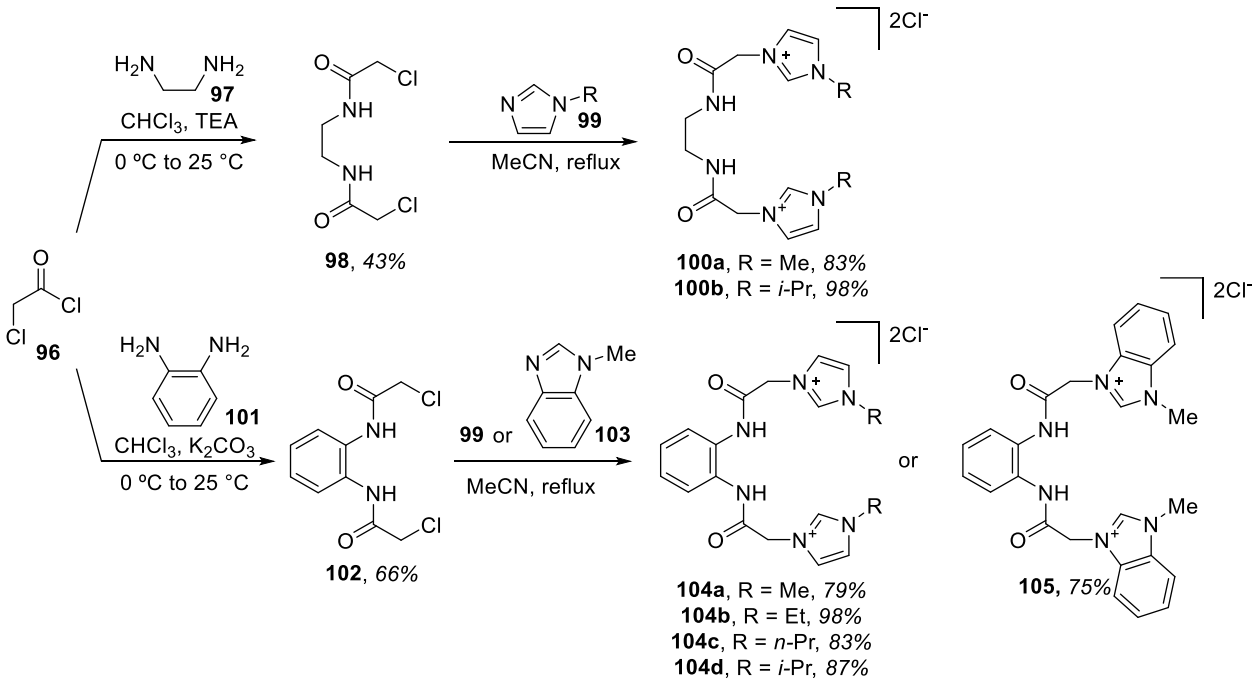

Scheme 24. Synthesis of ligand precursors.

and **105** with yields from 79% to 98%. All bisimidazolium salts were isolated as white powders. With the ligand precursors in hands, complexation to silver was attempted. First, bisimidazolium salt **100a** was treated with 1.3 equivalents of silver oxide. The reaction led to the formation of the desired chelate complex **106a**, which was isolated in 75% yield. When ligand precursor **104a** was treated with 1.3 equivalents of silver oxide, the corresponding complex **107a** was isolated in a lower 53% yield. Unsatisfied with the result, the ligand precursor **104a** was treated with 2 equivalents of silver oxide, in an attempt to increase the yield. Interestingly, the reaction proceeded with the formation of unprecedented tetranuclear complex **108**, as shown in Scheme 25. The analysis of this complex proved to be quite challenging due to insolubility in all organic solvents. Attempts to reproduce such a complex with ligand precursor **100a** were undertaken even using bases, such as sodium hydride, however, no such complex was ever isolated.

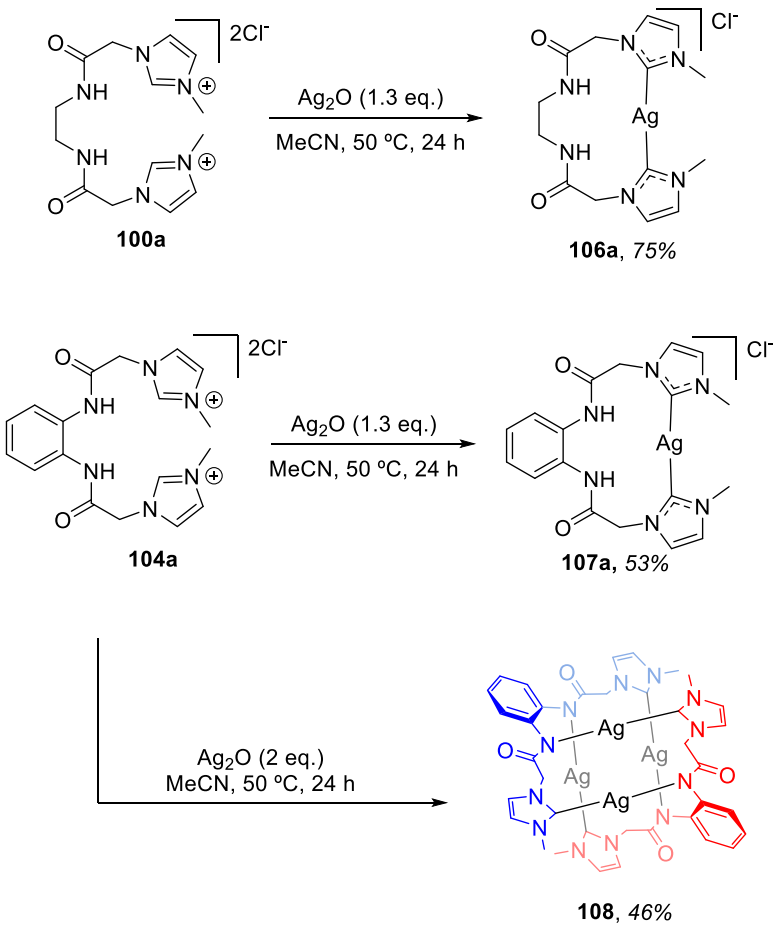

Scheme 25. Silver complexation with ligand precursor **100a** and **104a**.

The formation of complexes **106a**, **107a**, and **108** was confirmed through NMR, HRMS, and X-ray analysis. The NMR spectra showed that the acidic imidazolium signals disappeared in the ^{1}H NMR, indicating carbene formation. In complex **106a**, a broad signal at 8.54 ppm corresponding to the amide protons suggested that the amide group does not participate in complexation. Two doublets at 7.38 and 7.41 ppm were assigned to the imidazolium core. Additionally, three singlets were observed at 4.80 ppm (methylene protons, intensity of four), 3.83 ppm (methyl groups on the imidazole core, intensity of six), and 3.24 ppm (ethylene linker of the bisamide backbone, intensity of four). For complex **107a**, signals at 7.48 ppm and 7.40 ppm were attributed to the imidazole moiety, while signals at 7.34 ppm and 7.17 ppm were linked to the aromatic ring of the backbone. The methylene bridge appeared at 5.14 ppm, and the methyl protons at 3.86 ppm. Both complexes **106a** and **107a** displayed symmetrical characteristics.

The analysis of complex **108** was challenging due to its insolubility, granting only the ^{1}H NMR spectra in deuterated DMSO to be recorded. This analysis revealed signals for the imidazole units (7.46 ppm and 7.39 ppm), aromatic ring (7.30 ppm and 7.23 ppm), methyl

groups (3.15 ppm), and the methylene bridge. Unlike the previous complexes, the methylene bridge signals appeared as two doublets at 4.76 ppm and 5.42 ppm, indicating that the two geminal protons were in different chemical environments. Another key observation was the absence of the amide protons, which were present in both monomeric complexes.

In the ^{13}C NMR spectra of complexes **106a** and **107a**, signals for the backbone and imidazolium moieties were recognised. However, the signal around 180 ppm, that corresponds to the carbene carbons bonded to silver, was absent (Figure 16, A, and B). This absence is likely due to the slow relaxation of these carbons or coupling with ^{107}Ag and ^{109}Ag, causing signal splitting and very low intensity. Nonetheless, these signals were extrapolated from the 2D HMBC spectra. For complex **106a**, the carbene carbon signal was detected at 182.5 ppm, showing a cross-peak with methyl and methylene hydrogens (3.84 ppm and 4.80 ppm, respectively) (Figure 16, C). Similarly, the carbene carbon in complex **107a** was identified at 182.1 ppm through cross-interaction with methyl and methylene protons (Figure 16, D).

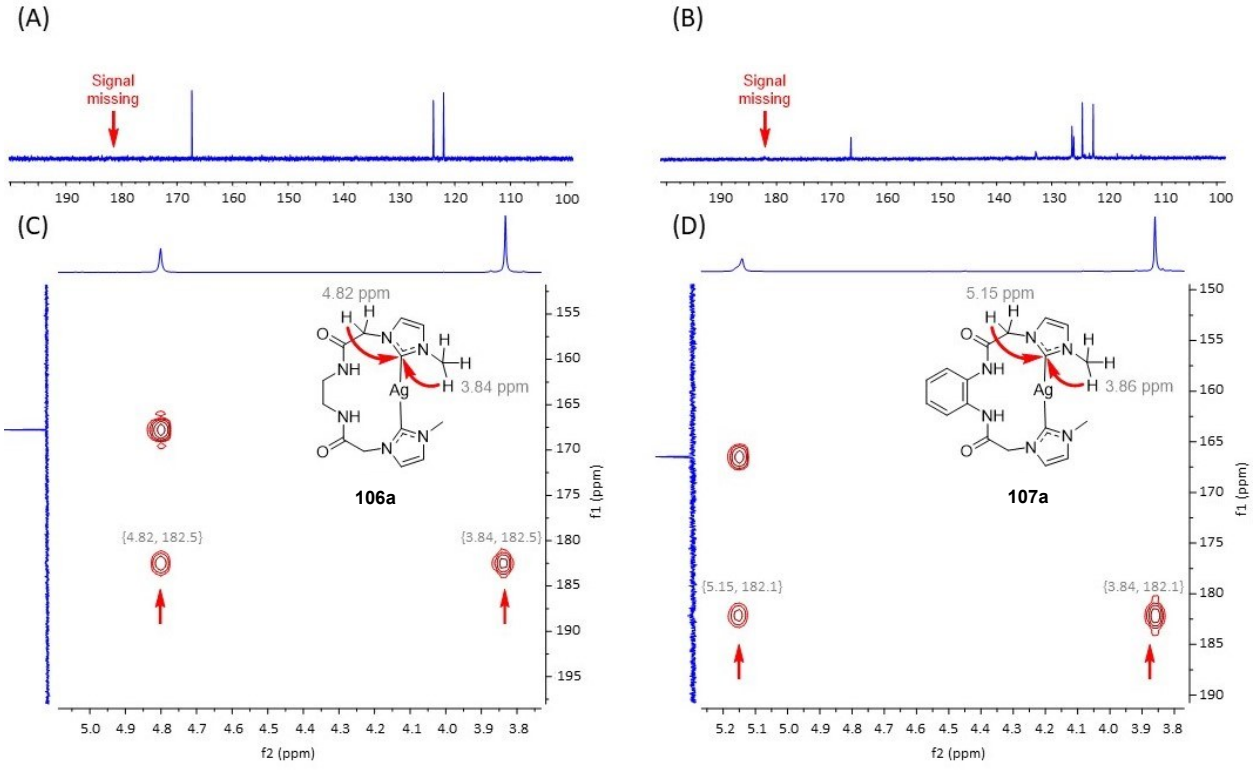

Figure 16. Lack of the carbene carbon signals in ^{13}C NMR spectra of complexes **106a** (A) and **107a** (B) and identification of the carbene carbon frequencies via HMBC correlations with selected protons.

The structure of complexes **106a** and **108** was further confirmed through X-ray crystallography, providing critical insight into the chelating nature of these complexes. For complex **106a**, a suitable crystal was obtained by the slow diffusion of diethyl ether into a saturated acetonitrile solution of the complex at room temperature. This method allowed for the formation of single crystals necessary for detailed structural analysis. The crystallographic data revealed that compound **106a** crystallised in a monoclinic system with the space group *P21/c*. The analysis unequivocally confirmed the chelating nature of the ligand, where the central silver ion is coordinated by two NHC moieties. The Ag1-C5 and Ag1-C11 bond lengths were measured at 2.09 Å, indicating a strong interaction between the silver ion and the NHC ligands. Additionally, the bond angle of C5-Ag1-C11 was found to be nearly linear at 172°, which is characteristic of a stable chelate complex (Figure 17). This nearly linear geometry supports the robustness of the chelating interaction, which is essential for the complex's stability and functionality. The consistent chelating behaviour observed across this complex underscores the reliability of the synthetic method used to produce them. The precise bond lengths and angles obtained from the X-ray data are crucial for understanding the electronic environment around the silver ion, which directly influences the complex's reactivity and potential applications.

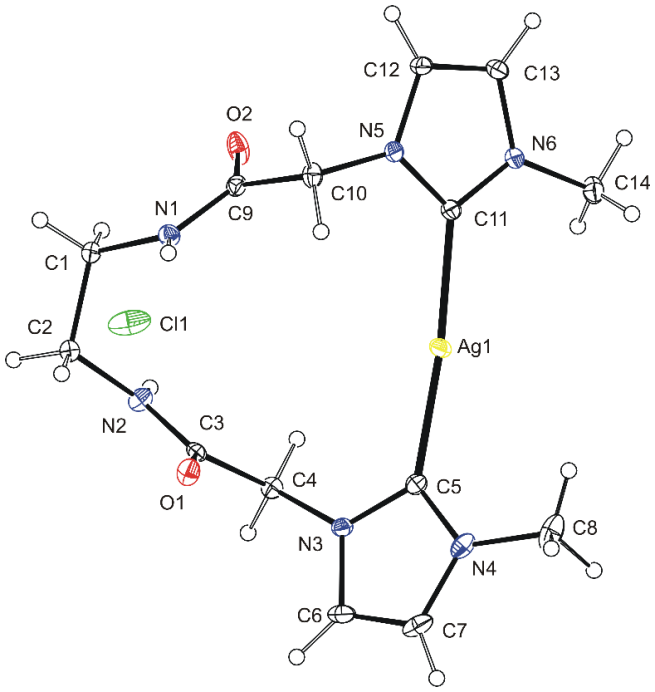

Figure 17: View on the molecule of **106a** the displacement ellipsoids at 30% probability level.

A suitable crystal of complex **108** was obtained by slowly cooling a hot DMSO solution. Crystallographic analysis showed that the complex belongs to the orthorhombic crystal system with the space group *Pca21*. This analysis revealed that the four silver atoms are arranged in a distorted tetrahedral shape, stabilized by two ligand molecules. Unlike the mononuclear complex **106a**, the amide groups in complex **108** are deprotonated and coordinate to the silver atoms as anionic ligands, forming an overall neutral complex. Each silver atom is bonded to one NHC moiety and one deprotonated amide, with the silver-carbon bond being slightly shorter (2.07 Å) than the silver-nitrogen bond (2.10 Å). The coordination geometry is nearly linear, with carbon-silver-nitrogen bond angles between 174° and 177°. A notable feature of complex **108** is the π-π stacking interaction between the NHC moieties of the two ligands that coordinate the silver ions (Figure 18). This stacking interaction likely contributes to the stability of the complex. The formation of such a tetranuclear structure is particularly significant because, to our knowledge, while binuclear silver complexes with a carbene-silver-amidate arrangement have been described before, complex **108** is the first example of a tetranuclear complex with this specific bonding arrangement.

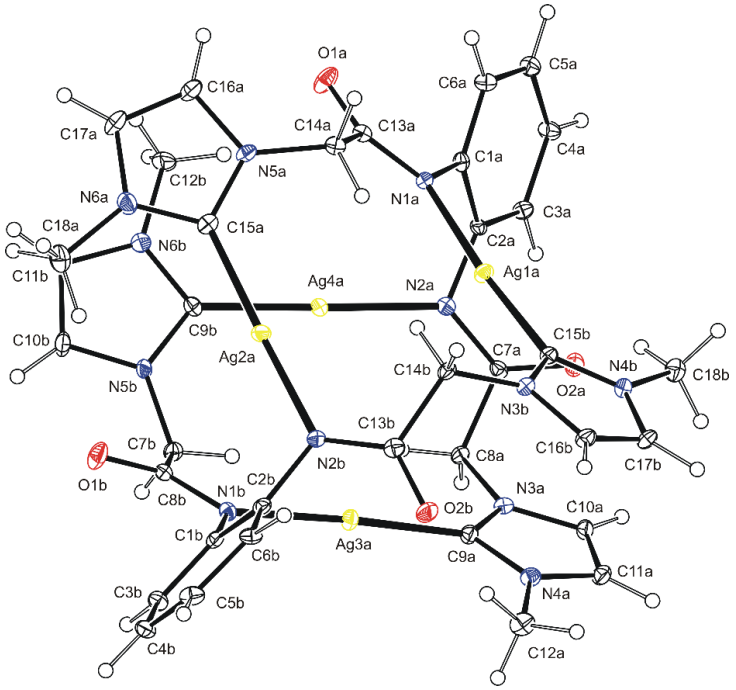

Figure 18. View on the molecule of **108** the displacement ellipsoids at 30% probability level.

With the successful synthesis of complexes **106a** and **107a** and confirmation of the desired chelating feature, the investigation of the impact of the side chain in the imidazole moiety was explored. The remaining synthesised ligand precursors were used for the silver complexation. Once again, each ligand was treated with 1.3 equivalents of silver oxide.

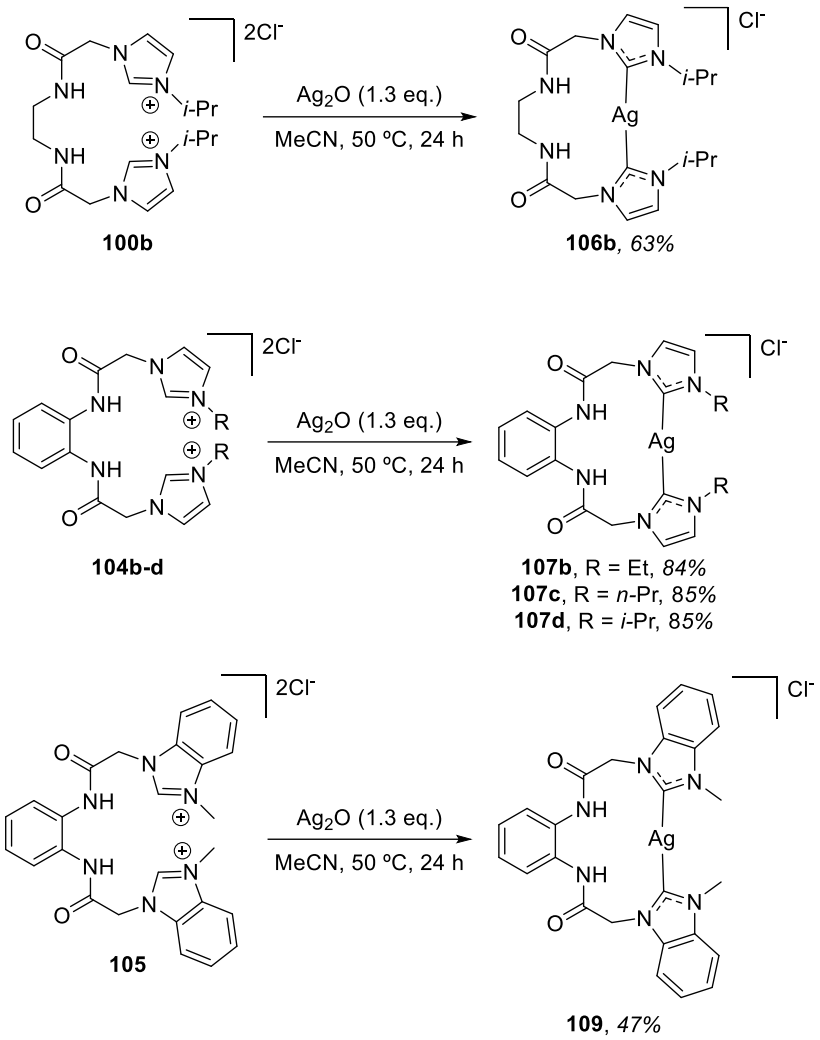

Scheme 26. Silver complexation with ligand precursor **100b**, **104b-d** and **105**.

For the ethylene backbone ligand **100b**, the desired silver complex **106b** was isolated in a lower yield of 63% when compared to the respective methyl analogue **106a**. The decrease in the yield might be attributed to the flexibility of the backbone and the steric demand of the isopropyl group, leading to the formation of non-chelate complexes, such as the dimeric version where two ligand units are coordinated to two silver cations. In the opposite direction, all the phenyl backbones with bigger such chain ligands **104c-d**, provided the desired chelate complexes **107b**, **107c** and **107d** in great yields of 84%, 85% and 85% respectively. This significant increase in yield might be attributable to two factors. Firstly, the increase of the side chain removes the possibility of forming any complex similar to the tetranuclear complex **108**

due to steric reasons. Secondly, the solubility of complexes **107b**, **107c** and **107d** is vastly superior to the methyl analogue **107a**, as can be seen in Table 1. For comparison, all three complexes **107b**, **107c** and **107d** are soluble in DCM, $CHCl_3$ and acetonitrile, which **107a** is not. This makes the purification process much simpler and more efficient. Lastly, the ligand containing two benzimidazole groups **105** likewise led to the respective chelate silver complex **109** with a moderate yield of 47%.

The structure of the synthesised complexes was ascertained by NMR and HRMS. Unfortunately, no suitable crystal was obtained for X-ray crystallography analysis.

Table 1: Solubility of the different silver complexes

Complex	Solubility									
	MeCN	MeOH	EtOH	H_2O	Et_2O	Acetone	DMSO	DMF	CH_2Cl_2	$CHCl_3$
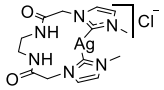	NO	YES	YES	YES (heated)	NO	NO	YES	YES	NO	NO
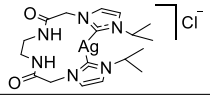	YES	NO	NO	NO	NO	NO	YES	YES	YES	YES
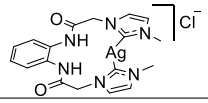	NO	NO	NO	NO	NO	NO	YES	YES	NO	NO
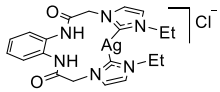	YES (heated)	YES	YES	YES (heated)	NO	NO	YES	YES	YES (poorly)	YES (poorly)
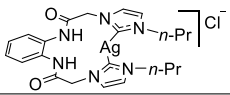	YES	YES	YES	YES (heated)	NO	NO	YES	YES	YES	YES
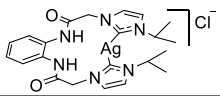	YES	NO	YES	YES (heated)	NO	NO	YES	YES	YES	YES

4.2. Transmetalation of silver to other transition metals

4.2.1. Transmetalation to palladium and nickel

As demonstrated before, NHC-silver complexes can serve as a carbene transfer group to more exotic and appealing transition metals. With that in mind, a clear demonstration of the efficiency and robustness of the method was proven when nickel **110** and palladium **111** and complexes were synthesised with great overall yields by transmetalation of the respective silver complexes. As shown in scheme 27, the synthesis of both complexes was previously reported, however with low yield for the nickel complex **110a** or unsuccessful in the case of the palladium complex **111a**.[117] As demonstrated in the introduction section, using strong bases to generate the desired carbenes can lead to unexpected results and in this instance, to avoid the sterical hindrance of the two methyl groups, the formation of complexes with abnormal carbenes **111a'** and **111a"** was preferred.

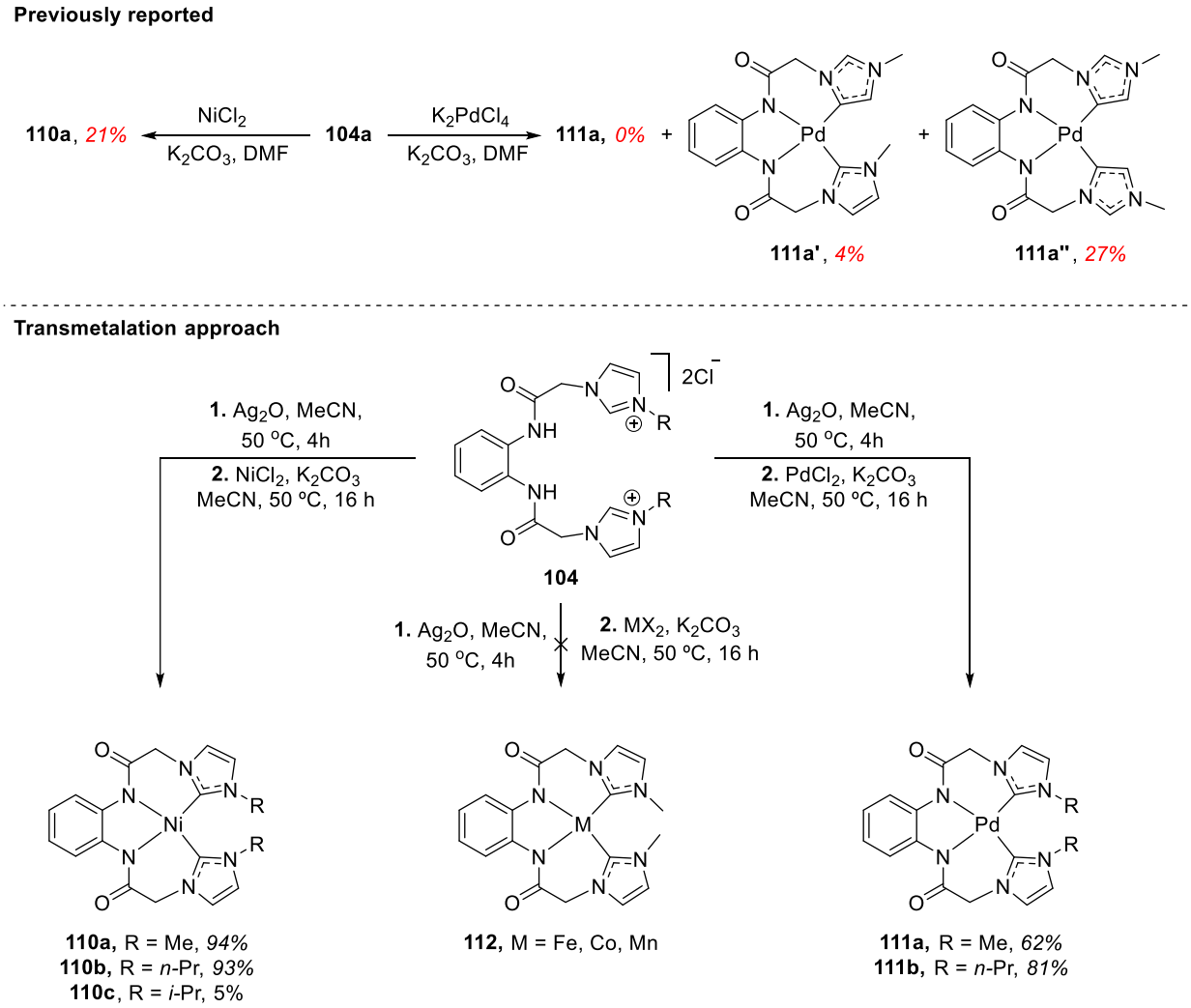

Scheme 27. Synthesis of nickel complexes **110** and palladium complex **111**.

When isolated silver complex **107a** is treated with $NiCl_2$, in the presence of a weak base, such as potassium carbonate, the desired nickel complex **110a** is isolated in 93% yield. This leads to an overall yield of 49% over two steps, due to the low yield provided by the synthesis of the silver complex **107a**. As stated in the introduction, even polymeric versions of silver complexes can lead to chelate transition metal complexes. For that reason and not satisfied with the results, a one-pot reaction was attempted, eliminating the necessity of isolating the silver complex **107a**. Treatment of the ligand precursor **104a** with Ag_2O and subsequent direct treatment of the *in situ* formed silver complex with $NiCl_2$ leads to the elimination of the isolation step and at the same time to the improved yield of the nickel complex, which is in this case isolated in 94%. The nature of the complex was confirmed, by comparing the analytical data with the complex reported previously. A good match in the ^{1}H and ^{13}C NMR spectra was observed and therefore confirmed that our method led effectively to the formation of the desired complex with both carbenes, coordinated to the metal centre in the normal fashion.

The size of the substitution can be further extended to *n*-propyl, without compromising the yield of the formation of the nickel complex **110b**, which was isolated at 93% yield. The use of the isopropyl substitution proved to be the limitation. When ligand precursor **104d** was treated with Ag_2O followed by $NiCl_2$, the reaction revealed a formation of three products, the desired nickel complex **110c** alongside the two respective nickel complexes containing abnormal carbenes (similar to palladium complex **111a'** and **111a"**). All complexes were distinguishable in ^{1}H NMR, due to the very characteristic deshielded singlet peaks of the abnormal carbenes. Nevertheless, the reaction yielded 5% of the desired nickel complex **110c** and it was possible to isolate it from the abnormal carbenes complexes using simple column chromatography.

Regarding the treatment of the ligand precursor **104a** with Ag_2O followed by $PdCl_2$, in the presence of a weak base, resulted in the formation of palladium complex **111a** in 62%. The structure of the complex was determined by ^{1}H NMR, ^{13}C NMR spectroscopy, high-resolution mass spectrometry, and X-ray crystallography. The ^{1}H NMR spectra in the aromatic region, we could identify two signals (8.31 ppm and 6.71 ppm) for the four protons of the phenyl ring as well as two signals (7.53 ppm and 7.40 ppm) for the four protons of the imidazole moieties. Further, we could observe a broad signal at 4.85 ppm, which belongs to the four protons of both the methylene bridges and one signal at 3.38 for both the methyl groups. Such a doubling of the signals suggests a symmetrical nature of the complex, which can be observed only in the case of the complex with both normal carbenes. The characteristic NMR for the abnormal carbenes complexes is known and the major difference is visible in the ^{1}H NMR spectra. No proton with

a relatively high chemical shift of 8.84 ppm, characteristic of the proton attached to the carbon in between the two nitrogens of the imidazole ring in case of abnormal coordination, is observed. Moreover, in the ^{13}C NMR spectra, a signal at 162.8 ppm is visible, which is a chemical shift typical for the carbon of the normal carbene coordinated with palladium metal. The chemical shift of the carbon of abnormal carbene coordinated with palladium metal was reported to appear at 144.8 ppm. These spectral features indicate that the complex with both normal carbenes was indeed formed. The size of the substitution can also be further extended to *n*-propyl forming palladium complex **111b** with an increase of the yield to 81%. The substantial increase in the yield can be ascribed to the improved solubility of the *n*-propyl derivative, which results in the minimisation of the losses during the isolation of the product.

Upon the synthesis of the five complexes, a remarkable feature was visible, the diastereotopic signals present in the nickel complexes **110a**, **110b** and **110c** and the palladium complex **111b**. However, such diastereotopic signals were not present in complex **111a**. In Figure 19 is depicted the diastereotopic signals in complex **110a**. The presence of diastereotopic signals suggests a presence of a chiral element within the structure, which must be of a *chiral-at-metal* origin, due to the lack of any chiral centre at the ligand precursor itself.

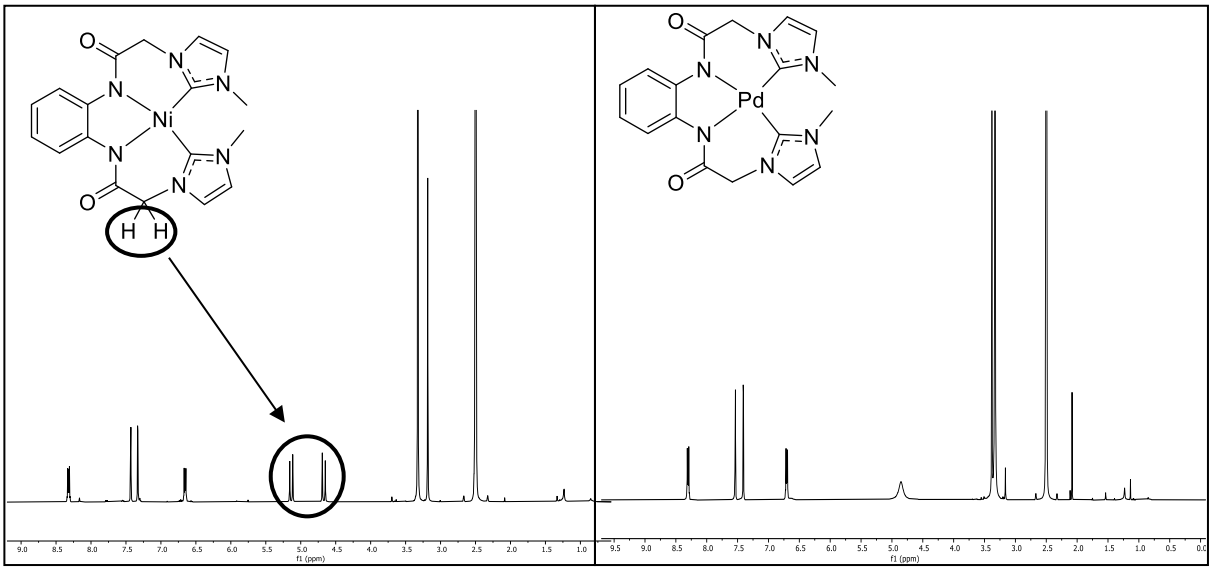

Figure 19. Diastereotopic signals visible in complex **110a** but absent in complex **111a.**

It is noteworthy that several attempts were made to synthesise other transition metal complexes, specifically those involving iron, cobalt, and manganese. Despite these efforts, none of the desired complexes were successfully detected. In certain cases, the starting silver complex was recovered, while in other attempts, only the ligand precursor was isolated.

4.2.2. Solid state studies of the conformational stability

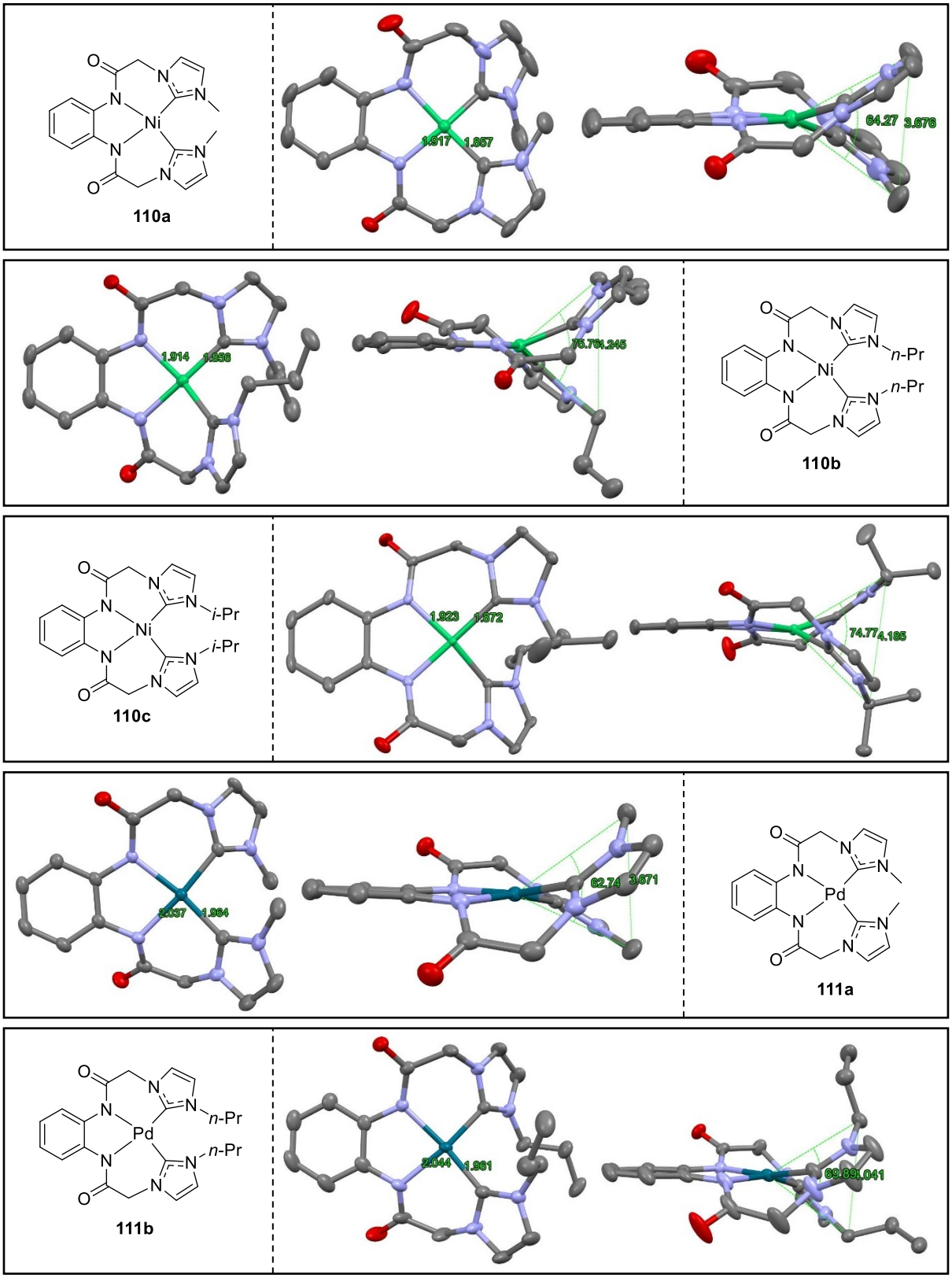

Figure 20. X-Ray crystals of all the Nickel **110** and Palladium **111** synthesised.

With great satisfaction, obtaining a single crystal suitable for X-ray crystallography from all the newly synthesised complexes **110b**, **110c**, **111a** and **111b** was possible and the result of the analysis is visible in Figure 20. The R-Xay of complex **110a** was retrieved from the available article.[117] By analysing and comparing all the respective crystal structures, some conclusions can be taken.

The bond length for NHC-Ni(II) is 1.857 Å for complex **110a**, 1.856 Å for complex **110b** and 1.872 Å for complex **110c**. The bond length NHC-Ni (II) is therefore very similar for the three complexes, meaning the side chain of the NHC does not interfere with its ability to coordinate to the metal centre. These values are in line with the reported literature for NHC-Ni(II) bonds.[118] On the other side of the complexes, the length of the amideNi(II) bond is also very similar for all three complexes, with bond lengths of 1.917 Å, 1.914 Å and 1.923 Å, respectively. With regards to the palladium complexes, the NHC-Pd (II) bond length is 1.964 Å for complex **111a** and 1.961 Å for complex **111b**. The amide bond N-Pd (II) length is 2.037 Å and 2.044 Å, respectively. The bond lengths of NHC-Pd (II) are also in accordance with the literature.[119] When comparing the bond length of complexes is possible to establish a difference of 0.1 Å from the palladium complexes to the nickel complexes. Since the palladium complexes are larger, the interference and hindrance of the side chain may not be so expressive, leading to lower configurational stability of the enantiomers. This goes along with our NMR observations for palladium and nickel complexes in solution, described above (Figure 18).

Another point that can explain the increased stability of the complexes with bigger side chains, such as propyl or isopropyl, is the distortion angle. The distortion angle for complexes nickel **110a**, with smaller methyl groups, is 64°. It is already quite a distorted complex, considering that the complex was hypothesised to be planar. The palladium complex **111a**, also with methyl groups, presents a distortion angle of 62°. A value very similar to the nickel complex. On the other hand, the distortion angles of complexes bearing the propyl group **110b** and **111b** and isopropyl group **110c** are 76°, 75° and 70°, respectively. There is more than a 10° increase in the nickel complexes from methyl to propyl and isopropyl ligand, suggesting that the steric bulk can have an effect on the configurational properties, including stability.

4.2.3. NMR studies of conformational stability

The diastereotopic nature of the methylene protons allowed us to investigate the conformational stability of the helicity in solution. At room temperature, the ^{1}H NMR of the diastereotopic signal from the methylene bridge of nickel complex **110a** appeared as a doublet of doublets. Yet, the same signal for the palladium complex **111a** appeared as a broad singlet. This suggests that at room temperature the dynamic switch of the two enantiomeric forms is significantly pronounced for the palladium complex. This is rationalised by the structural features observed in the solid state, namely the length of the metal-carbene and metal-amide bonds, and the subsequent opening of the helix, which is more pronounced in the palladium case. The incremental heating of the solution of nickel complex **110a** led to a gradual merging of the diastereotopic signals to the point of coalescence observed at 125 °C, which corresponds to a rate constant of $k = 310.8\ s^{-1}$ and the Gibbs free energy for nickel complex **110a** is 58.6 9 kJ/mol^{-1}.

Our synthetic method allowed us to prepare the complexes with a sterically more demanding substitution on the terminal imidazole nitrogen. The confirmation of the nickel complex **110b**, having propyl substituents, was locked even at temperatures elevated to 130 °C with no indication of a conformational switch. The signals of the diastereotopic protons remained a clear doublet-of-doublets. As expected, the same behaviour was observed for isopropyl-bearing nickel complex **110c**. The increase in conformational stability was observed for palladium complex **111b**, having terminal propyl substitution. At room temperature, we identified a doublet-of-doublets, suggesting a slowdown of the dynamic process, compared to complex **110a.** However, even the slide elevation of the temperature to 45 °C led to a coalescence of the diastereotopic signals, represented in Figure 21.

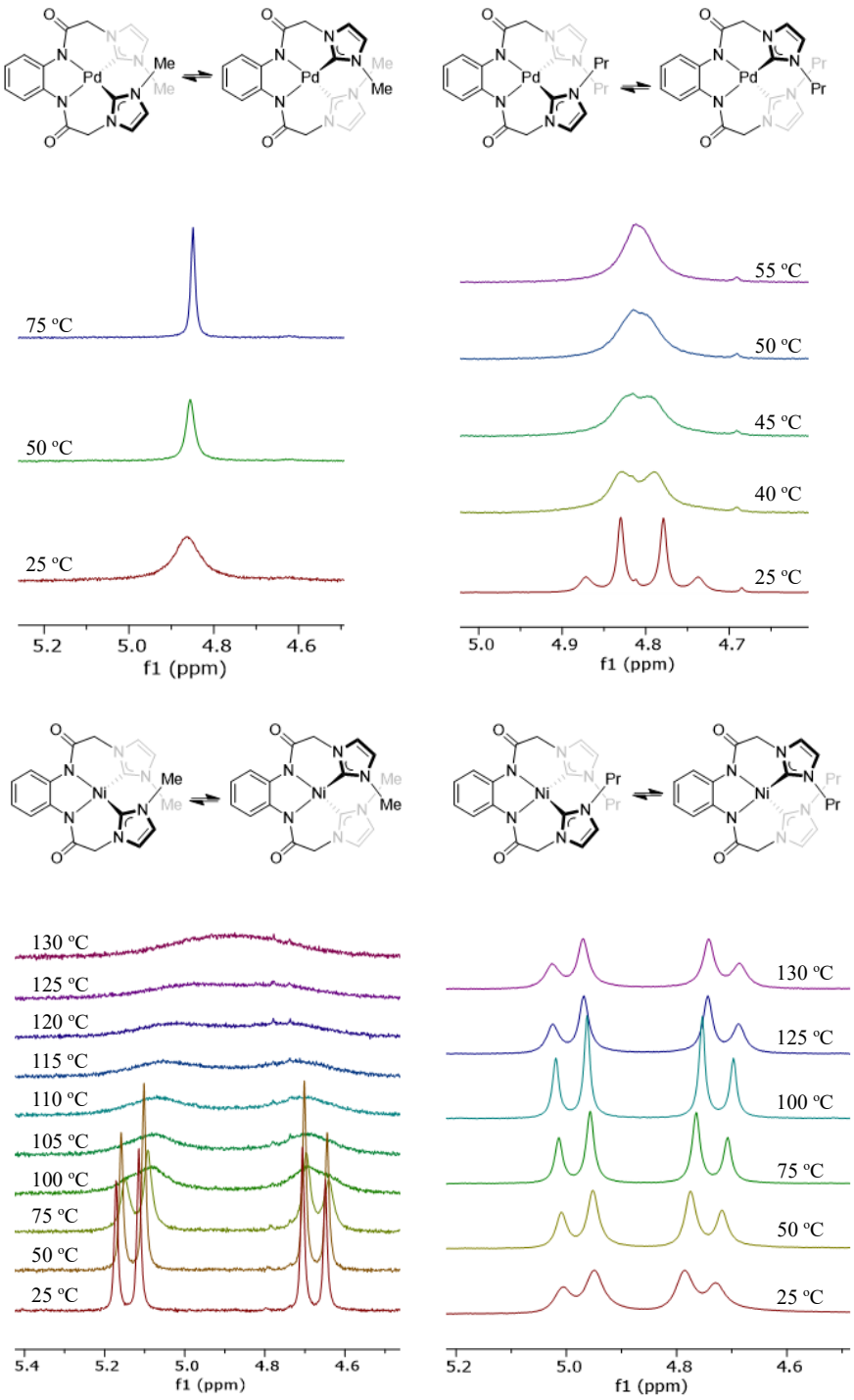

Figure 21. ^{1}H NMR coalescence point.

We hypothesised, that the conformational flip can happen via two distinct pathways. In pathway I, depicted in red, decomplexation of the carbene is followed by a loss of the chiral information and subsequent re-complexation of the ligand to the metal. Alternatively, pathway II, depicted in blue, consists of a simple interconversion without a decomplexation. To gain some insight into the mechanism of the flip, we carried out a trapping experiment, where nickel complex **110a** was heated to 130 °C in the presence of sulphur. Sulphur can promptly react with

free carbenes, and in the case of the decomplexation pathway I, a formation of the imidazole-2-thione should be observed.[120] However, the formation of the thione was not detected, which suggests that the conformational flip does not occur with decomplexation. This was further supported by DFT calculation. We evaluated the Gibbs free energy of the complex in the ground state and the possible transition state of the conformational interconversion. The calculation revealed that the calculated activation energy is close to the observed energy in the case of the nickel complex **110a**. The Gibbs free energy for palladium complex **111a** is about 15.9 kJ/mol^{-1} lower. Furthermore, the DFT studies also propose a saddle transition state as shown in Figure 22. Such a transition state makes the side chains of the imidazole ring in very close proximity to each other. This aligns with the findings from the NMR studies where the bigger propyl group was conformationally more stable than the methyl counterpart. These results strongly support the alternative pathway II, where the chiral switch takes place without the decomplexation of the carbene ligands.

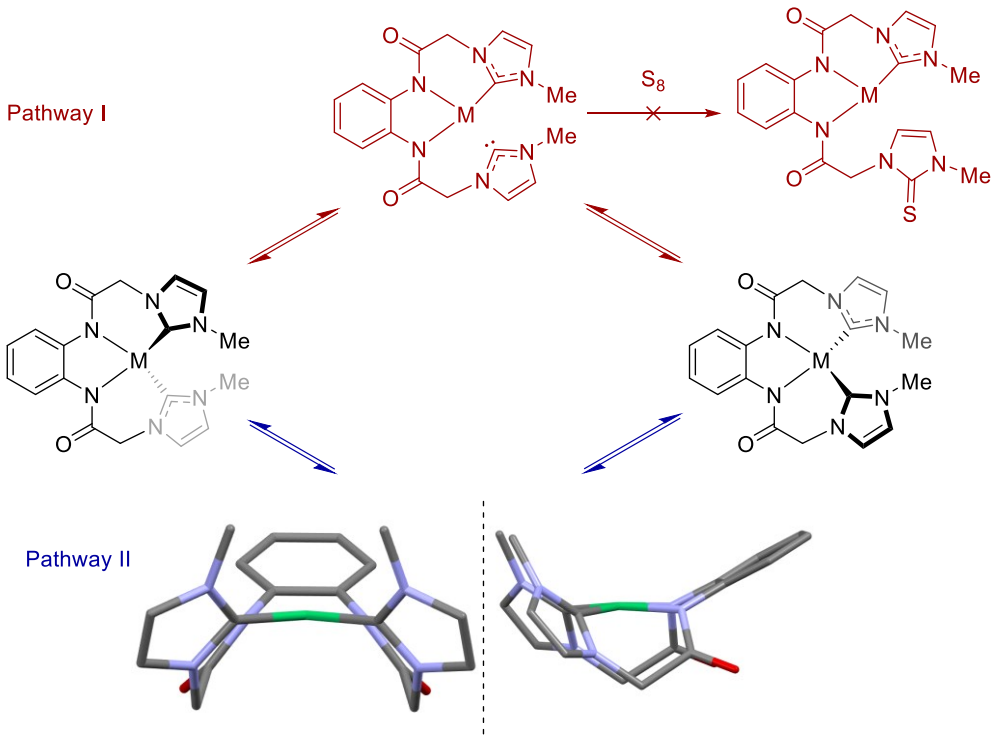

Figure 22. Possible pathways for the conformational switch.

4.2.4. Application of the synthesised palladium and nickel complexes

We aimed to find applications for the synthesised nickel complexes, either in classical couplings or, preferably, in reactions that could be further developed into asymmetric processes. Our initial focus was to explore the reactivity before proceeding to the enantiopure synthesis of the complex. One of the first applications was the use of the complex in the Suzuki cross-coupling reaction. In all the experiments de complex **110a** was always pre-treated with a reducing agent such as $NaBH_4$ and Et_3SIH in order to form the reactive nickel species. After stirring for 30 minutes the aryl halide **114** was added alongside the boronic acid **115**. Different aryl halides were used, such as bromobenzene and 4-bromoanisole, as well as boronic acids, such as 4-methoxyphenylboronic acid and 4-fluorophenylboronic acid. The idea of the fluor boronic acid was to help the control of the reaction by ^{19}F NMR. Complex **110c** was also tested in the reaction due to the higher solubility when compared to complex **110a**. However, no traces of the desired coupled compound **116** were ever detected.

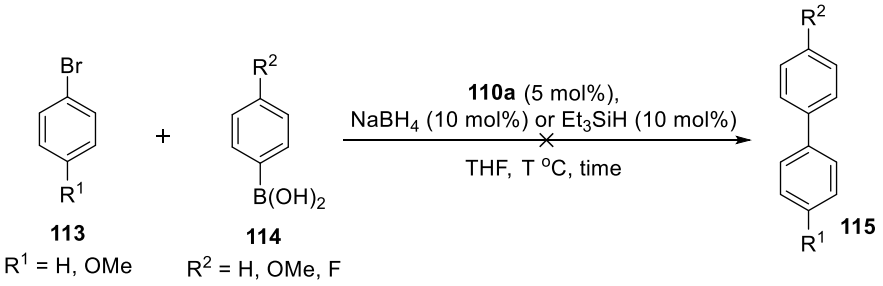

Scheme 28. Suzuki cross-coupling reaction attempted with complex **110a.**

Another cross-coupling reaction tested was the Kumada cross-coupling. With the Kumada cross-coupling we hypothesised that the Grignard reagent could be used as a reducing agent.[121] For that reason, the nickel complex was pre-treated with Grignard reagent **116** in order to generate the reactive species. Afterwards, the aryl bromide **113** was added to the reaction mixture. Once again, no traces of the desired final product where observed.

Scheme 29. Kumada cross-coupling reaction attempted with complex 110a.

Unsatisfied with the results, a new experiment was performed using *n*-butyllithium, a cross-coupling reaction recently reported by Ben Feringa.[122] The concept was that, once again, *n*-butyllithium would be used in excess in order to reduce the metal. However, in this case, we hypothesised that the lithium cation could interact with the amide bond, liberating the metal centre. Surprisingly, the reaction formed the desired compound **119** in a quantitative yield. Delighted with these results, the next logical step was to test the reaction without the presence of the catalyst. Once again, to our surprise, the desired compound was isolated. The proposed mechanism for this reaction is that first, a lithium/halogen exchange forms the phenyllithium **117** and bromobutane intermediates. Since the lithium species formed is nucleophilic, a nucleophilic attack will take place forming the desired compound **118**, as shown in Scheme 30.[123] It is worth mentioning that the solvent, tetrahydrofuran, plays a crucial role in the reaction. The reaction does not take place if toluene is used instead.

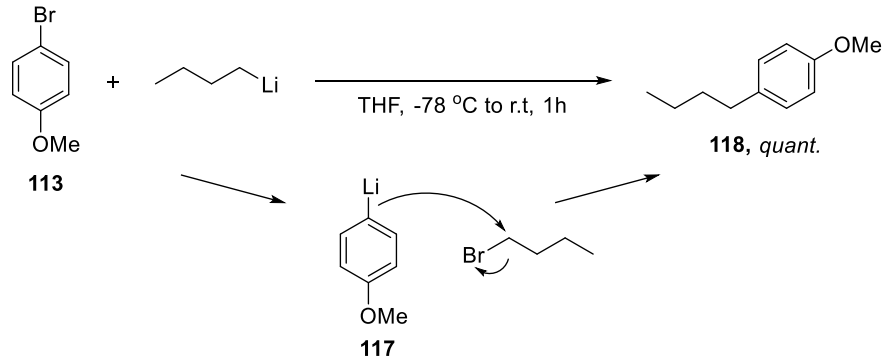

Scheme 30. Reaction of 4-bromoanisole and *n*-butyllithium.

Unfortunately, when the solvent was changed to toluene and in the presence of complex **110a** the reaction did not occur. Furthermore, when *sec*-BuLi and *tert*-BuLi were used, no reaction also occurred, rendering the complex unreactive.

Lastly, the nickel complex was used as a Lewis acid in a Michael addition reaction between dimethyl malonate **119** and diethyl maleate **120**. When the reaction was carried out without any catalyst in neat conditions, no reaction happened. When the catalyst was used, the reaction

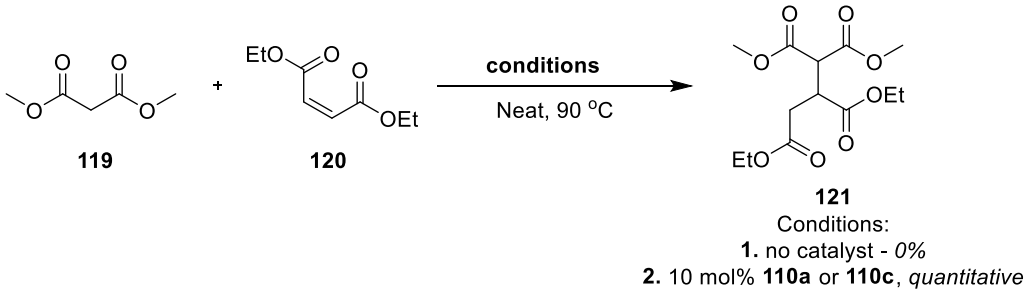

Scheme 31. Michael addition catalysed by complex **110**.

performed gave the desired compound in quantitative yield. Furthermore, the catalyst was recovered at the end of the reaction, so there is the possibility for reusability.

To take the Michael addition a step further, we envisioned making a chiral nickel complex to accomplish an asymmetrical Michael addition. We initially attempted to separate the enantiomers of the helical complex **110a** using chiral HPLC. However, our attempts failed, as no suitable system for the separation was identified. We hypothesised that adding a chiral centre into the ligand structure would lead to the formation of diastereoisomers, which could be separable by simple chromatography. This approach would also allow us to evaluate the cooperative effect of the two chiral aspects – the helicity and the "classical" chirality of the ligand. We envisioned, that an amino acid could be incorporated into the ligands previously synthesised. In scheme 32, the retrosynthesis of such ligand is depicted. The necessary imidazolium salt precursor can be achieved by reacting imidazole **122** with an appropriate electrophile, such as 1-chloroproparne. On ligand **122**, the imidazole ring can be assembled *via* a multicomponent reaction between the amine **123**, glyoxal, formaldehyde and an ammonium source.[124] Amine **123** could be accessed between the coupling of *o*-phenylenediamine **101** and an amino acid. In this case, alanine **124a** and valine **124b** seemed the suitable choices.

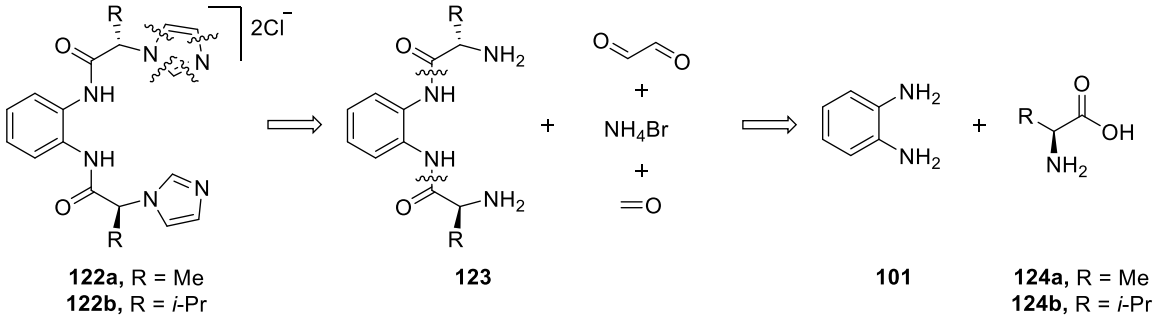

Scheme 32. Retrosynthesis of ligands containing amino acids.

The synthesis of the chiral ligand precursors began with the reaction of *o*-phenylenediamine **101** with the Boc-L-valine **124b**. The peptide bond was formed with the assistance of N,N'-dicyclohexylcarbodiimide (DCC). The Boc protecting group could be cleaved straight away with the use of acetyl chloride in methanol, a method commonly used for the controlled release of hydrochloric acid. The respective ammonium salt **125** was achieved in a quantitative fashion, without the need for purification. The multicomponent reaction to assemble the desired imidazole ring proved to be problematic and the desired compound was never achieved. The outcome of the attempted reactions was normally a complex mixture of products.

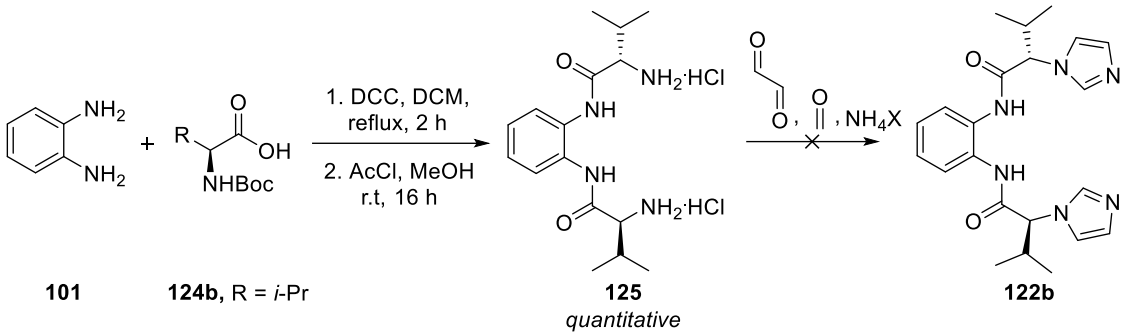

Scheme 33. Attempted synthesis of the chiral ligand **122b**.

Unpleased with the results, a new strategy was planned. In order to avoid constructing the imidazole ring in the later stages of the synthesis, the imidazole ring synthesis took place as the first reaction, leading to the formation of imidazole **126a** and **126b** in a quantitative manner. The resulting imidazole amino acids **126a** and **126b** were highly hygroscopic and needed to be stored in the oven. Since the next step was the amide bond formation, any presence of water could render the reaction futile. The coupling reaction between the carboxylic acids **126** and *o*-phenylenediamine **101** proved to be more challenging than expected. Initially, the same conditions adopted in the previous reaction were attempted (Table 2, Entry 1). Starting materials were isolated. Next, different solvents with higher boiling points as well as the addition of additives to facilitate the reaction were used (Table 2, Entry 2-8). The DCC/DMAP system was also replaced by EDC/HOBt (Table 2, Entry 9), however the outcome of the reaction remained unchanged. From this point, a new approach was attempted by the formation of the respective acyl chloride. Thionyl chloride (Table 2, Entry 10) proved to be unreactive. On the other hand, oxalyl chloride (Table 2, Entry 11) led to the decomposition of the starting material. The reactant was then switched to phosphorous pentachloride. The usage of PCl_5 generated the desired acyl chloride, since with crude ^{13}C NMR was visible the disappearance of the peak corresponding to the carboxylic acid. Nevertheless, the reaction led to the formation of a complex mixture of products that proved to be impossible to separate. We hypothesised that the decomposition of the product could be taking place due to the acidity of the mixture. Therefore, DIPEA or TEA were added as additives (Table 2, Entries 11 and 12), however, the opposite effect was observed with the decomposition of the starting material.

Table 2. Reaction conditions attempted to couple **126b** and **101.**

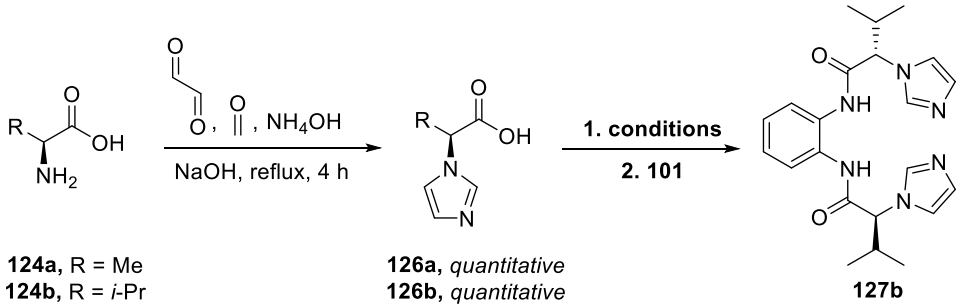

Entry	Reactant	Additive	Solvent	Conditions	Outcome
1	DCC	-	DCM	Reflux, 16 h	S.M recovery
2	DCC	-	$CHCl_3$	Reflux, 16 h	S.M recovery
3	DCC	-	DMSO	100 ºC, 16 h	S.M recovery
4	DCC	DMAP cat.	DCM	Reflux, 16 h	S.M recovery
5	DCC	DMAP	DCM	Reflux, 16 h	S.M recovery
6	DCC	DMAP	MeCN	Reflux, 16 h	S.M recovery
7	DCC	DMAP	DMSO	100 ºC, 16 h	S.M recovery
8	DCC	DMAP	DMF	70 ºC, 16 h	Purification problem due to complex mixture.
9	EDC	HOBt	DCM	Reflux, 16 h	S.M recovery
10	Thionyl chloride		DCE	Reflux, 16 h	S.M recovery
11	Oxalyl chloride		MeCN	Reflux, 16 h	Decomposition
12	PCl_5	-	DCM	Reflux, 16 h	Purification problem due to complex mixture.
13	PCl_5	-	$CHCl_3$	Reflux, 16 h	Complex mixture
14	PCl_5	DIPEA	$CHCl_3$	Reflux, 16 h	Decomposition
15	PCl5	TEA	$CHCl_3$	Reflux, 16 h	Decomposition

4.3. Antimicrobial properties of complexes 106a and 107a

With the silver complexes in hand, we focused on their antimicrobial properties in collaboration with Professor Tomasz M. Karpiński from the Poznań University of Medical Sciences in Poland. Complexes 106a and 107a were tested against Gram-positive and Gram-negative bacteria, and fungi (Table 3). Minimal inhibitory concentrations (MICs) were determined for complexes **106a** and **107a**, as well as their ligand precursors **100a** and **104a**.

Complex **106a** inhibited the growth of Gram-positive bacteria, with MIC values of 2-4 μg/mL for *Staphylococcus aureus* and 1-2 μg/mL for *Staphylococcus epidermis*. It also inhibited Gram-negative bacteria, with MIC values of 16 μg/mL for Escherichia coli, 8 μg/mL for *Klebsiella pneumoniae*, and 8 μg/mL for *Pseudomonas aeruginosa*. For fungi, MIC values were 8 μg/mL for *Candida albicans* and *Candida glabrata*, and 16 μg/mL for *Rhodotorula rubra*.

Complex **107a** showed similar results, though with slightly higher MIC values, inhibiting *Staphylococcus aureus* and *Staphylococcus epidermis* with MIC values of 8-16 μg/mL and 2 μg/mL, respectively. For Gram-negative bacteria, MIC values were 31 μg/mL for *Escherichia coli*, 16 μg/mL for *Klebsiella pneumoniae*, and 16-31 μg/mL for *Pseudomonas aeruginosa*. Antifungal effects against *Candida albicans* and *Candida glabrata* were seen at 16 μg/mL, and against *Rhodotorula rubra* at 16-32 μg/mL.

Ligand precursors **100a** and **104a** exhibited negligible antimicrobial effects, with MIC values ranging from 1000 to 2000 μg/mL, indicating that the antimicrobial activity derives from the silver.

The comparison of the results with the reported literature must be considered with precaution since different strains of bacteria could have been employed leading to different MIC values. However, a comparison with the outcome gathered by Silvia Figueiredo Costa and co-workers[125], where several strains of gram-positive and gram-negative bacteria were employed against silver nitrate, and the work by Kashif Raees and co-workers[126], in which several strains of gram-positive and gram-negative bacteria and fungi were employed against silver nanoparticles (Ag-NPs) can help understand the results. Overall, complex **106a** performed better than **107a** and the reason for this difference might be due to the overall lower solubility of complex 107a. When compared to silver nitrate, both complexes **106a** and **107a** seem to have better antimicrobial properties against gram-positive bacteria, with lower MIC values. On the other hand, the complexes seem to be worse against gram-negative bacteria. When

compared to the results obtained with the silver nanoparticles, then complexes **106a** and **107a** are much stronger antimicrobials and antifungals with MIC values ranging from two times to thirty times lower. The most notorious difference is against fungi species, where the silver nanoparticles performed quite poorly.[125] The overall good results obtained with complexes 106a and 107a mean that both complexes release silver cation necessary for the antimicrobial and antifungal activity. The incapability of the silver nanoparticles to generate the silver cation might be a reason for the higher MIC values. Another valid reason for the good activity of the complexes might reside in the importance of the counter anion. As stated, and presented in **Chapter 2.4**, the presence of chloride anions tends to lower the MIC value and both complexes have chlorine as the counterion.

Table 3. Evaluation of antimicrobial properties of complexes **106a** and **107a**.

Entry	**Organism**		**106a (μg/mL)**	**107a (μg/mL)**	**$AgNO_3$ (μg/mL)**	**AgNPs (μg/mL)**
1	G. positive	*Staphylococcus aureus*	2–4	8–16	13.5	31
2		*Staphylococcus epidermis*	1–2	2	6.7	-
3	G. negative	*Escherichia coli*	16	31	-	31
4		*Klebsiella pneumoniae*	8	16	6.7	62
5		*Pseudomonas aeruginosa*	8	16–31	1.6	62
6	Fungi	*Candida albicans*	8	16	-	62
7		*Candida glabrata*	8	16	-	250
8		*Rhodotorula rubra*	16	16–31	-	-

4.4. Catalysts in A^3 coupling reaction

We evaluated complex **107a** in the A3 coupling reaction to optimize the reaction conditions using cyclohexanecarboxaldehyde (**75**), pyrrolidine (**128**), and phenylacetylene (**65**) as a model system. We hypothesised that the transformation could proceed under solvent-free conditions. Initially, we performed the reaction with 1 mol% of the catalyst at 80 °C. To our delight, we observed full consumption of the starting reactants, and the desired product was isolated with an impressive yield of 89% (Table 4, Entry 1).

Encouraged by the high yield at 1 mol% catalyst, we decided to reduce the catalyst loading to 0.5 mol%. At 80 °C, after 5 hours, we again observed full consumption of the starting materials, and the product yield was slightly lower but still high at 85% (Table 4, Entry 2). This result indicated that the reaction could proceed effectively with half the amount of catalyst, thus making the process more cost-effective.

Next, we aimed to investigate the effects of reaction temperature and catalyst loading further. We chose two directions for this investigation: lowering the reaction temperature while keeping the catalyst load at 0.5 mol% and reducing the catalyst load further to 0.1 mol%. When the reaction was conducted at 60 °C for 5 hours, we found that 14% of the aldehyde remained unreacted (Table 4, Entry 3), identifiable by the characteristic peak at 9.62 ppm. Extending the reaction time to 36 hours led to nearly complete conversion, with only about 3% of the aldehyde remaining, and the desired product was isolated in 88% yield (Table 4, Entry 4). Further reducing the reaction temperature to 40 °C and extending the reaction time to 36 hours resulted in only 4% of the aldehyde remaining, with the product yield being 87% (Table 4, Entry 5). At 25 °C, after 36 hours, 12% of the starting aldehyde was still present in the crude mixture, and the desired product yield dropped to 72% (Table 4, Entry 6). These findings indicated that while lower temperatures can be used, they require longer reaction times and may result in slightly lower yields. To examine the effects of using an even lower catalyst load, we conducted the reaction with 0.1 mol% of the catalyst at 80 °C for 36 hours. Under these conditions, 2% of the aldehyde remained unreacted, and the product yield was 74% (Table 4, Entry 7). This showed that while it is possible to significantly reduce the catalyst load, it necessitates a longer reaction time to achieve high conversion rates without severely compromising the yield.

Overall, the data suggest that the reaction reaches completion with 1 mol% of the catalyst in just 5 hours. Lowering the catalyst load to 0.5 mol% does not compromise the catalyst's effectiveness, maintaining high yields with a similar reaction time. Reducing the catalyst load

to 0.1 mol% requires extending the reaction time to 36 hours to maintain high yields. Moreover, with 0.5 mol% of the catalyst, the reaction can be effectively conducted at room temperature without significant loss of efficiency, demonstrating the robustness and versatility of the catalyst under various conditions.

Without the catalyst, the reaction does not proceed, as evidenced by only residual traces of the product being detected after 36 hours at 80 °C (Table 4, Entry 8). This underscores the crucial role of the catalyst in facilitating the A3 coupling reaction and highlights the potential for optimizing reaction conditions to maximize efficiency and yield in a practical and cost-effective manner.

Table 4. Optimization table A^3 coupling reaction.

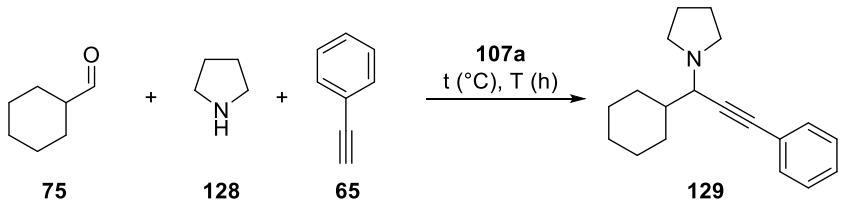

75 128 65 129

Entry	Catalyst load (mol%)	Temperature (°C)	Time (h)	Ratio 75:129	Isolated yield (%)
1	1	80	5	>1:99	89
2	0.5	80	5	>1:99	85
3	0.5	60	5	14:86	n.d.
4	0.5	60	36	3:97	88
5	0.5	40	36	4:96	87
6	0.5	25	36	3:97	72
7	0.1	80	36	2:98	74
8	None	80	36	n.d	<5%

With the optimised conditions in hand, we set to explore the scope of the transformation catalysed by complex **107a** (Figure 23). Reactions were carried out with 0.5 mol% of the catalyst at 80°C for 5 hours. Since the A^3 coupling reactions comprehend the use of three different starting materials, we first studied the use of different aldehydes. When benzaldehyde was used, the reaction proceeded to completion, yielding 87% of the propargyl amine **130**. The result was quite surprising since it is reported in the literature that some NHC-silver(I) complexes lead to poor yields with benzaldehyde. When using benzaldehydes containing electron-withdrawing groups, such as 2-bromobenzaldehyde **131** and 2,5-dichlorobenzaldehyde **132**, the yield lowered to moderate yields of 57% and 54%, respectively. In the opposite direction, when an electron-donating was present such as *p*-anisaldehyde, the reaction led to the formation of propargyl amine **133** with an excellent yield of 94%. To no surprise, the use of more reactive aliphatic aldehydes, such as pivaldehyde **134**, isobutyraldehyde **135**, and hexanal **136** led to excellent yields of 89%, 99% and 93%, respectively.

The study then proceeded to the use of different amines. The use of the cyclic amines piperidine and morpholine proved to be suitable leading to the formation of the desired propargyl amines **137** and **138** with overall high yields of 85% and 77%, respectively. The cyclic amine azepane was also suitable for the reaction even when reacted with benzaldehyde resulting in the propargyl amine **139** with 90% yield. At this point, a limitation of the method was encountered with the use of either acyclic secondary amines or primary amines. Surprisingly, when diisopropylamine and dibutylamine were used, the reaction did not progress as expected and, instead of the propargyl amines **140** and **141**, the starting material was isolated. Similarly, the outcome of the experiments using the primary amines, aniline and isobutylamine, led to an identical result, the isolation of the starting materials. However, concerning the primary amines, the explanation for the negative results can lie in the fact of catalyst poison by the primary amines rendering the catalyst unreactive. Furthermore, with primary amines, the reaction does not form the iminium cation leading to a less reactive intermediate.

Lastly, the alkyne moiety was explored. The change from phenylacetylene to 1-chloro-4-ethynylbenzene, containing an electron-withdrawing group, led to the formation of the propargyl amine **144** with a good yield of 71%. In a reverse way, the use of an electron-donating group, such as 4-ethynylanisole led to the formation of propargyl amine **145** with a great yield of 86%. The use of a linear alkyne was also attempted with 1-heptyne, leading to the formation of the respective product **146** with a moderate yield of 50%. Unfortunately, when alkynes

containing functional groups were used the reaction did not proceed as expected leading to the formation of complex mixtures or isolation of starting materials. This was the case when using trimethylsilylacetylene, propargyl alcohol and propargyl bromide. Regarding trimethylsilylacetylene the reason for the complex mixture can be hypothesised with some side reaction of silver and the silyl group, since the use of silver to cleave silyl groups has been previously reported.[127] The reaction of propargyl alcohol and propargyl bromide resulted in a complex mixture. The alcohol moiety can act as a nucleophile and react with the formed

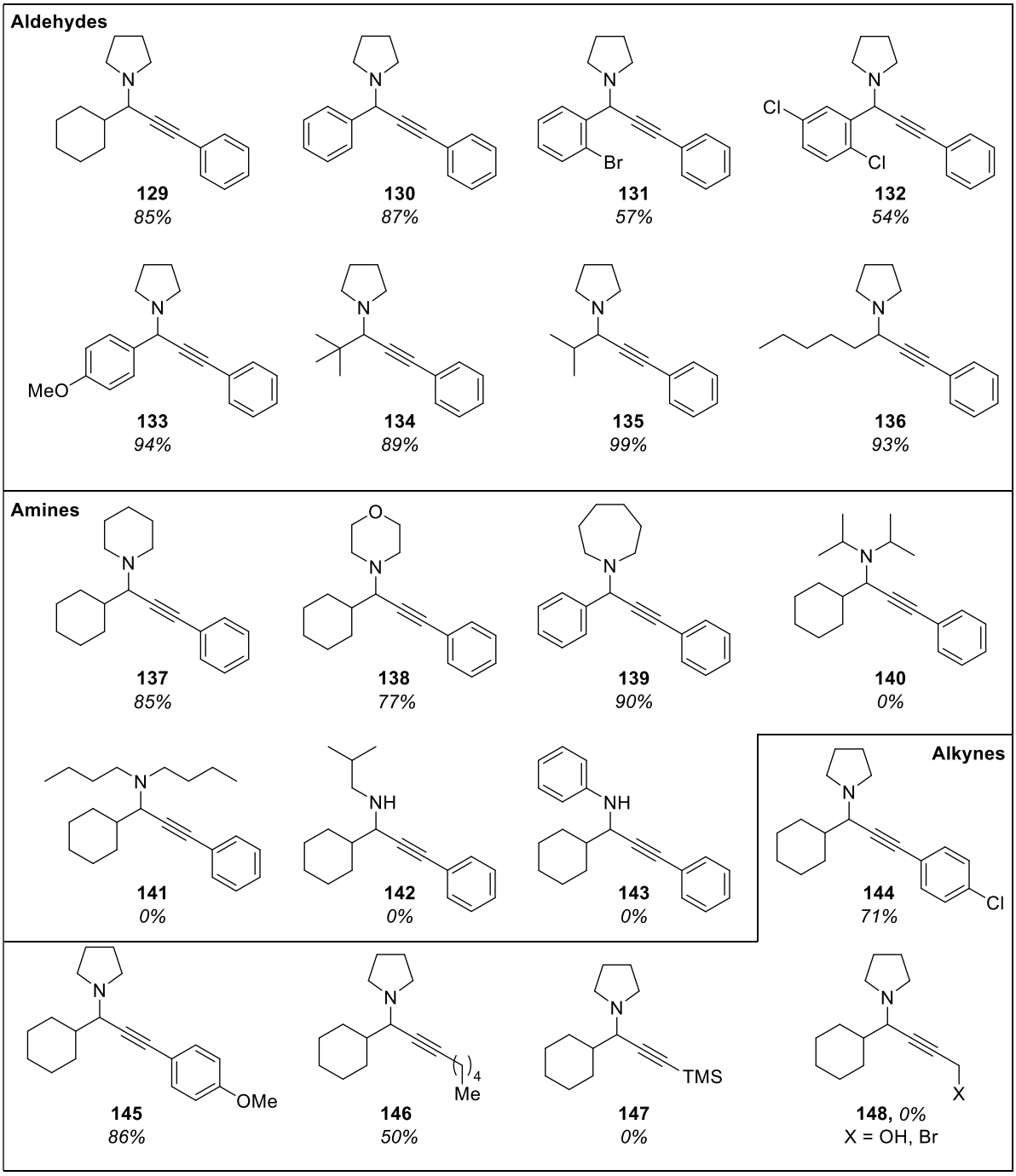

Figure 23. A[3] coupling reaction scope.

propargyl amine since the silver can activate the internal alkyne. The bromine group in the propargyl bromide may decrease the reactive of the alkyne moiety rendering the incapability to form the necessary silver alkynide for the reaction to proceed.

In conclusion, complex **107a** showed remarkable activity in the multicomponent A^3 coupling. Overall, the reaction proved to be suitable for all types of aldehydes, even the less reactive ones. Regarding the amine moiety, only secondary cyclic amines proved to be suitable. Alkynes containing functional groups that decrease the overall reactivity of the alkyne moiety and/or that can react with silver are also unsuitable for this application.

4.5. Catalysts in KA^2 coupling reaction

The delightful results obtained with the A^3 coupling reaction led us also to attempt the use of the silver complexes in the KA^2 coupling reaction. KA^2 coupling stands for the coupling of ketone, amine, and alkyne, hence very closely related to the A^3 coupling reaction, yet more challenging due to the less reactive nature of ketones over aldehydes. First, our attention was focused on the optimisation of the reaction conditions, which is summarised in Table 5. For the KA^2 coupling reaction, instead of the previously used silver complex **107a**, silver complex **107c** was used instead. The reason for this change is tied to the more efficient and better isolation of complex, leading to a synthesis with higher yield. We started the optimisation procedure with cyclohexanone, pyrrolidine, and phenylacetylene, using 5 mol% of the catalyst under neat conditions at 110 °C (Table 5, Entry 1). To our satisfaction, the reaction was finished in 4 hours, yielding 87% of the desired product **150**. To make the protocol more ecologically and economically friendly, we further investigated if decreasing the reaction temperature and catalytic loading was possible. When the reaction was carried at 80 °C it was necessary to extend the reaction time to 16 hours for full consumption of the starting material and a drop of yield was observed (Table 5, Entry 2). A further decrease to 50°C leads to full consumption of the starting material after 72 hours, being the product isolated in 69% yield (Table 5, Entry 3). The reaction can also be carried out at room temperature, however, there is the necessity to extend the time of the reaction to 72 hours and with a decrease of the yield to 64% (Table 5, Entry 4). An experiment was conducted to attempt increasing the yield at room temperature, by adding ethyl acetate to the reaction mixture (Table 5, Entry 5). However, the opposite effect was observed, with the decrease of the overall yield to 32%. The drop in the yield and the large extension of reaction time led us to perform further experiments at 110 °C.

Regarding the catalyst loading, reducing it to 2.5 mol% did not impact the outcome, with the product being isolated with a 90% yield (Table 5, Entry 6). Further decrease of the catalytic loading to 1 mol% resulted in the drop of the yield to 71% (entry 7) and using 0.1 mol% led to the formation of the product in 51% (Table 5, Entry 8). For comparison, we evaluated other catalysts as well. Complex **107a**, previously used in the A^3 coupling, showed a comparable activity as complex **107c** (Table 5, Entry 9). The use of the isopropyl-containing complex **107d** resulted in a decrease in the reaction yield to 71% (Table 5, Entry 10). The use of commercially available silver chloride only gave 34% of the desired compound (Table 5, Entry 11), which emphasises the highly reactive nature of complex **107a** and complex **107c**. As expected, when

no catalyst is used, the reaction does not take place, leading to the isolation of all the starting materials (Table 5, Entry 12).

Table 5. Optimization table KA^2 coupling reaction.

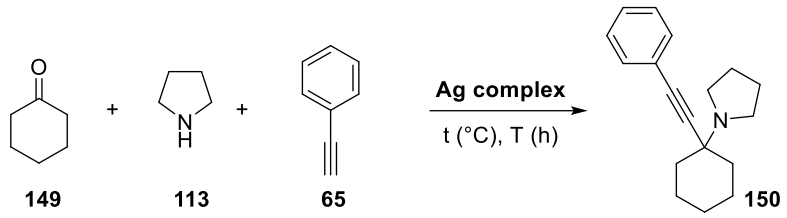

Entry	Catalyst used	Catalyst load (mol%)	Temperature (°C)	Time (h)	Solvent	Isolated yield (%)
1	**107c**	5	110	4	Neat	87
2	**107c**	5	80	16	Neat	71
3	**107c**	5	50	72	Neat	67
4	**107c**	5	r.t	72	Neat	64
5	**107c**	5	r.t	72	EtOAc	32
6	**107c**	2.5	110	4	Neat	90
7	**107c**	1	110	4	Neat	71
8	**107c**	0.1	110	4	Neat	51
9	**107a**	2.5	110	4	Neat	90
10	**107d**	2.5	110	4	Neat	71
11	AgCl	2.5	110	4	Neat	34
12	none	-	110	4	Neat	0

Further, we investigated the scope of the KA^2 coupling reaction, catalysed by complex **107c**. First, we explored various alkynes, while keeping cyclohexanone as the ketone and pyrrolidine as the secondary amine. When electron-rich 4-methoxyacetylene was applied, the reaction yielded corresponding propargylic amine **151** with an excellent 94% yield. Applying electron-

deficient 4-trifluorophenylacetylene led to the formation of amine **152** in 82% yield. Reaction with structurally more complex 1-ethynyl-2-methoxynaphthalene resulted in a drop in yield of the desired amine **153** to 53%. The loss of yield may be explained due to sterical reasons surrounding the alkyne centre. Reaction with 2-methylbut-3-yn-2-ol proceeded smoothly and the desired amine **154** was obtained in 95% yield. In the next stage, we investigated various ketones. First, we applied the simplest ketone, acetone, in the reaction with pyrrolidine and alkynes with different electronic properties. Reaction with electron-neutral phenylacetylene granted amine **155** in an excellent 89% yield. A negligible yield drop was observed when the reaction was carried with electron-donating 4-methoxyphenylacetylene or electron-withdrawing 4-trifluorophenylacetylene. Respectively, reaction with the earlier yielded the desired product **156** in 70%, while reaction with the latter provided amine **157** in 87%. Changing the amine to piperidine, while keeping electron-neutral phenylacetylene led to **158** with a drop in the reaction yield to an acceptable value of 50%. Adamantane has been often referred to as having a beneficial effect on bioactive molecules since it increases the bioavailability or solubility of compounds. Therefore, we investigated 2-adamantanone as the ketone substrate. The reaction of 2-adamantane with pyrrolidine and phenylacetylene led to the formation of the desired product **159** in 95%. Using 4-methoxyacetylene provided the tertiary amine **160** in 90%, and reaction with 4-trifluorophenylacetylene afforded **161** in 84% yield. Reaction of 2-adamantanone with phenylacetylene and piperidine yielded the product **162** in 68% yield. Cyclobutene ring is often found in drug candidates for its favourable properties, such as increased metabolic stability, restricted cis/trans isomerisation observed for alkenes, and others. Therefore, cyclobutanone seemed to be a proper candidate for exploration in the KA^2 coupling. Its reaction with phenylacetylene and pyrrolidine yielded amine **163** in 72% yield. Changing to 4-methoxyphanylacetylene and 4-trifluorophenylacetylene did not compromise the yields and products **164** and **165** were obtained in respective 81% and 75% yields. In the next step, we evaluated various secondary amines, including piperidine, morpholine, dibutyl amine, and *N*-benzylmethylamine. Corresponding propargylic amines were obtained in 87%, 63%, 25%, and 54%, in the respective order. The drop in the yields observed for the acyclic amines can be rationalised by the higher freedom of rotation of the aliphatic chains, which might cause bigger steric interaction, compared to the locked cyclic secondary amines.

To further demonstrate the utility of the catalyst, we performed the reaction of biologically relevant natural product-derived compounds. First, phenylacetylene and pyrrolidine were subjected to the reaction with estrone, which led to the formation of a single diastereomer **170** in 74% yield. Our method is complementary to a previously reported reaction on the epi-estrone.

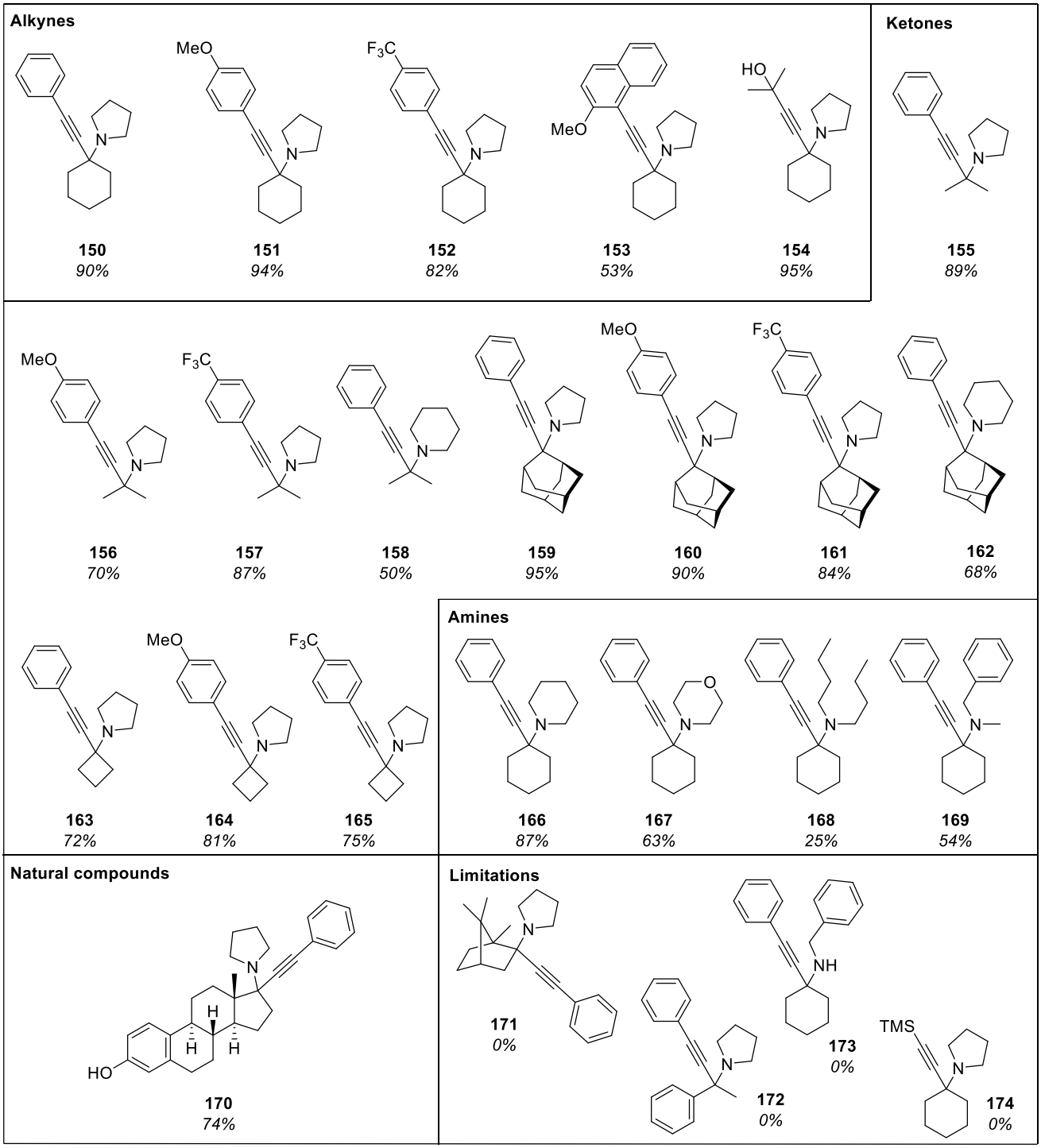

Figure 24. KA^2 coupling reaction scope.

Some limitations with the catalyst were encountered. The use of ketones such as camphor **171**, resulted in the isolation of starting material. The logical explanation for the negative result can be attributed to the sterical hindrance of the ketone, which may interfere with the alkynylation insertion. The reaction with acetophenone **172** also did not produce the expected propargyl amine. Instead, the aldol condensation product was isolated. Lastly, the reaction with the primary amine benzylamine to form **173** and TMS-acetylene to produce **174** also did not occur. Primary amines may have the ability to coordinate to the metal centre, poisoning the catalyst. On the other hand, silver has a high affinity to silicon and in some instances can be used to deprotect trimethylsilyl acetylenes.

To further demonstrate the importance and versatility of propargyl amines and the KA^2 methodology, additional experiments with the isolated products were carried out. Firstly, it is worth mentioning that the reaction can be scaled up to gram scale reaction without the need for solvent or purification and with no decrease in yield, as shown in Scheme 34. When 1 gram of cyclohexanone leads to the formation of the respective propargyl amine **150** with a 97%. Furthermore, alkyne **154**, when treated with a strong base, can release acetone leading to the formation of the terminal alkyne **175**. A first experiment was carried out with the treatment of alkyne **154** with sodium hydride in toluene. The reaction was over after one hour and alkyne **175** was isolated in a quantitative yield. Since the KA^2 reaction is carried out at neat conditions, this leads to the hypothesis that the terminal alkyne could be achieved in a one-pot synthesis with the addition of toluene and sodium hydride once the KA^2 reaction is over. Indeed, the reaction can be carried out in a one-pot reaction with a surprising overall yield of 94%. This

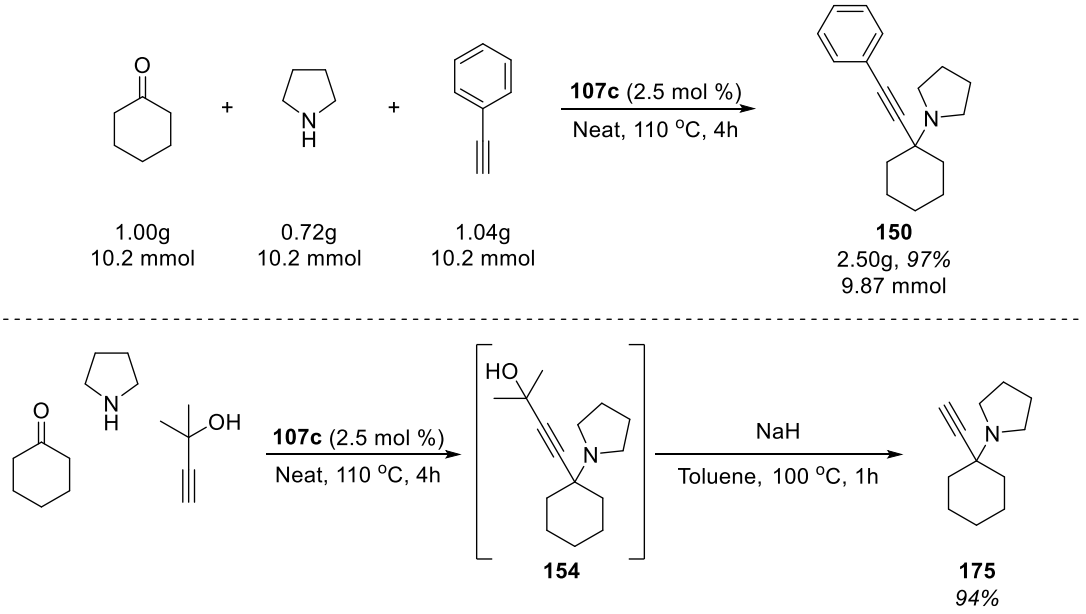

Scheme 34. Gram scale synthesis of compound **150** and one-pot reaction of terminal alkyne **175**.

makes a very straightforward and efficient synthesis for either internal or terminal alkynes. It is noteworthy that previous attempts to prepare terminal alkynes via KA2 coupling using diethyl but-2-ynedioate as a surrogate resulted in limited success. The final products were typically obtained in poor yields, rarely exceeding 50%.[103] This highlights the significant improvement our method offers, achieving substantially higher yields and demonstrating greater efficiency and practicality in synthesising terminal alkynes.

4.6. Data storage

The great catalytic activity of the developed silver complex suited our interest in investigating if a predefined set of propargylamines could be applied for data storage. The choice for such application was due to the simple and efficient method to access a small library of compounds *via* the A^3 coupling where we could finetune the reaction conditions to our needs. Since we had done a scope of the reactions, we set upon to ensure the stability of the compounds. Firstly, a thin layer chromatography (TLC) was performed to ensure that the compounds were bench-stable and to great surprise, all compounds were bench-stable and had somehow distinct retention factor values, as depicted in Figure 25.

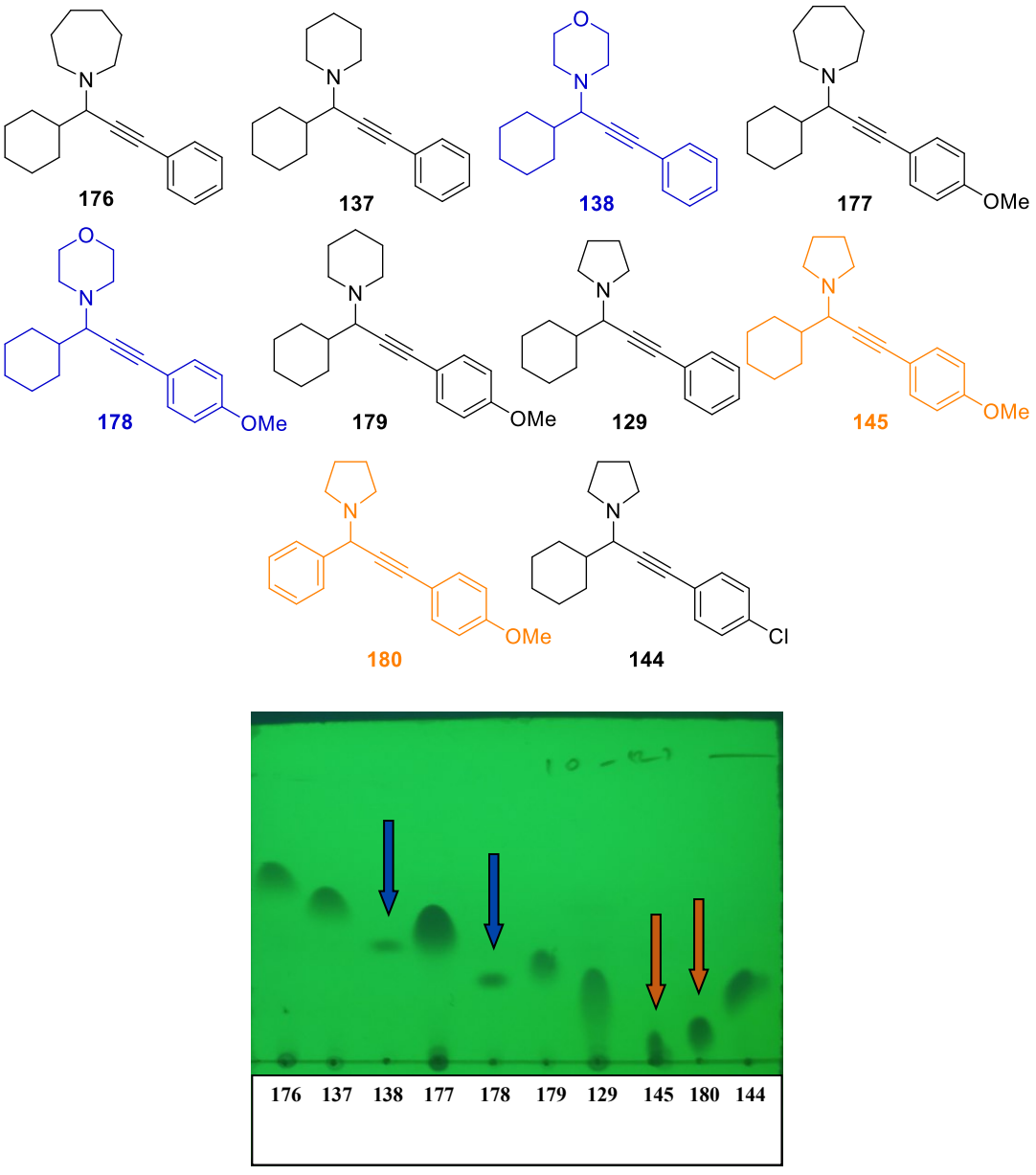

Figure 25. First TLC made with propargyl amines synthesised in the A^3 coupling reaction.

Consequently, we envisioned that such property could be further explored within their application in data storage. There are two main reasons to use propargyl amines for data storage: The ability to synthesise more compounds allowing to make small modifications that can slightly change the retention factor and the use of TLCs for decoding the data stored, as a cheap and easy alternative to methods presented in **chapter 2.6**, which involves hampered and expensive machinery. The TLC plates present a virtually cost free and user-friendly alternative, given that even chemists in their early days know how to operate with the TLCs.

Satisfied with the possibility of using TLCs for decoding the stored data, the next logical step was to further investigate the influence of each starting material (aldehyde, amine, alkyne) on the retention factor of the produced propargyl amine. From the initial TLC it was possible to take some conclusions. We focused on two factors, one being the retention factor of the compound and second being the shape of the spot on the TLC plate. For instance, we noticed that compounds containing azepane and piperidine seem to have a higher retention factor than pyrrolidine or morpholine. Similarly, propargyl amines derived from benzaldehyde showed higher retention factors than those, derived from cyclohexanecarboxaldehyde. Morpholine presented itself as a good starting material since the two propargyl amines **138** and **178** (depicted in blue) containing morpholine formed a very tidy and well-defined spot. On the other hand, we avoided azepane from the further investigations, because we observed, that the propargylic amines that contain this heterocycle show spots on the TLC plate with a significant tailing. This complicates the analysis of the storing mixture (the recovery of the saved information), and therefore it is undesired. With this knowledge insight, the next step was to increase the number of the library members, distinguishable on TLC, to increase the storing capacity of the system.

Illustrated in Figure 26 is a list of all the propargyl amines synthesised for this purpose. The A^3 coupling reaction proved to be a simple and efficient methodology for accessing a small library of compounds. The method is very versatile and tolerates many functional groups. Pyrrolidine and piperidine were the most used amines since they presented better results and gave compounds with good properties for TLC usage. Surprisingly, the best amine candidate, morpholine, proved to be unfortunately unreactive when using less reactive aldehydes, such as benzaldehyde.

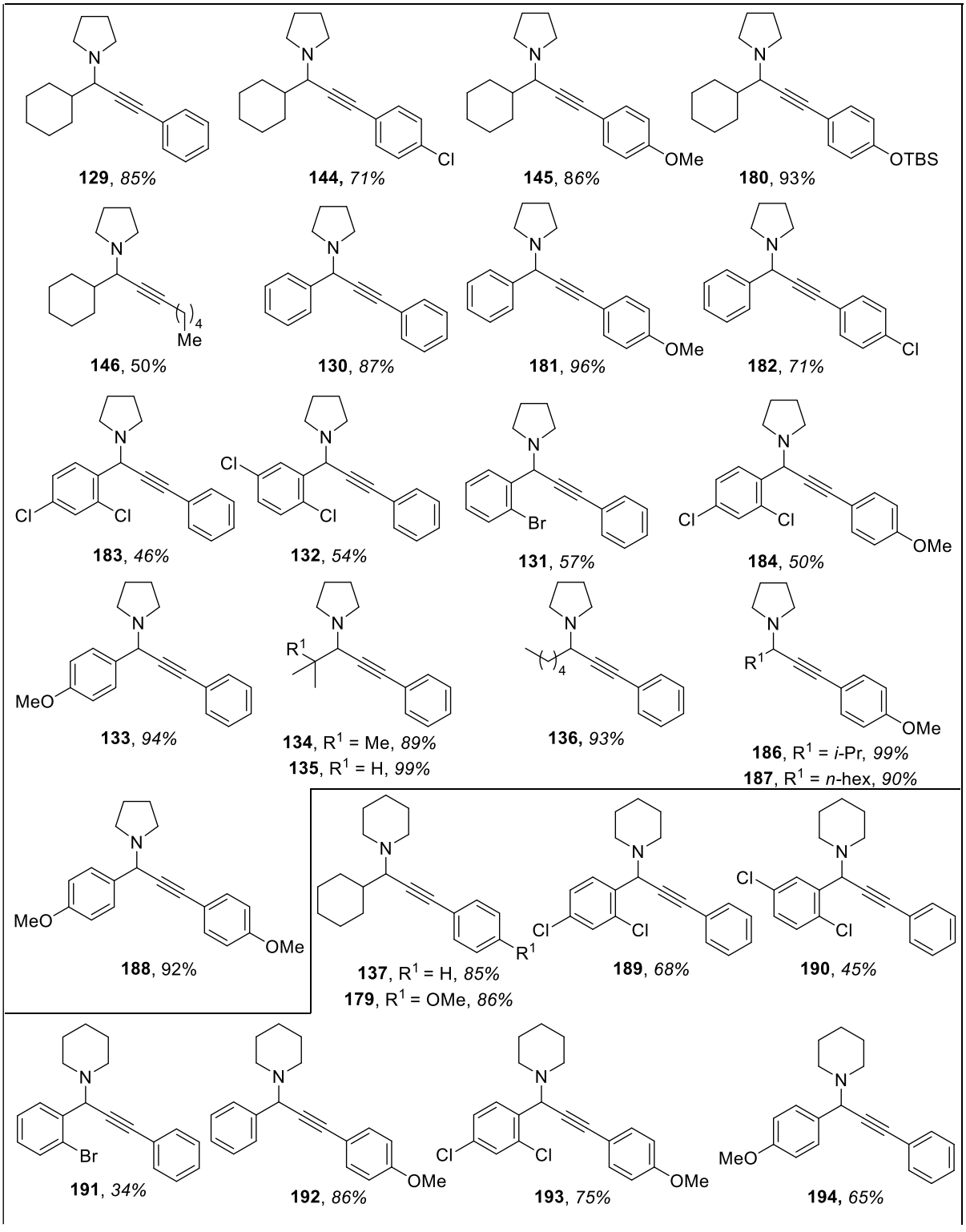

129, *85%*
144, *71%*
145, *86%*
180, 93%
146, 50%
130, *87%*
181, *96%*
182, *71%*
183, *46%*
132, *54%*
131, *57%*
184, *50%*
133, *94%*
134, R^1 = Me, *89%*
135, R^1 = H, *99%*
136, *93%*
186, R^1 = *i*-Pr, *99%*
187, R^1 = *n*-hex, *90%*
188, 92%
137, R^1 = H, *85%*
179, R^1 = OMe, *86%*
189, *68%*
190, *45%*
191, *34%*
192, *86%*
193, *75%*
194, *65%*

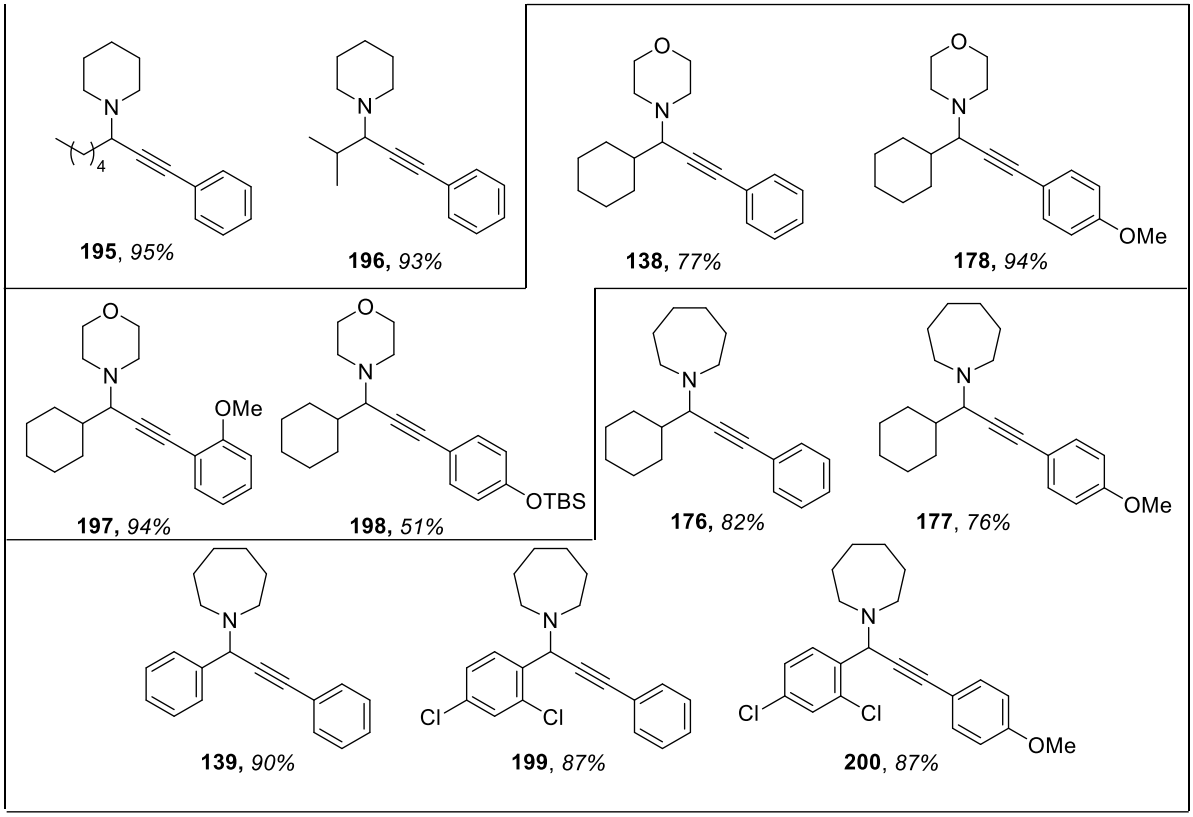

Figure 26. Propargyl amines synthesised for data storage.

With the library of compounds in hand, the next step was to apply it in data storage for proof of concept. Firstly, it is important to clarify the workflow on how the information is stored. We envisioned that the data could be stored in 96-well plates commonly used in the microbiology field since these plates are readily available and cheap. Another reason for this choice is the existence of twelve-channel pipettes that make the encoding process much faster and more efficient. The process begins with the transformation of the data input into binary code. This is carried out either by online available software,[128] or by a software developed in our group, using python programming language and artificial intelligence driven coding (the software principles and development are beyond the scope of this thesis, therefore will not be described here in detail). Practically, we chose to encode a QR code encoding the group website into a binary code, as depicted in the Figure 27, Step 1. In the step 2, the binary code is translated into a distribution of compounds over the well-plate. This is achieved by dividing the binary code into substrings (the length of which corresponds to the number of molecules used for encoding – eight in this case). Each substring represents one well of the well plate. Each position of the substring is assigned to one specific molecule of choice. If there is a binary one at the particular position of the substring, the molecule assigned to this position is present in the corresponding well, and vice versa, the presence of binary zero at the particular position is encoded by the absence of the corresponding molecule. The developed software is capable of analysing the presence of each molecule over the well plate and provides eight separate "molecular maps" for a distribution of each compound, as depicted in the Figure 27, Step 2.

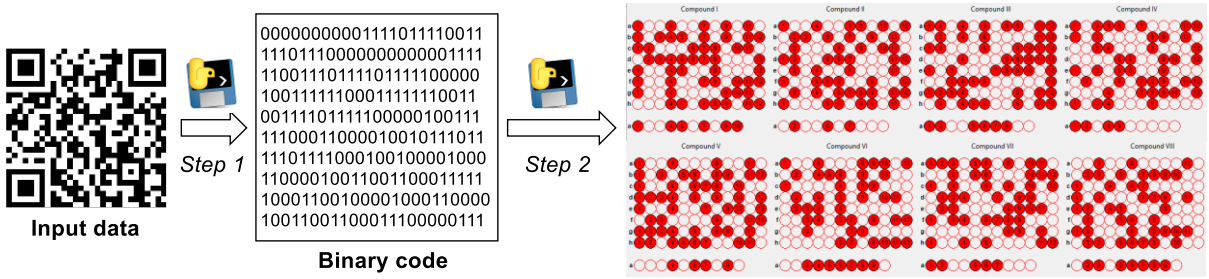

Figure 27. Transformation of the input data into the distribution of each compound on the 96-well plate.

After the converting of the input data into the distribution of each compound in the 96-well plate, we turned our attention to the encoding process meaning the storage of the data in the well plate. For an efficient encoding three 96-well plates were used, as shown in Figure 28 The encoding process takes place one compound at a time. On the first 96-well plate (Figure 28, plate A), the tips of the pipette are arranged in order of the presence or absence of the compound in each well given by the distribution generated by the software. If the compound should be

present then a tip is placed (black dot), if the compound should be absent then no tip is placed. Afterwards, the tips are attached in the twelve-channel pipette and the compound is retrieved from the reservoir 96-well (Figure 28, plate B). In this 96-well plate, each line was filled with a solution of one specific molecule. This well-plate served as a reservoir for the compounds used for the encoding. Consequently, the retrieved tips with the compound are placed in the storing well plate (Figure 28, plate C), in which the data is encoded. When all the 96-well plate **C** is filled with compound I, then the process repeats with compound II. The tips are placed in the well plate **A**. With the pipette, compound II is retrieved from line B of well plate **B** and placed in the well plate **C**. When all the compounds are deposited in the 96-well plate **C**, then the data is encoded.

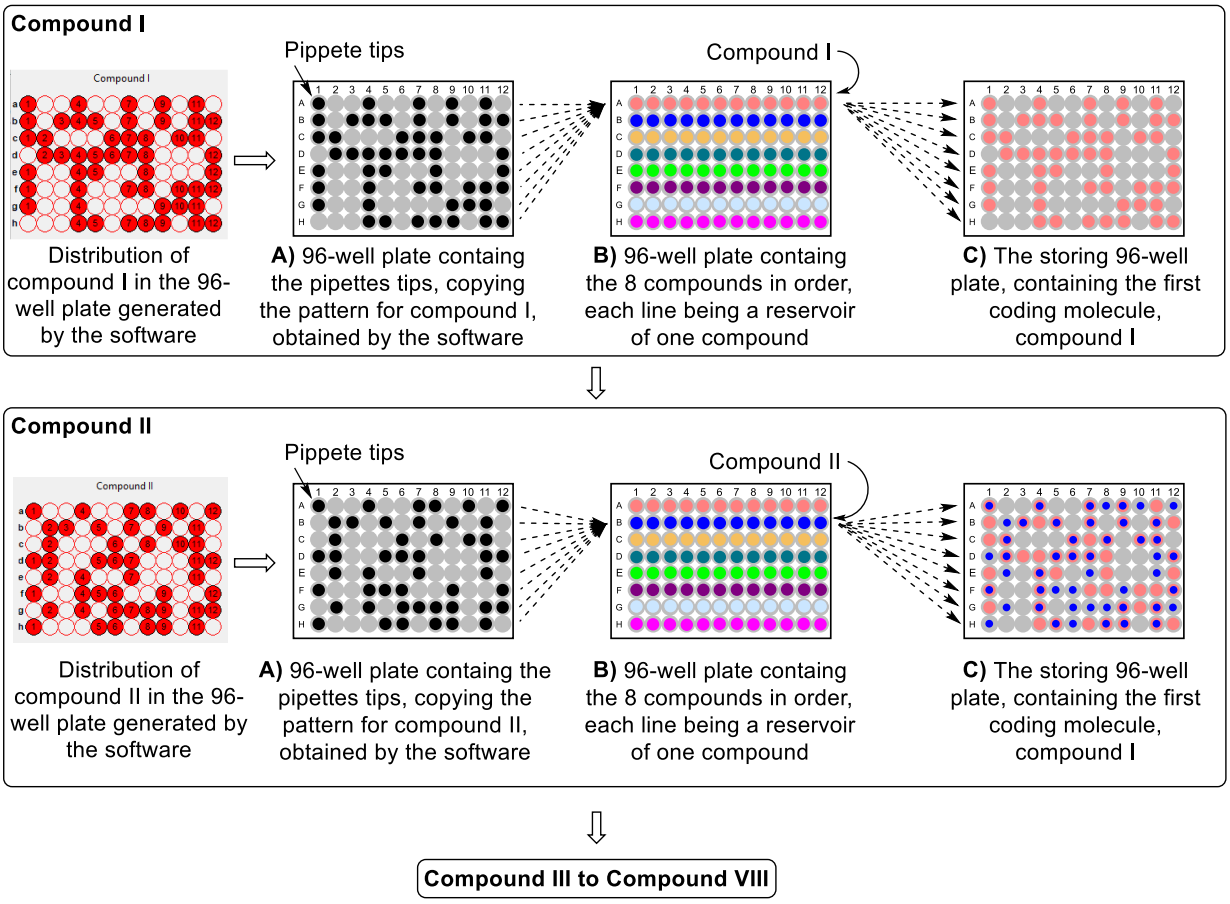

Figure 28. Encoding method using 96-well plates.

Once the data is stored in the 96-well plate, then the TLCs can be used to decode the data. The decoding is possible by spotting each well in the TLC plate. A 96-well plate means that 96 TLC spots are required. Upon running all the TLCs, a software was created to decode the TLCs and restore the encrypted binary code. This automatisation makes the recovery of the data practical and fast. Once the binary code is recovered, another software was designed responsible

for detecting any possible errors in the recovered binary codes. This is achieved by comparing the input binary code with the recovered binary code. The software is capable to compare these codes and identify the wells where the error occurred. Such a well can be easily repaired by adding the corresponding molecules, if they are missing, or removing the mixture and equipping the well with the correct mixture, allowing an easy repair. This makes this method advantageous over others presented in **chapter 2.6** since each well can be accessed independently. After such check, that data can be stored without the errors and recovered any time needed.

With the methodology developed and the compounds synthesised, the first application was to store the QR code of our research group website. In Figure 29 is represented the eight compounds (I-VIII) used for the proof of concept and the complete workflow of the data storage

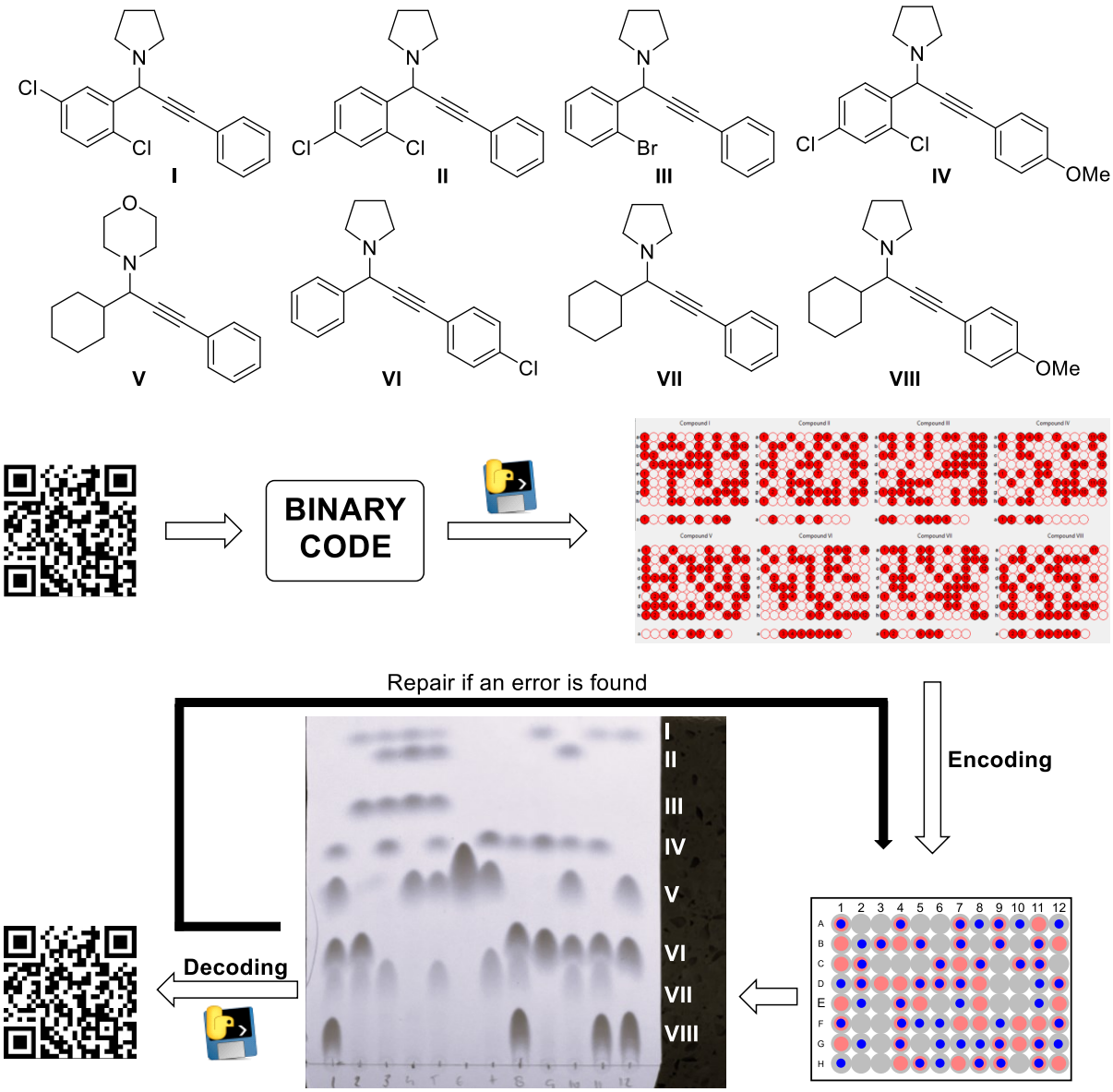

Figure 29. Data storage procedure and first set of compounds used.

process. First, we generated the QR code, transformed it into binary codes, and divided it into substrings. The second program generated each compound position in the 96-well plate, as in detail described in Figure 27. We then proceed with the encoding of the data in the 96-well plates, as described in detail in Figure 28. For the QR code, two 96-well plates were necessary in order to store all the necessary information. Upon completing the fulfilment of the well plates, all 106 wells were spotted in the TLC. Upon spotting, all the TLCs were developed to recover the stored data by the software. The corresponding binary code was regenerated first, which was in turn converted back into QR code.

One of the "eluted" TLCs can be seen in Figure 29. All eight compounds were distinguishable, yet the results were not satisfactory since compound VI presents itself with a tail disguising compound VII. This makes the recovery of the data prone to reading errors. Therefore, some of the compounds were changed.

The change in the eight compounds produced an immediate impact on the TLC outlook. The compounds used for the second set are represented in Figure 30 as well as one of the developed TLCs obtained from the decoding process. In order to make the decoding process easier, in all the TLCs a spot containing all compounds was added, as a reference. It was also concluded that the tail of the compounds such as **VI**, **VII** and **VIII** is very much dependent on the concentration of said compound. After the first run, the recovered binary code had a 98.5% similarity with the starting binary code. After the repair and rerun, the data was fully recovered with 100% data similarity, meaning that the concept was proven and working.

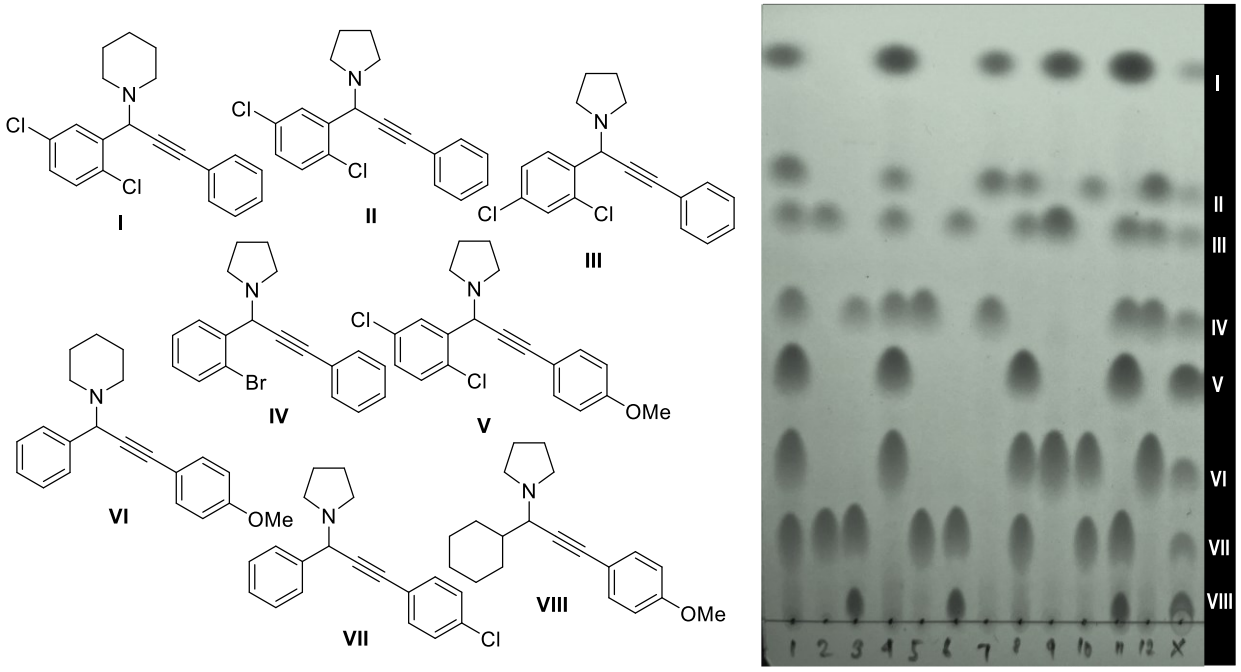

Figure 30. Second set of eight compounds used.

The next step is to include an extra 3 or 4 compounds to make the process more efficient. Additionally, the storage of other data input, such as text and images will be attempted.

5. Conclusions

The synthesis of mononuclear chelate silver complexes was approached by employing a variety of bidentate ligands with diverse backbones, linker moieties, and NHC parts. Initial attempts with simple alkane linkers were unsuccessful, leading to a shift towards bisamide linkers. The successful synthesis of bisimidazolium salts from bisamide precursors allowed for the complexation with silver, yielding mononuclear chelate silver complexes and a novel tetranuclear complex. Complexation outcomes varied based on the ligand structure, with ethylene backbones showing lower yields, while bulkier side chains on phenyl backbones improved yields and solubility, facilitating easier purification. Structural analyses confirmed the chelating nature of the ligand and coordination details of the complexes, with significant insights gained from NMR, HRMS, and X-ray crystallography, though some structural confirmations were limited due to the lack of suitable crystals.

The study successfully demonstrated the efficiency and robustness of NHC-silver complexes as carbene transfer agents to transition metals, particularly nickel and palladium. Transmetalation of silver complex with $NiCl_2$ and $PdCl_2$ yielded nickel and palladium complexes with high overall yields. The use of a one-pot reaction further improved the yield of all the complexes. Extending the side chain to *n*-propyl maintained high yields, although isopropyl substitution resulted in the formation of undesirable abnormal carbenes. Structural analyses confirmed the formation of desired complexes, with spectral features indicating the presence of normal carbenes and highlighting diastereotopic signals indicative of helical *chiral-at-metal* complexes. The chirality of the complexes was further studied. It was proved that both nickel and palladium complexes bearing the propyl side chain are more stable than their respective methyl analogues.

The antimicrobial properties of some of the silver complexes were investigated, showing promising results against various Gram-positive and Gram-negative bacteria, and fungi. In general, both complexes with MIC values ranging from 1 to 31 μg/mL. In contrast, the ligand precursors showed negligible antimicrobial activity, confirming that the silver ion is essential for the observed effects. Comparisons with literature indicate that these silver complexes are more effective against Gram-positive bacteria and fungi than silver nitrate and significantly outperform silver nanoparticles, particularly in antifungal activity.

The silver complexes demonstrated significant catalytic efficiency in the A^3 coupling reaction, successfully transforming a variety of aldehydes, amines, and alkynes into propargyl

amines under optimised conditions. With 0.5 mol% of the catalyst at 80°C, the reactions proceeded smoothly, yielding high to excellent results for most substrates. Furthermore, the catalytic load could go as low as 0.1% while maintaining a good outcome. Notably, the aldehyde portion was highly tolerated even when using less reactive aromatic aldehydes. Cyclic secondary amines were effective, but primary and acyclic secondary amines failed to react, likely due to catalyst poisoning or lack of iminium ion formation. The alkyne scope was more limited, with functional groups often leading to unreacted starting materials.

The investigation into the KA^2 coupling reaction catalysed by the silver complexes revealed it as an effective catalyst for the synthesis of propargyl amines from ketones, amines, and alkynes. Optimisation studies indicated that 2.5 mol% of the catalyst at 110°C provided the best yields, and while lower temperatures and catalyst loadings were feasible, they resulted in decreased efficiency. The scope of the reaction was broad, successfully accommodating various alkynes, ketones, and secondary amines, with notable high yields for electron-rich and electron-deficient substrates. However, limitations were encountered with sterically hindered ketones, acyclic secondary amines, and primary amines, which either did not react or led to side products. The methodology proved versatile, including applications to natural product derivatives, and could be scaled up without loss of efficiency. Additionally, a one-pot synthesis demonstrated the ability to convert propargyl amines to terminal alkynes efficiently, underscoring the practical utility of the catalyst in complex synthetic routes.

The synthesised propargyl amines were explored for data storage applications due to their tunable retention factors, accessible via A^3 coupling reactions. TLC was identified as a cost-effective and user-friendly method for decoding data, leveraging the distinct TLC spots of propargyl amines derived from various starting materials. By creating a small library of these compounds and optimising their TLC separation, a proof-of-concept was achieved, demonstrating the storage and accurate retrieval of binary data, including a QR code, in 96-well plates. This method, capable of independent well access and error correction, was shown to store data efficiently and accurately, with future plans to expand the number of compounds used, enhancing storage capacity and versatility for various data types. Such investigations are underway.

6. Experimental Section

6.1. Materials and physical measurements

All the chemicals were purchased from the common sources: Sigma Aldrich, Acros Organics, Alfa Aesar, Strem Chemicals, PENTA Chemicals, Fluorochem, and Cambridge Isotope Laboratories, Inc. All the reagents were used without further purification unless otherwise noted. Solvents used in the reactions were distilled and dried before use. The reactions were monitored by TLC using Merck TLC silica gel 60 F254 plates, using a UV lamp (254 nm) detection. NMR spectra were recorded on a Bruker Avance III spectrometer (400 MHz and 600 MHz for ^{1}H NMR and 100 MHz and 150 MHz for ^{13}C NMR, respectively) and Varian NMR Solutions 300 (300 MHz for ^{1}H NMR and 75 MHz for ^{13}C NMR). All chemical shifts δ are reported in ppm with a reference to a residual solvent. Mass spectrometry was performed on a VG-Analytical ZAB SEQ. Infrared spectrum were measured in KBr with a Hermo Nicolet AVATAR 370 FT-IR spectrometer. Unless otherwise stated, reactions requiring heating were carried out with the oil bath as the heat source.

6.2. Silver complex synthesis

***N1,N2*-bis((1H-imidazol-1-yl)methyl)-N1,N2-dimethylethane-1,2-diamine (92)**

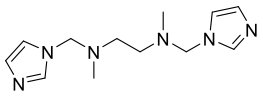

A solution of DMEDA (0.05 mol, 5.4 mL of 85%) and imidazole (0.1 mol, 6.807 g) in water (10 mL) was carefully acidified using Hydrochloric acid to a pH 5. Then, an aqueous solution of formaldehyde (37 %, 0.22 mol, 6.1 mL) was added and the mixture was stirred at room temperature for 60 h. The reaction mixture was basified using 10 M KOH solution to a pH. Afterwards, it was placed in an ice bath and 55 g of K_2CO_3 was added in portions and the mixture was stirred for 20 min. 60 mL of $CHCl_3$ were added and the mixture was stirred for 15 min. at room temperature. After that time, the layers were separated, and the aqueous layer was extracted with 3x15 mL of $CHCl_3$. The combined organic phase was washed with 10 mL of brine, dried over Na_2SO_4, filtered and concentrated, to yield 27% (6.6 g) of desired product as a colourless oil.

^{1}H NMR (400 MHz, $CDCl_3$) δ 7.39 (s, 2H), 6.96 (s, 2H), 6.85 (m, 2H), 4.65 (s, 4H), 2.45 (s, 4H), 2.21 (s, 6H).

^{13}C NMR (101 MHz, $CDCl_3$) δ 137.4, 129.1, 119.5, 68.3, 51.4, 39.3.

HRMS (ESI) m/z: Calcd for $C_{12}H_{21}N_6^+$ = 249.1823; Found = 249.1825

IR (DRIFT): 2962, 1689,1454, 1237, 1045, 920, 794, 647 cm^{-1}.

***N*,*N*'-(ethane-1,2-diyl)bis(2-chloroacetamide) (98)**

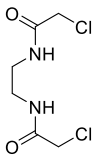

In a flame-dried flask, ethylene diamine (**97**) (1.1 mL, 17 mmol) and TEA (4.6 mL, 35 mmol) were added and dissolved with dry $CHCl_3$ (50 mL). The mixture was stirred at 0 °C. To this mixture, a solution of chloroacetylchloride (**96**) (2.8 mL, 33 mmol) in dry $CHCl_3$ (50 mL) was added dropwise and the mixture was stirred for 4 hours at room temperature. The desired amide precipitates as a white powder and simple filtration yielded 43% (1.5 g) of the final product.

^{1}H NMR (400 MHz, DMSO-d_6) δ 7.08 (s, 2H), 4.07 (s, 4H), 3.68 – 3.34 (m, 4H).

^{13}C NMR (101 MHz, DMSO) δ 166.2, 42.6, 38.5.

The data is in accordance with the one reported in the literature.[129]

_N_,_N_'-3,3'-((ethane-1,2-diylbis(azanediyl))bis(2-oxoethane-2,1-diyl))bis(1-methyl-1H-imidazol-3-ium) (100a)

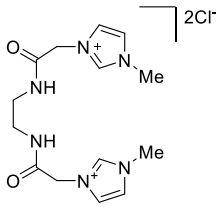

A round bottom flask was loaded with *N*,*N*'-(ethane-1,2-diyl)bis(2-chloroacetamide) **(98)** (0.5 g, 2.3 mmol), 1-methylimidazole (0.4 ml, 5.2 mmol) and 40 mL of CH_3CN. The reaction mixture was stirred for 16 hours under reflux. After, the solvent was evaporated, yielding 83% (0.6 g) of the desired compound as a white powder.

^{1}H NMR (400 MHz, DMSO-d_6) δ 9.21 (s, 2H), 8.96 (s, 2H), 7.76 (s, 2H), 7.70 (s, 2H), 5.06 (s, 4H), 3.89 (s, 6H), 3.25 – 3.16 (m, 4H).

^{13}C NMR (101 MHz, DMSO-d_6) δ 165.7, 138.2, 124.2, 123.5, 51.1, 38.8, 36.3.

The data is in accordance with the one reported in the literature.[129]

1,1'-((ethane-1,2-diylbis(azanediyl))bis(2-oxoethane-2,1-diyl))bis(3-isopropyl-1H-imidazol-3-ium) (100b).

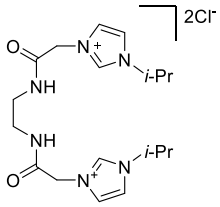

Protocol identical to **100a**. *N*,*N*'-(ethane-1,2-diyl)bis(2-chloroacetamide) (**98**) (1.2 g, 5.6 mmol) and 1-isopropylimidazole (1.3 ml, 11.8 mmol) yielded 79% (1.9g) of the desired compound 98% (1.81 g) as a white solid.

MP (DCM): 250.1 ºC

^{1}H NMR (400 MHz, DMSO-d_6) δ 9.49 (s, 2H), 9.08 (s, 2H), 7.93 (m, 2H), 7.81 (m, 2H), 5.07 (s, 4H), 4.69 (hept, J = 6.7 Hz, 2H), 3.26 – 3.12 (m, 4H), 1.48 (s, 6H), 1.47 (s, 6H).

^{13}C NMR (101 MHz, DMSO-d_6) δ 165.3, 136.1, 123.9, 119.9, 52.2, 50.7, 38.3, 22.3.

HRMS (ESI) m/z: Calcd for $C_{18}H_{30}N_6O_2^{2+}$ = 181.1210; Found = 181.1208

IR (ATR): ν 3396, 3155, 2978, 2875, 1658, 1556, 1348, 1217, 1151, 754, 613cm^{-1}.

_N_,_N_'-(1,2-phenylene)bis(2-chloroacetamide) (102)

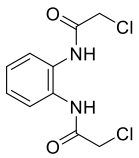

To a round bottom flask containing *o*-phenylenediamine (**101**) (10.0 g, 92.5 mmol) and 125 mL of CH_2Cl_2 was added TEA (25.8 mL, 184.9 mmol). A solution of 2-chloroacetylchloride (**96**) (14.7 mL, 184.9 mmol) in 125 mL of CH_2Cl_2 was slowly added via a dropping funnel over 1 hour at 0 ºC. After, the reaction mixture was warmed up to

room temperature and stirred for an additional 3 hours. The desired amide precipitates as a white powder and simple filtration yielded 66% (16.1 g) of the desired compound as a white powder.

^{1}H NMR (400 MHz, DMSO-d_6) δ 9.68 (s, 2H), 7.54 (dd, J = 6.0, 3.5 Hz, 2H), 7.22 (dd, J = 6.1, 3.5 Hz, 2H), 4.32 (s, 4H).

^{13}C NMR (101 MHz, DMSO-d_6) δ 165.6, 130.7, 126.1, 125.6, 49.1, 43.7.

The data is in accordance with the one reported in the literature.[129]

1,1'-((1,2-phenylenebis(azanediyl))bis(2-oxoethane-2,1-diyl))bis(3-methyl-1H-imidazol-3-ium) (104a)

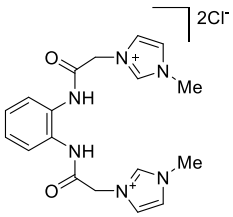

A round bottom flask was loaded with *N,N'*-(1,2-phenylene)bis(2-chloroacetamide) (**102**) (2.5 g, 9.6 mmol), 1-methylimidazole (1.6 mL, 20.1 mmol) and 40 ml of CH_3CN. The reaction mixture was stirred for 16 hours under reflux. After, the solvent was evaporated, yielding 79% (3.2 g) of the desired compound as a white powder.

^{1}H NMR (400 MHz, DMSO-d_6) δ 10.74 (s, 2H), 9.34 (s, 2H), 7.89 (m, 2H), 7.75 (m, 2H), 7.61 (dd, J = 6.1, 3.5 Hz, 2H), 7.17 (dd, J = 6.1, 3.5 Hz, 2H), 5.48 (s, 4H), 3.92 (s, 6H).

^{13}C NMR (101 MHz, DMSO-d_6) δ 164.8, 138.3, 130.2, 125.6, 125.2, 124.3, 123.5, 51.9, 36.3. The data is in accordance with the one reported in the literature.[129]

1,1'-((1,2-phenylenebis(azanediyl))bis(2-oxoethane-2,1-diyl))bis(3-ethyl-1H-imidazol-3-ium) (104b)

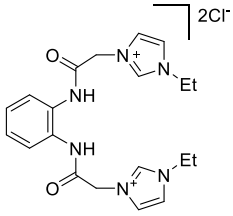

Protocol identical to **104a**. *N,N'*-(1,2-phenylene)bis(2-chloroacetamide) (**102**) (1.05 g, 4.0 mmol) and 1-ethylimidazole (0.84 ml, 8.4 mmol) yielded 98% (1.81 g) of the desired compound as a white solid.

MP (DCM): 261.8 ºC

^{1}H NMR (300 MHz, , DMSO-d_6) δ 10.70 (s, 2H), 9.41 (s, 2H), 7.89 (s, 2H), 7.85 (s, 2H), 7.62 (dd, J = 6.1, 3.6 Hz, 2H), 7.18 (dd, J = 6.2, 3.6 Hz, 2H), 5.46 (s, 4H), 4.27 (q, J = 7.3 Hz, 4H), 1.44 (t, J = 7.3 Hz, 6H).

^{13}C NMR (101 MHz, DMSO-d_6) δ 164.3, 137.1, 129.8, 125.2, 124.7, 123.9, 121.6, 51.5, 44.3, 15.1.

HRMS (ESI) m/z: Calcd for $C_{20}H_{26}N_6O_2^{2+}$ = 191.1053; Found = 191.1053

IR (DRIFT)**:** ν 3369, 3128, 2978, 1657, 1565, 1446, 1232, 829, 719, 573 cm^{-1}.

1,1'-((1,2-phenylenebis(azanediyl))bis(2-oxoethane-2,1-diyl))bis(3-propyl-1H-imidazol-3-ium) (104c)

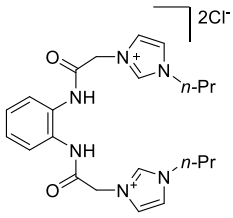

Protocol identical to **104a**. *N,N'*-(1,2-phenylene)bis(2-chloroacetamide) (**102**) (2.0 g, 7.7 mmol) and 1-propylimidazole (1.8 ml, 15.7 mmol) yielded 83% (3.1 g) of the desired compound as a white solid.

MP (DCM): 267.1 ºC

^{1}H NMR (400 MHz, DMSO-d_6) δ 10.73 (s, 2H), 9.41 (m, 2H), 7.91 (m, 2H), 7.83 (m, 2H), 7.62 (dd, J = 6.1, 3.5 Hz, 2H), 7.18 (dd, J = 6.1, 3.5 Hz, 2H), 4.21 (t, J = 7.0 Hz, 4H), 1.83 (h, J = 7.3 Hz, 4H), 0.86 (t, J = 7.4 Hz, 6H).

^{13}C NMR (101 MHz, DMSO-d_6) δ 164.3, 137.4, 129.7, 125.2, 124.7, 123.9, 121.8, 51.5, 50.4, 22.8, 10.3.

HRMS (ESI) m/z: Calcd for $C_{22}H_{29}N_6O_2^{+}$ = 409.2347; Found = 409.2352

IR (DRIFT)**:** ν 3161, 2962, 1691, 1539, 1346, 1171, 764, 536 cm^{-1}.

1,1'-((1,2-phenylenebis(azanediyl))bis(2-oxoethane-2,1-diyl))bis(3-isopropyl-1H-imidazol-3-ium (104d)

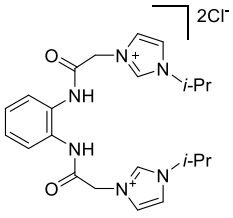

Protocol identical to **104a**. *N,N'*-(1,2-phenylene)bis(2-chloroacetamide) (**102**) (1.00 g, 3.8 mmol) and 1-isopropylimidazole (0.91 ml, 8.0 mmol) yielded 87% (1.6 g) of the desired compound as a white solid.

MP (DCM): 245.4 ºC

^{1}H NMR (300 MHz, DMSO-d_6) δ 10.69 (s, 2H), 9.50 (s, 2H), 7.95 (m, 2H), 7.90 (m, 2H), 7.63 (dd, J = 6.1, 3.6 Hz, 2H), 7.18 (dd, J = 6.1, 3.6 Hz, 2H), 5.44 (s, 4H), 4.72 (p, J = 6.6 Hz, 2H), 1.51 (s, 6H), 1.49 (s, 6H).

^{13}C NMR (101 MHz, DMSO-d_6) δ 164.3, 136.2, 129.8, 125.2, 124.7, 124.1, 120.0, 52.3, 51.5, 22.3.

HRMS (ESI) m/z: Calcd for $C_{22}H_{30}N_6O_2^{2+}$= 205.1210; Found = 205.1211

IR (ATR): ν 3101, 2968, 1689, 1543, 1294, 1153, 964, 754, 534 cm^{-1}

1,1'-((1,2-phenylenebis(azanediyl))bis(2-oxoethane-2,1-diyl))bis(3-methyl-1H-benzo[d]imidazol-3-ium) (105)

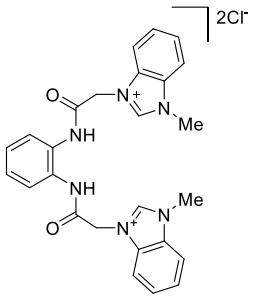

Protocol identical to **104a**. *N,N'*-(1,2-phenylene)bis(2-chloroacetamide) (**102**) (0.25 g, 1.0 mmol) and 1-methylbenzimidazole (0.26 g, 2.0 mmol) yielded 75% (0.38g) of the desired compound as a white solid.

MP (DCM): 289.1 ºC

^{1}H NMR (400 MHz, DMSO-d_6) δ 10.87 (s, 2H), 9.96 (s, 2H), 8.23 (d, J = 8.3 Hz, 2H), 8.04 (d, J = 8.1 Hz, 2H), 7.72 – 7.66 (m, 2H), 7.66 – 7.57 (m, 4H), 7.16 (dd, J = 6.1, 3.5 Hz, 2H), 5.89 (s, 4H), 4.17 (s, 6H).

^{13}C NMR (101 MHz, DMSO-d_6) δ 164.1, 143.8, 131.7, 131.5, 129.8, 126.6, 126.5, 125.3, 124.7, 113.9, 113.6, 49.3, 33.4.

HRMS (ESI) m/z: Calcd for $C_{26}H_{26}N_6O_2^{2+}$ = 227.1053; Found = 227.1051

IR (ATR): ν 3022, 2972, 1676, 1552, 1300, 1036, 791, 580 cm^{-1}

Silver complex 106a

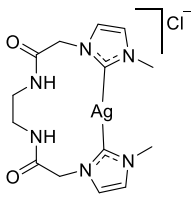

A solution of **100a** (1.0 g, 2.7 mmol) in 40 mL of CH_3CN was treated with silver oxide (0.68 mg, 2.9 mmol). The mixture was stirred at 50 ºC for 24 h. Afterwards, the solvent was removed, and the mixture was resuspended in MeOH. Filtration through Celite®, to remove unreacted silver oxide and consequent solvent evaporation, yielded 75% (0.820 mg) of the desired complex as a grey powder.

MP (DCM): 145 ºC

^{1}H NMR (400 MHz, DMSO-d_6) δ 8.54 (s, 2H), 7.42 (d, J = 1.8 Hz, 2H), 7.39 (d, J = 1.8 Hz, 2H), 4.80 (s, 4H), 3.83 (s, 6H), 3.25 (s, 4H).

^{13}C NMR (101 MHz, DMSO-d_6) δ 182.50 (from 2D), 167.32, 123.84, 122.00, 52.67, 38.16, 37.98.

HRMS (ESI) m/z: Calcd for $C_{14}H_{20}AgN_6O_2$ = 411.06987; Found = 411.0690

IR (ATR): ν 3070, 2937, 1676, 1558, 1371, 1190, 941, 656, 451 cm^{-1}.

Silver complex 106b

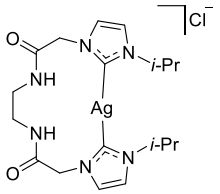

Protocol identical to **106a**. **100b** (0.85 g, 2.0 mmol) and silver oxide (0.5 g, 2.2 mmol) yielded 63% (0.62 g) of the desired compound as a grey solid.

MP (DCM): 125-134 ºC

^{1}H NMR (400 MHz, DMSO-d_6) δ 8.19 (s, 2H), 7.55 (s, 2H), 7.42 (s, 2H), 4.76 (s, 4H), 4.71 – 4.58 (m, 2H), 3.27 (m, 4H), 1.47 (s, 6H), 1.45 (s, 6H).

^{13}C NMR (101 MHz, DMSO-d_6) δ 179.3, 167.1, 123.9, 117.8, 53.3, 52.9, 38.1, 23.5.

HRMS (ESI) m/z: Calcd for $C_{18}H_{28}AgN_6O_2^+$ = 467.1320; Found = 467.1317

IR (ATR): ν 3075, 2931, 1668, 1552, 1369, 1132, 1074, 737, 575 cm^{-1}.

Silver complex 107a

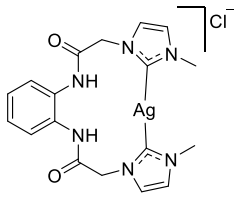

Protocol identical to **106a**. **104a** (1.0 g, 2.4 mmol) and silver oxide (0.6 g, 2.6 mmol) yielded 53% (0.57 g) of the desired compound as a grey solid.

MP (DCM): 192 ºC

^{1}H NMR (400 MHz, DMSO-d_6) δ 7.48 (d, J = 1.7 Hz, 2H), 7.40 (d, J = 1.7 Hz, 2H), 7.34 (dd, J = 5.9, 3.5 Hz, 2H), 7.16 (dd, J = 6.0, 3.6 Hz, 2H), 5.14 (s, 4H), 3.86 (s, 6H).

^{13}C NMR (101 MHz, DMSO-d_6) δ 181.9 (from 2D), 166.0, 125.9, 125.5, 123.9, 121.9, 53.2, 38.2.

HRMS (ESI) m/z: Calcd for $C_{18}H_{20}AgN_6O_2^+$ = 459.0699; Found = 459.0693.

IR (ATR): ν 3120, 2952, 1684, 1558, 1456, 1178, 837, 598 cm^{-1}.

Tetranuclear silver complex 108

A solution of ligand precursor **104a** (0.3 mg, 0.7 mmol) in 10 mL of CH3CN was treated with silver oxide (0.4 mg, 1.8 mmol). The mixture was stirred at 50 ºC for 24 h. Afterwards, the solvent was evaporated. The mixture was resuspended in hot DMSO, and it was filtrated through Celite, to remove solids. Upon cooling down the mixture to room temperature a black precipitate was formed. Filtration and removal of DMSO residual using H_2O and Et_2O yielded the desired product in 51% (414 mg).

^{1}H NMR (400 MHz, DMSO-d_6) δ 7.57 (s, 4H), 7.24 (dd, J = 6.0, 3.6 Hz, 4H), 7.12 (s, 4H), 6.80 (dd, J = 6.0, 3.6 Hz, 4H), 5.42 (m, 4H), 4.75 (m, 4H), 3.15 (s, 12H).

Silver complex 107b

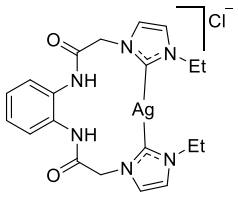

Protocol identical to **106a**. **104b** (0.57 g, 1.2 mmol) and silver oxide (0.30 mg, 1.3 mmol) yielded 84% (0.55 g) of the desired compound as a grey solid.

MP (DCM): 189 ºC

^{1}H NMR (400 MHz, DMSO) δ 7.51 – 7.48 (m, 4H), 7.32 (dd, *J* = 5.9, 3.6 Hz, 2H), 7.24 (dd, *J* = 5.9, 3.6 Hz, 2H), 5.08 (s, 4H), 4.19 (q, *J* = 7.2 Hz, 4H), 1.42 (t, *J* = 7.3 Hz, 6H).

^{13}C NMR (101 MHz, DMSO) δ 181.5 (from 2D) 166.0, 126.3, 123.9, 120.5, 53.1, 46.1, 16.9.

HRMS (ESI) m/z: Calcd for $C_{20}H_{24}AgN_6O_2^+$ = 487.1007; Found = 487.1004

IR (ATR): ν 3128, 2978, 1657, 1560, 1381, 1171, 829, 573 cm^{-1}.

Silver complex 107c

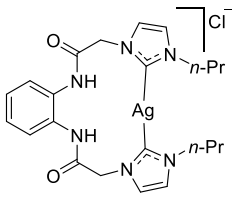

Protocol identical to **106a**. **104c** (0.50 g, 1.1 mmol) and silver oxide (0.27 mg, 1.2 mmol) yielded 85% (0.49 g) of the desired compound as a grey solid.

MP (DCM): 170 ºC

^{1}H NMR (400 MHz, DMSO) δ 7.52 – 7.44 (m, 2H), 7.30 (dd, J = 5.9, 3.6 Hz, 1H), 7.13 (dd, 1H), 5.11 (s, 2H), 4.11 (t, J = 7.1 Hz, 2H), 1.83 (h, J = 7.3 Hz, 2H), 0.88 (t, J = 7.3 Hz, 3H).

^{13}C NMR (101 MHz, DMSO) δ 165.8, 132.9, 125.7, 125.2, 123.9, 120.9, 53.6, 52.6, 24.5, 10.9.

HRMS (ESI) m/z: Calcd for $C_{22}H_{28}AgN_6O_2^+$ = 515.1325; Found = 515.1328

IR (ATR): ν 3111, 2968, 1660, 1560, 1381, 744, 536 cm^{-1}.

Silver complex 107d

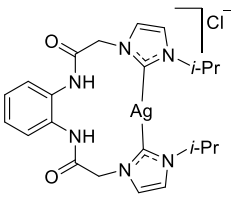

Protocol identical to **106a**. **104d** (0.50 g, 1.1 mmol) and silver oxide (0.27 g, 1.2 mmol) yielded 85% (0.41 g) of the desired compound as a grey solid.

MP (DCM): 212 ºC

^{1}H NMR (400 MHz, DMSO-d_6) δ 7.57 – 7.42 (m, 4H), 7.32 (dd, J = 5.9, 3.6 Hz, 2H), 7.24 (dd, J = 5.9, 3.6 Hz, 2H), 5.08 (s, 4H), 4.19 (q, J = 7.3 Hz, 4H), 1.42 (t, J = 7.3 Hz, 6H).

^{13}C NMR (101 MHz, DMSO-d_6) δ 180.4 (from 2D), 166.0, 126.3, 123.9, 120.5, 53.1, 46.1, 16.9

HRMS (ESI) m/z: Calcd for $C_{22}H_{28}AgN_6O_2^+$ = 515.1320; Found = 515.1317

IR (ATR): ν 3128, 2978, 1657, 1560, 1446, 1171, 739, 573 cm^{-1}.

Silver complex 109

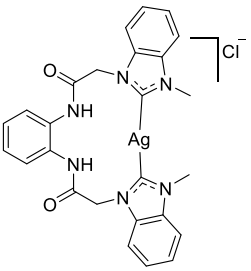

Protocol identical to **106a**. **105** (0.30 g, 0.6 mmol) and silver oxide (0.16 mg, 0.7 mmol) yielded 47% (0.16. g) of the desired compound as a grey solid.

MP (DCM): 209.7 ºC

^{1}H NMR (400 MHz, DMSO-d_6) δ 9.94 (s, 2H), 7.95 – 7.72 (m, 4H), 7.55 – 7.43 (m, 4H), 7.42 – 7.20 (m, 4H), 5.50 (s, 4H), 4.17 (s, 6H).

^{13}C NMR (101 MHz, DMSO-d_6) δ 166.3, 134.9, 134.0, 127.0, 124.5, 124.3, 112.6, 112.4, 50.8, 36.1.

HRMS (ESI) m/z: Calcd for $C_{26}H_{24}AgN_6O_2^+$ = 559.1007; Found = 559.1009.

IR (ATR): ν 3102, 2985, 1676, 1512, 1368, 1078, 760, 598 cm^{-1}.

6.3. Transmetalation

Nickel complex 110a

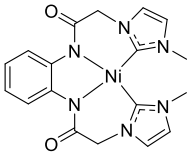

A solution of **104a** (1.0 g, 2.4 mmol) in 40 mL of CH_3CN was treated with silver oxide (0.60 mg, 2.6 mmol). The mixture was stirred at 50 ºC for 2h. Afterwards, nickel chloride (0.40 g, 3.1 mmol) and K_2CO_3 (1.3 g, 9.4 mmol) were added, and the reaction was stirred at 50 ^{0}C for an additional 16 h. The solvent was removed, and the mixture was resuspended in MeOH. Filtration through Celite® and consequent solvent evaporation yielded 94% (0.9 g) of the desired complex as a yellow powder.

^{1}H NMR (400 MHz, DMSO-d_6): 8.36 – 8.27 (m, 2H), 7.43 (d, J = 1.8 Hz, 2H), 7.33 (d, J = 1.9 Hz, 2H), 6.69 – 6.62 (m, 2H), 5.14 (d, J = 17.0 Hz, 2H), 4.67 (d, J = 17.1 Hz, 2H), 3.18 (s, 6H).

^{13}C NMR (101 MHz, DMSO-d_6): δ 166.5, 162.7, 143.4, 123.8, 121.6, 121.3, 120.0, 54.5, 36.2.

The data is in accordance with the one reported in the literature.[130]

Nickel complex 110b

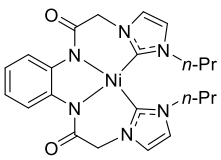

A solution of **104c** (1.0 g, 2.4 mmol) in 40 mL of CH_3CN was treated with silver oxide (0.60 mg, 2.6 mmol). The mixture was stirred at 50 ºC for 2h. Afterwards, nickel chloride (0.40 g, 3.1 mmol) and K_2CO_3 (1.3 g, 9.4 mmol) were added, and the reaction was stirred at 50 ^{0}C for an additional 16 h. The solvent was removed, and the mixture was resuspended in MeOH. Filtration through Celite® and consequent solvent evaporation yielded 93% (0.9 g) of the desired complex as a yellow powder.

MP (MeCN): 349.7 ºC.

^{1}H NMR (400 MHz, DMSO-d_6) δ 8.28 (dd, J = 6.2, 3.5 Hz, 2H), 7.47 (d, J = 1.9 Hz, 2H), 7.42 (d, J = 1.9 Hz, 2H), 6.66 (dd, J = 6.2, 3.5 Hz, 2H), 4.85 (m, 4H), 3.71 – 3.58 (m, 2H), 3.20 – 3.06 (m, 2H), 2.00 – 1.88 (m, 2H), 1.80 – 1.66 (m, 2H), 0.78 (t, J = 7.3 Hz, 6H).

^{13}C NMR (101 MHz, DMSO-d_6) δ 166.7, 162.7, 143.9, 123.3, 122.1, 122.1, 120.5, 54.9, 51.5, 24.7, 11.5.

HRMS (ESI) m/z: Calcd for $C_{22}H_{27}N_6NiO_2^+$ = 465.1544; Found = 465.1540

IR (ATR): ν 3149, 2968, 1597, 1479, 1298, 1043, 806, 555 cm^{-1}.

Nickel complex 110c

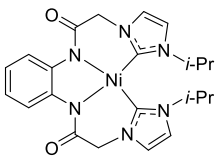

A solution of **104d** (0.50 g, 1.0 mmol) in 25 mL of CH_3CN was treated with silver oxide (0.27 g, 1.1 mmol). The reaction mixture was stirred for 2 hours at 50 ºC. Nickel chloride (0.18 g, 1.4 mmol) and K_2CO_3 (0.57 g, 4.2 mmol) were added, and the reaction was allowed to react for an additional 16 hours at 50 ºC. Afterwards, the mixture was filtered through Celite®. Upon purification through chromatographic column (DCM/MeOH, 20/1) the desired complex was isolated in 5% (26 mg) yield.

MP (MeCN): 320 ºC (decomposes before reaching the melting point).

^{1}H NMR (400 MHz, CD_3CN) δ 8.28 (dd, *J* = 6.2, 3.6 Hz, 2H), 7.20 – 7.14 (m, 4H), 6.74 (dd, *J* = 6.2, 3.5 Hz, 2H), 5.10 (d, *J* = 17.0 Hz, 2H), 4.63 (d, *J* = 17.0 Hz, 2H), 4.09 (hept, *J* = 6.8 Hz, 2H), 1.56 (s, 3H), 1.54 (s, 3H), 1.03 (s, 3H), 1.02 (s, 3H).

^{13}C NMR (101 MHz, CD_3CN) δ 167.6, 164.3, 144.7, 123.0, 123.0, 121.3, 55.9, 53.0, 25.5, 21.4.

HRMS (ESI) m/z: Calcd for $C_{22}H_{27}N_6NiO_2^+$= 465.1544; Found = 465.1531

IR (ATR): 3126, 2924, 1595, 1354, 1132, 968, 692, 422 cm^{-1}

Palladium complex 111a

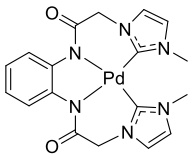

A solution of **104a** (0.30 g, 0.6 mmol) in 25 mL of CH_3CN was treated with silver oxide (0.16 g, 0.7 mmol). The reaction mixture was stirred for 2 hours at 50 ºC. Palladium chloride (0.14 g, 0.8 mmol) and K_2CO_3 (0.35 g, 2.5 mmol) were added, and the reaction was allowed to react for an additional 16 hours at 50 ºC. Afterwards, the mixture was filtered through Celite® and washed with $CHCl_3$. The desired complex was isolated in 81% (0.26 g) yield.

MP (MeCN): 320 ºC (decomposes before reaching the melting point).

^{1}H NMR (400 MHz, DMSO-d_6): δ 8.37 – 8.25 (m, 2H), 7.53 (d, J = 1.9 Hz, 2H), 7.40 (d, J = 1.9 Hz, 2H), 6.75 – 6.66 (m, 2H), 4.85 (s, 4H), 3.38 (s, 6H).

^{13}C NMR (101 MHz, DMSO-d_6): δ166.08, 163.22, 144.14, 123.53, 123.11, 122.20, 120.79, 56.69, 37.41.

HRMS (ESI) m/z: Calcd for $C_{18}H_{18}N_6O_2Pd^+$ = 457.0599; Found = 457.0605

IR (DRIFT): ν 3159, 2949, 2665, 1861, 1653, 1477, 1184, 985, 750, 532 cm^{-1}

Palladium complex 110b

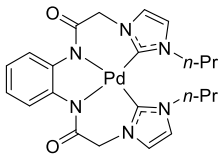

A solution of **104c** (0.30 g, 0.6 mmol) in 25 mL of CH_3CN was treated with silver oxide (0.16 g, 0.7 mmol). The reaction mixture was stirred for 2 hours at 50 ºC. Palladium chloride (0.15 g, 0.7 mmol) and K_2CO_3 (0.35 g, 2.5 mmol) were added, and the reaction was allowed to react for an additional 16 hours at 50 ºC. Afterwards, the mixture was filtered through Celite® and washed with $CHCl_3$. The desired complex was isolated in 62% (0.20 g) yield.

MP (MeCN): 297.2 ºC

^{1}H NMR (400 MHz, DMSO) δ 8.28 (dd, J = 6.2, 3.6 Hz, 2H), 7.57 (s, 2H), 7.48 (s, 2H), 6.72 (dd, J = 6.4, 3.6 Hz, 2H), 4.81 (q, J = 16.8 Hz, 4H), 3.74 (s, 2H), 1.81 – 1.60 (m, 4H), 0.71 (t, J = 7.4 Hz, 6H).

^{13}C NMR (101 MHz, DMSO) δ 165.5, 162.4, 143.7, 123.1, 121.9, 121.7, 120.4, 56.2, 51.4, 24.3, 10.9.

HRMS (ESI) m/z: Calcd for $C_{22}H_{26}N_6O_2PdNa^+$ = 535.1045; Found = 535.1048

IR (DRIFT): 3122, 2922, 1593, 1254, 1184, 989, 810, 723, 532 cm^{-1}.

2,3-diethyl 1,1-dimethyl propane-1,1,2,3-tetracarboxylate (121)

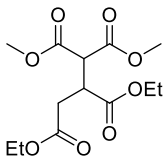

To a round bottom flask loaded with the nickel complex **110a** (77 mg, 0.19 mmol) was added malonic acid dimethyl ester (0.22 ml, 1.89 mmol) and diethyl maleate (0.31 ml, 1.89 mmol). The mixture was stirred at 90 ºC for 24h at neat conditions. Upon completion, EtOAc was added, and the reaction was filtered to remove the catalyst. Evaporation of the solvent yielded 99% (0.57 g) of the desired compound as a yellow oil.

^{1}H NMR (400 MHz, $CDCl_3$) δ 4.20 – 4.11 (m, 4H), 3.93 (d, *J* = 7.1 Hz, 1H), 3.75 (s, 3H), 3.74 (s, 3H), 3.58 (td, *J* = 7.4, 5.2 Hz, 1H), 2.85 – 2.64 (m, 2H), 1.24 (q, *J* = 7.3 Hz, 6H).

^{13}C NMR (101 MHz, $CDCl_3$) δ 171.7, 171.3, 168.4, 168.2, 61.6, 61.0, 52.9, 52.9, 52.2, 40.7, 33.6, 14.3, 14.1.

The data is accordance with the literature.[131]

(2R,2′R)-N,N'-(1,2-phenylene)bis(2-aminopropanamide) dihydrochloride (125a)

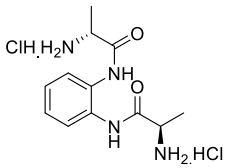

To a flame-dried flask containing L-boc-alanine (1.0 g, 5.3 mmol) in CH_2Cl_2 was added N,N′-Dicyclohexylcarbodiimide (1.2 g, 5.6 mmol) at 0 ºC and stirred for 30 minutes. 1,2-Phenylenediamine (0.29 g, 2.64 mmol) was then added and the reaction was stirred at reflux for 2 hours and followed by TLC. A white precipitate is formed upon allowing the reaction mixture to cool down to room temperature. The precipitate corresponds to urea so it was filtered off. The solvent was evaporated and the mixture resuspended in dry MeOH. Acetyl chloride was slowly added at -78 ºC. The reaction was then allowed to warm up to room temperature and stirred for 16 hours. The solvent was evaporated and the product was washed with EtOAc to yield 99% (850 mg) as a white powder.

^{1}H NMR (400 MHz, DMSO) δ 10.49 (s, 2H), 8.44 (s, 6H), 7.65 (dd, *J* = 6.0, 3.6 Hz, 2H), 7.22 (dd, *J* = 6.1, 3.5 Hz, 2H), 4.32 (p, *J* = 6.1 Hz, 2H), 1.51 (s, 3H), 1.49 (s, 3H).

^{13}C NMR (101 MHz, DMSO) δ 169.1, 130.0, 125.9, 125.2, 49.3, 17.6.

The data is accordance with the literature.[132]

(2R,2′R)-N,N'-(1,2-phenylene)bis(2-amino-3-methylbutanamide) dihydrochloride (125b)

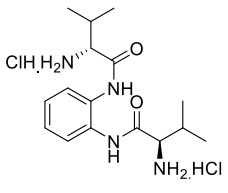

To a flame-dried flask containing L-boc-valine (2.0 g, 9.1 mmol) in CH_2Cl_2 was added N,N′-Dicyclohexylcarbodiimide (2.1 g, 10.1 mmol) at 0 ºC and stirred for 30 minutes. 1,2-Phenylenediamine (0.50mg, 4.6 mmol) was then added and the reaction was stirred at reflux for 2 hours and followed by TLC. A white precipitate is formed upon allowing the reaction mixture to cool down to room temperature. The precipitate corresponds to urea so it was filtered off. The solvent was evaporated and the mixture resuspended in dry MeOH. Acetyl chloride was slowly added at -78 ºC. The reaction was then allowed to warm up to room temperature and stirred for 16 hours. The solvent was evaporated and the product was washed with EtOAc to yield 98% (1.71 g) as a white powder.

^{1}H NMR (400 MHz, DMSO) δ 10.51 (s, 2H), 8.48 (s, 6H), 7.65 (dd, *J* = 6.0, 3.5 Hz, 2H), 7.23 (dd, *J* = 6.1, 3.5 Hz, 2H), 4.18 (s, 2H), 2.23 (h, *J* = 6.8 Hz, 2H), 1.04 (m, 12H).

^{13}C NMR (101 MHz, DMSO) δ 168.1, 130.1, 126.0, 125.3, 58.3, 30.3, 19.0, 18.4.

The data is accordance with the literature.[132]

(S)-2-(1H-imidazol-1-yl)propanoic acid (126a)

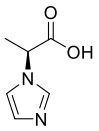

A two-neck flask was loaded with formaldehyde solution (36% 8.5 ml, 112 mmol) and glyoxal solution (40%, 5.2 ml, 45 mmol). A condenser and drop-funnel were coupled to the flask. The mixture was heated up to 50 ºC. A solution of NaOH (20%, 9 ml) containing L-alanine (2.0 g, 23 mmol) and ammonium hydroxide (25%, 7.15 ml, 45 mmol), previously loaded into the drop-funnel, was slowly added over a period of 30 minutes. The reaction was stirred for an additional 4 hours at 50 ºC. Afterwards, it was cooled down to 0 ºC and neutralized with 2M HCl. The product was extracted with EtOAc. The organic layer was washed with brine and dried with MgSO4. Evaporation of the solvent yielded 63% (2.0 g) of the title compound as a yellow solid stored in the oven due to its high hygroscopicity.

^{1}H NMR (400 MHz, DMSO) δ 7.56 (m, 1H), 7.09 (m, 1H), 6.76 (m, 1H), 4.43 (q, *J* = 7.2 Hz, 1H), 1.46 (d, *J* = 7.2 Hz, 3H).

^{13}C NMR (101 MHz, DMSO) δ 172.8, 136.3, 126.8, 118.7, 61.6, 57.9, 20.2.

The data is accordance with the literature.[133]

(S)-2-(1H-imidazol-1-yl)-3-methylbutanoic acid (126b)

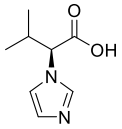

To a two-neck flask was added formaldehyde solution (36%, 16.2 ml, 213 mmol) and glyoxal solution (40%, 10.3 ml, 85.3 mmol). A condenser and drop-funnel were coupled to the flask. The mixture was heated up to 50 ºC. A solution of NaOH (20%, 17 ml) containing L-valine (5 g, 42.7 mmol) and ammonium hydroxide (25%, 13.6 ml, 85.3 mmol) loaded into the drop-funnel, was slowly added over a period of 30 minutes. The reaction was stirred for an additional 4 hours at 50 ºC. Afterwards, it was cooled down to 0 ºC and neutralized with 2M HCl. The product was extracted with EtOAc. The organic layer was washed with brine and dried with MgSO4. Evaporation of the solvent yielded 50% (3.82g) of the title compound as a yellow solid stored in the oven due to its high hygroscopicity.

^{1}H NMR (400 MHz, DMSO) δ 7.60 (m, 1H), 7.18 (m, 1H), 6.76 (m, 1H), 3.97 (d, *J* = 8.7 Hz, 1H), 2.21 (dp, *J* = 8.7, 6.7 Hz, 1H), 0.87 (d, *J* = 6.7 Hz, 3H), 0.61 (d, *J* = 6.7 Hz, 3H).

^{13}C NMR (101 MHz, DMSO) δ 172.1, 137.1, 126.6, 119.4, 70.1, 66.4, 31.7, 19.9, 18.6.

The data is accordance with the literature.[124]

6.4. Minimal Inhibitory Concentration (MIC) study

All the MIC studies were performed, in collaboration, with professor Tomasz M. Karpiński from Department of Medical Microbiology, Poznań University of Medical Sciences, Poland. In the MIC study, there were investigated clinical strains of Gram-positive bacteria *Staphylococcus aureus* and *S. epidermidis*, Gram-negative bacteria *Escherichia coli*, *Klebsiella pneumoniae* and *Pseudomonas aeruginosa* and fungi *Candida albicans, C. glabrata* and *Rhodotorula rubra.* All strains were obtained from the collection of the Chair and Department of Medical Microbiology at Poznań University of Medical Sciences (Poland). The species of bacteria were grown at 35°C for 24 h, in tryptone soy agar (TSA; Graso, Poland) and fungi were grown on Sabouraud agar (Graso, Poland).

The MICs of selected substances were determined by the micro-dilution method using 96-well plates (Nest Scientific Biotechnology, China). Studies were conducted according to our previous publications.[134,135] Concentrations of tested compounds were in the range of serial dilutions from 2000 to 1 μg/mL. The analyses were repeated three times.

6.5. A^3 coupling reaction and data storage

General procedure: To a round bottom flask the catalyst (0.5 mol% or 3 mol%) and aldehyde were added (1 eq.), together with amine (1 eq.), and acetylene (1 eq.). The reaction was stirred for 5 hours at 80 ºC in neat conditions. Afterwards, the mixture was dissolved in EtOAc (20 mL) and filtered to remove the catalyst. The removal of unreacted aldehyde, when necessary, was done by following the procedure of Maria M. Boucher *et al.*[136] The crude mixture was dissolved in 2 ml of MeOH. A saturated solution of $NaHSO_3$ was added and the mixture was vigorously shaken. Addition of H_2O and extraction with EtOAc, followed by a brine wash, drying with $MgSO_4$ and evaporation of the solvent provided with the desired propargyl amine. Unless otherwise stated, no further purification was required.

1-(1cyclohexyl-3-phenylprop-2-yn-1-yl)pyrrolidine (129)

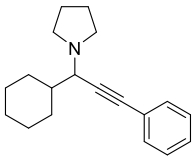

Following the general procedure: cyclohexanecarboxaldehyde (0.17 mL, 1.5 mmol), pyrrolidine (0.15 mL, 1.5 mmol), phenylacetylene (0.15 mL, 1.5 mmol) and catalyst (0.5 mol%) were used as starting substrates, yielding 85% (0.34 g) of the desired compound as a yellow oil.

^{1}H NMR (400 MHz, $CDCl_3$) δ 7.43 – 7.44 (m, 2H), 7.28 – 7.29 (m, 3H), 3.37 (d, 1H, *J* = 5.6 Hz), 2.75 (d, 2H, *J* = 5.2 Hz), 2.66 (d, 2H, *J* = 3.6 Hz), 2.10 (d, 1H, *J* = 8.8 Hz), 1.96 (d, 1H, *J* = 8.8 Hz), 1.79 (m, 6H), 1.68 (d, 1H, *J* = 8.0 Hz), 1.59 (m, 1H), 1.18 (m, 5H).

^{13}C NMR (151 MHz, $CDCl_3$) δ 131.8, 128.3, 127.8, 123.8, 88.0, 85.9, 61.4, 50.2, 41.5, 30.8, 30.4, 29.8, 26.8, 26.4, 23.7.

The data is in accordance with the one reported in the literature.[129]

1-(3-(4-chlorophenyl)-1-cyclohexylprop-2-yn-1-yl)pyrrolidine (144)

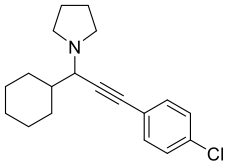

Following the general procedure: cyclohexanecarboxaldehyde (0.17 mL, 1.5 mmol), pyrrolidine (0.15 mL, 1.5 mmol), *p*-chlorophenylacetylene (0.21 g, 1.5 mmol) and catalyst (0.5 mol%) were used as starting substrates, yielding 89% (0.40 g) of the desired compound as a pale-yellow oil.

^{1}H NMR (400 MHz, $CDCl_3$) δ 7.33 – 7.36 (m, 2H), 7.24 – 7.27 (m, 2H), 3.33 (d, 1H, *J* = 12.6 Hz), 2.73 – 2.69 (m, 2H), 2.64 – 2.59 (m, 2H), 2.06 (d, 1H, *J* = 18.0 Hz), 1.94 (d, 1H, *J* = 19.2 Hz), 1.77 (m, 6H), 1.69 (m, 1H), 1.57 (m, 1H), 1.28 – 1.05 (m, 5H).

^{13}C NMR (151 MHz, $CDCl_3$) δ 133.8, 133.1, 122.3, 89.2, 84.8, 61.4, 50.0, 41.4, 30.8, 30.4, 26.8, 26.3, 26.3, 23.7.

The data is in accordance with the one reported in the literature.[129]

1-(1-cyclohexyl-3-(4-methoxyphenyl)prop-2-yn-1-yl)pyrrolidine (145)

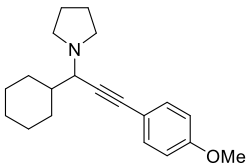

Following the general procedure: cyclohexanecarboxaldehyde (0.17 mL, 1.5 mmol), pyrrolidine (0.15 mL, 1.5 mmol), 4-ethynilanisole (0.20 mL, 1.5 mmol) and catalyst (0.5 mol%) were used as starting substrates, yielding 86% (0.38 g) of the desired compound as a pale-yellow oil.

^{1}H NMR (400 MHz, $CDCl_3$) δ 7.36 (d, 2H, *J* = 4.4 Hz), 6.82 (d, 2H, *J* = 7.8 Hz), 3.80 (s, 3H), 3.33 (d, 1H, *J* = 8.4 Hz), 2.73 (d, 2H, *J* = 6.6 Hz), 2.64 (d, 2H, *J* = 6.6 Hz), 2.08 (d, 1H, *J* = 12.6 Hz), 1.94 (d, 1H, *J* = 11.4 Hz), 1.78 (m, 6H), 1.67 (d, 1H, *J* = 12.0 Hz), 1.57 (m, 1H), 1.06 – 1.29 (m, 6H).

^{13}C NMR (151 MHz, $CDCl_3$) δ 159.3, 133.2, 116.0, 113.9, 86.3, 85.6, 61.5, 55.4, 50.2, 41.5, 30.9, 30.4, 26.8, 26.4, 23.7.

The data is in accordance with the one reported in the literature.[129]

1-(3-(4-((tert-butyldimethylsilyl)oxy)phenyl)-1-cyclohexylprop-2-yn-1-yl)pyrrolidine (180)

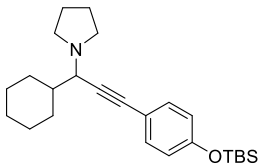

Following the general procedure: cyclohexanecarboxaldehyde (0.17 g, 1.5 mmol), pyrrolidine (0.11 g, 1.5 mmol), and tert-butyl(4-ethynylphenoxy)dimethylsilane (0.5 g, 1.5 mmol) were used as starting substrates, yielding 93% (0.56 g) of the desired compound as a transparent oil.

^{1}H NMR (400 MHz, $CDCl_3$) δ 7.33 (d, *J* = 8.6 Hz, 2H), 6.78 (d, *J* = 8.6 Hz, 2H), 3.35 (d, *J* = 8.5 Hz, 1H), 2.79 – 2.61 (m, 4H), 2.17 – 2.05 (m, 1H), 2.00 – 1.92 (m, 1H), 1.84 – 1.75 (m, 6H), 1.70 – 1.52 (m, 2H), 1.31 – 1.12 (m, 5H), 1.00 (s, 9H), 0.21 (s, 6H).

^{13}C NMR (101 MHz, $CDCl_3$) δ 155.5, 133.1, 120.2, 116.6, 86.5, 85.7, 61.4, 50.1, 41.5, 30.8, 30.4, 26.8, 26.4, 26.3, 25.8, 23.6, 18.3, -4.3.

HRMS (ESI) m/z: Calcd for $C_{25}H_{40}NOSi^+$: 398.2873; Found: 398.2873.

IR (DRIFT): 3046, 2966, 2201, 1612, 1423, 1190, 945, 749, 580 cm^{-1}

1-(1-cyclohexyloct-2-yn-1-yl)pyrrolidine (146)

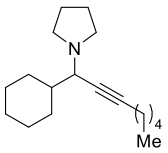

Following the general procedure: cyclohexanecarboxaldehyde (0.17 mL, 1.5 mmol), pyrrolidine (0.15 mL, 1.5 mmol), 1-heptyne (0.20 mL, 1.5 mmol) and catalyst (0.5 mol%) were used as starting substrates. After the work-up, the residue obtained was subjected to chromatographic column (DCM/EtOAc, 100/1), to give 50% (0.2 g) of the desired compound as a transparent oil.

^{1}H NMR (400 MHz, $CDCl_3$) δ 3.04 (dt, 1H, *J* = 8.0 Hz, *J* = 2.0 Hz), 2.64 – 2.58 (m, 2H), 2.54 – 2.48 (m, 2H), 2.17 (td, 2H, *J* = 7.2 Hz, *J* = 2.4 Hz), 1.98 – 1.95 (m, 1H), 1.84 – 1.81 (m, 1H), 1.75 – 1.67 (m, 5H), 1.50 – 1.14 (overlapped multiplets, 10H), 0.87 (t, 3H, *J* = 7.2 Hz).

^{13} C NMR (101 MHz, $CDCl_3$) δ 85.57, 77.76, 61.06, 41.45, 31.15, 30.77, 30.04, 28.93, 26.84, 26.37, 26.32, 23.55, 22.26, 18.73, 14.09.

The data is in accordance with the one reported in the literature.[129]

1-(1,3-diphenylprop-2-yn-1-yl)pyrrolidine (130)

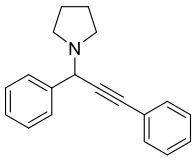

Following the general procedure: benzaldehyde (0.19 mL,1.5 mmol), pyrrolidine (0.15 mL, 1.5 mmol), phenylacetylene (0.21 mL, 1.5 mmol) and catalyst (0.5 mol%) were used as starting substrates, yielding 87% (0.43 g) of the desired compound as a yellow oil.

^{1}H NMR (400 MHz, $CDCl_3$) δ 7.67 – 7.62 (m, 2H), 7.54 – 7.51 (m, 2H), 7.42 – 7.36 (m, 2H), 7.34 (tt, *J* = 4.0, 2.6 Hz, 4H), 4.94 (s, 1H), 2.84 – 2.69 (m, 4H), 1.91 – 1.79 (m, 4H).

^{13}C NMR (101 MHz, $CDCl_3$) δ 139.7, 131.9, 128.4, 128.4, 128.2, 127.7, 123.4, 87.0, 86.9, 59.3, 50.4, 23.6.

The data is in accordance with the one reported in the literature.[129]

1-(3-(4-methoxyphenyl)-1-phenylprop-2-yn-1-yl)pyrrolidine (181)

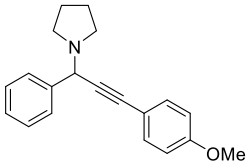

Following the general procedure: benzaldehyde (0.19 mL, 1.5 mmol), pyrrolidine (0.15 mL, 1.5 mmol), 4-ethynylanisole (0.24 mL, 1.5 mmol) and catalyst (0.5 mol%) were used as starting substrates, yielding 96% the desired (0.53 g) compound as a yellow oil.

^{1}H NMR (400 MHz, $CDCl_3$) δ 7.64 – 7.55 (m, 2H), 7.45 – 7.38 (m, 2H), 7.39 – 7.33 (m, 2H), 7.28 (s, 2H), 6.88 – 6.80 (m, 2H), 4.86 (s, 1H), 3.81 (s, 3H), 2.75 – 2.62 (m, 4H), 1.86 – 1.75 (m, 4H).

^{13}C NMR (101 MHz, $CDCl_3$) δ 139.7, 131.9, 128.4, 128.4, 128.2, 127.7, 123.4, 87.0, 86.9, 59.3, 50.4, 23.6.

The data is in accordance with the one reported in the literature.[129]

1-(3-(4-chlorophenyl)-1-phenylprop-2-yn-1-yl)pyrrolidine (182)

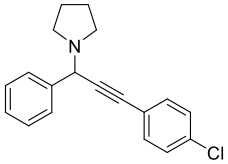

Following the general procedure, benzaldehyde (0.19 mL, 1.5 mmol), pyrrolidine (0.15 mL, 1.5 mmol), *p*-chlorophenylacetylene (205 mg, 1.5 mmol) and catalyst (0.5 mol%) were used as starting substrates. After the work-up, the residue obtained was subjected to chromatographic column (DCM/EtOAc, 100/1), yielding 71% (0.4 g) of the desired compound as a yellow oil.

^{1}H NMR (400 MHz, $CDCl_3$) δ 7.61 – 7.56 (m, 2H), 7.43 – 7.33 (m, 4H), 7.32 – 7.27 (m, 3H), 4.85 (s, 1H), 2.67 (td, J = 6.9, 5.7, 3.3 Hz, 4H), 1.88 – 1.74 (m, 4H).

^{13}C NMR (101 MHz, $CDCl_3$) δ 139.5, 134.2, 133.2, 128.7, 128.5, 128.4, 127.8, 121.8, 88.1, 85.8, 59.3, 50.5, 23.6.

The data is in accordance with the one reported in the literature.[129]

1-(1-(2,4-dichlorophenyl)-3-phenylprop-2-yn-1-yl)pyrrolidine (183)

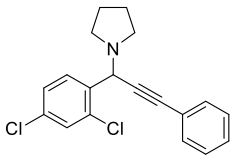

Following the general procedure: 2,4-dichlorobenzaldehyde (0.30 g, 1.7 mmol), pyrrolidine (0.15 mL, 1.7 mmol), phenylacetylene (0.19 mL, 1.7 mmol) and catalyst (3 mol%) were used as starting substrates. After the

work-up, the residue obtained was subjected to chromatographic column (Hexanes/EtOAc, 100/1) yielding 46% (0.26 g) of the desired compound as a yellow oil.

^{1}H NMR (400 MHz, $CDCl_3$) δ 7.73 (d, J = 8.4 Hz, 1H), 7.48 – 7.44 (m, 2H), 7.40 (d, J = 2.1 Hz, 1H), 7.34 – 7.30 (m, 3H), 7.28 (d, J = 2.2 Hz, 1H), 7.25 (s, 1H), 5.23 (s, 1H), 2.78 – 2.63 (m, 4H), 1.85 – 1.76 (m, 4H).

^{13}C NMR (101 MHz, $CDCl_3$) δ 136.1, 134.6, 134.0, 131.9, 131.1, 129.5, 128.4, 127.3, 122.9, 86.9, 85.9, 55.3, 50.5, 23.6.

HRMS (ESI) m/z: Calcd for $C_{19}H_{18}Cl_2N^+$ = 330.0811; Found = 330.0808

The data is in accordance with the one reported in the literature.[137]

1-(1-(2,5-dichlorophenyl)-3-phenylprop-2-yn-1-yl)pyrrolidine (132)

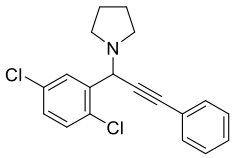

Following the general procedure: 2,5-dichlorobenzaldehyde (0.20 g, 1.1 mmol), pyrrolidine (0.09 mL, 1.1 mmol), phenylacetylene (0.12 mL, 1.1 mmol) and catalyst (3 mol%) were used as starting substrates After the work-up, the residue obtained was subjected to chromatographic column (Hexanes/EtOAc, 100/1) yielding 54% (0.20 g) of the desired compound as a yellow oil.

^{1}H NMR (400 MHz, $CDCl_3$) δ 7.91 (d, *J* = 2.5 Hz, 1H), 7.65 – 7.60 (m, 2H), 7.47 (dd, *J* = 4.1, 2.4 Hz, 3H), 7.45 (s, 1H), 7.36 (dd, *J* = 8.5, 2.6 Hz, 1H), 5.37 (s, 1H), 2.96 – 2.76 (m, 4H), 1.96 (ddd, *J* = 7.0, 4.7, 2.3 Hz, 4H).

^{13}C NMR (101 MHz, $CDCl_3$) δ 139.1, 132.7, 132.2, 131.9, 130.8, 130.1, 129.0, 128.5, 128.5, 122.9, 87.1, 85.6, 55.7, 50.5, 23.6.

HRMS (ESI) m/z: Calcd for $C_{19}H_{18}Cl_2N^+$ = 330.0811; Found = 330.0810

IR (DRIFT): 3078, 2966, 2231, 1599,1460, 1190, 980, 756, 580 cm^{-1}.

1-(1-(2-bromophenyl)-3-phenylprop-2-yn-1-yl)pyrrolidine (131)

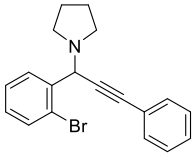

Following the general procedure: 2-bromobenzaldehyde (0.20 g, 1.1 mmol), pyrrolidine (0.09 mL, 1.1 mmol), phenylacetylene (0.12 mL, 1.1 mmol) and catalyst (3 mol%) were used as starting substrates After the work-up, the

residue obtained was subjected to chromatographic column (Hexanes/EtOAc, 100/1) yielding 57% (0.21 g) the desired compound as a yellow oil.

^{1}H NMR (400 MHz, $CDCl_3$) δ 7.80 (dd, *J* = 7.7, 1.8 Hz, 1H), 7.58 (dd, *J* = 8.0, 1.3 Hz, 1H), 7.51 – 7.45 (m, 2H), 7.37 – 7.29 (m, 4H), 7.15 (td, *J* = 7.6, 1.7 Hz, 1H), 5.27 (s, 1H), 2.87 – 2.63 (m, 4H), 1.88 – 1.74 (m, 4H).

^{13}C NMR (101 MHz, $CDCl_3$) δ 139.0, 133.1, 131.9, 130.3, 129.1, 128.3, 128.2, 127.4, 124.5, 123.2, 86.8, 86.5, 58.3, 50.4, 23.6.

HRMS (ESI) m/z: Calcd for $C_{19}H_{19}BrN^+$ = 340.0696; Found = 340.0693

The data is in accordance with the one reported in the literature.[138]

1-(1-(2,4-dichlorophenyl)-3-(4-methoxyphenyl)prop-2-yn-1-yl)pyrrolidine (184)

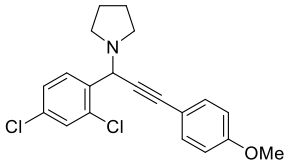

Following the general procedure: 2,4-dichlorobenzaldehyde (0.20 g, 1.1 mmol), pyrrolidine (0.09 mL, 1.1 mmol), 4-ethynilanisole (0.16 mL, 1.1 mmol) and catalyst (3 mol%) were used as starting substrates After the work-up, the residue obtained was subjected to chromatographic column (Hexanes/EtOAc, 100/1) yielding 50% (0.21 g) of the desired compound as a yellow oil.

^{1}H NMR (400 MHz, $CDCl_3$) δ 7.72 (d, *J* = 8.3 Hz, 1H), 7.44 – 7.35 (m, 3H), 7.26 (dd, *J* = 8.3, 2.2 Hz, 1H), 6.88 – 6.80 (m, 2H), 5.19 (s, 1H), 3.81 (s, 3H), 2.77 – 2.61 (m, 4H), 1.87 – 1.73 (m, 4H).

^{13}C NMR (101 MHz, $CDCl_3$) δ 159.7, 136.3, 134.6, 133.9, 133.3, 131.1, 129.5, 127.1, 115.1, 114.0, 86.7, 84.5, 55.4, 55.3, 50.5, 23.6.

HRMS (ESI) m/z: Calcd for $C_{20}H_{20}Cl_2NO^+$ = 360.0917; Found = 360.0917

IR (DRIFT): 3037, 2929, 2208, 1607, 1446, 1142, 897, 537 cm^{-1}.

1-(1-(4-methoxyphenyl)-3-phenylprop-2-yn-1-yl)pyrrolidine (133)

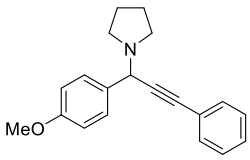

Following the general procedure: *p*-anisaldehyde (0.1 g, 0.73 mmol), pyrrolidine (0.06 mL, 0.73 mmol), phenylacetylene (0.08 mL, 0.73 mmol) and catalyst (0.5 mol%) were used as starting substrates, yielding 94% (0.20 g) of the desired compound as a yellow oil.

^{1}H NMR (400 MHz, $CDCl_3$) δ 7.58 (d, *J* = 8.5 Hz, 2H), 7.53 – 7.45 (m, 2H), 7.35 – 7.30 (m, 3H), 6.93 – 6.87 (m, 2H), 4.96 (s, 1H), 3.81 (s, 3H), 2.80 (s, 4H), 1.85 (s, 4H).

^{13}C NMR (101 MHz, $CDCl_3$) δ 159.7, 131.9, 130.0, 128.7, 128.4, 122.4, 113.9, 88.2, 84.6, 58.5, 55.3, 50.3, 23.6.

The data is in accordance with the one reported in the literature.[137]

1-(4,4-dimethyl-1-phenylpent-1-yn-3-yl)pyrrolidine (134)

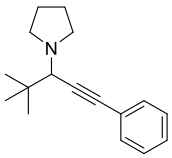

Following the general procedure: pivaldehyde (0.1 g, 1.2 mmol), pyrrolidine (0.10 mL, 1.2 mmol), phenylacetylene (0.13 mL, 1.2 mmol) and catalyst (0.5 mol%) were used as starting substrates, yielding 84% (0.24 g) of the desired compound as a yellow oil.

^{1}H NMR (400 MHz, $CDCl_3$) δ 7.46 – 7.42 (m, 2H), 7.29 (dd, *J* = 4.9, 2.3 Hz, 3H), 3.48 (s, 1H), 2.86 – 2.73 (m, 4H), 1.75 (h, *J* = 3.2 Hz, 4H), 1.07 (s, 9H).

^{13}C NMR (101 MHz, $CDCl_3$) δ 131.7, 128.2, 127.6, 123.8, 87.0, 86.9, 65.2, 51.7, 36.1, 27.7, 24.2.

The data is in accordance with the one reported in the literature.[137]

1-(4-methyl-1-phenylpent-1-yn-3-yl)pyrrolidine (135)

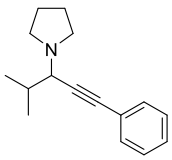

Following the general procedure: isobutyraldehyde (0.1 g, 1.4 mmol), pyrrolidine (0.11 mL, 1.4 mmol), phenylacetylene (0.15 mL, 1.4 mmol) and catalyst (0.5 mol%) were used as starting substrates, yielding 99% (0.31 g) of the desired compound as a yellow oil.

^{1}H NMR (400 MHz, $CDCl_3$) δ 7.46 – 7.41 (m, 2H), 7.31 – 7.27 (m, 3H), 3.26 (d, *J* = 8.0 Hz, 1H), 2.79 – 2.61 (m, 4H), 1.91 (dp, *J* = 8.0, 6.6 Hz, 1H), 1.84 – 1.77 (m, 4H), 1.12 (d, *J* = 6.7 Hz, 3H), 1.06 (d, *J* = 6.6 Hz, 3H).

^{13}C NMR (101 MHz, $CDCl_3$) δ 131.8, 128.3, 127.8, 123.8, 88.0, 85.6, 62.6, 50.5, 32.1, 23.7, 20.3, 19.6.

The data is in accordance with the one reported in the literature.[139]

1-(1-phenyloct-1-yn-3-yl)pyrrolidine (136)

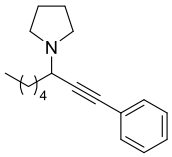

Following the general procedure: hexanal (0.1 g, 1.0 mmol), pyrrolidine (0.08 mL, 1.0 mmol), phenylacetylene (0.11 mL, 1.0 mmol) and catalyst (0.5 mol%) were used as starting substrates, yielding 93% (0.24 g) of the desired compound as a yellow oil.

^{1}H NMR (400 MHz, $CDCl_3$) δ 7.50 – 7.39 (m, 2H), 7.36 – 7.24 (m, 3H), 3.71 (t, *J* = 7.3 Hz, 1H), 2.88 – 2.63 (m, 4H), 1.86 – 1.32 (m, 12H), 0.97 – 0.86 (m, 3H).

^{13}C NMR (101 MHz, $CDCl_3$) δ 131.8, 128.3, 127.9, 123.6, 88.4, 85.4, 55.3, 49.9, 35.2, 31.8, 26.5, 23.6, 22.7, 14.2.

The data is in accordance with the one reported in the literature.[137]

1-(1-(4-methoxyphenyl)-4-methylpent-1-yn-3-yl)pyrrolidine (186)

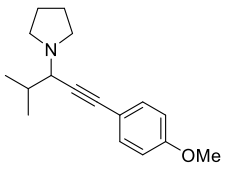

Following the general procedure: isobutyraldehyde (0.1 g, 1.4 mmol), pyrrolidine (0.11 mL, 1.4 mmol), 4-ethynylanisole (0.18 mL, 1.4 mmol) and catalyst (0.5 mol%) were used as starting substrates, yielding 99% (0.35 g) of the desired compound as a yellow oil.

^{1}H NMR (400 MHz, $CDCl_3$) δ 7.39 – 7.34 (m, 2H), 6.83 – 6.79 (m, 2H), 3.79 (s, 3H), 3.23 (d, *J* = 7.9 Hz, 1H), 2.77 – 2.69 (m, 2H), 2.65 (dtd, *J* = 7.8, 5.5, 4.8, 2.3 Hz, 2H), 1.89 (dp, *J* = 7.9, 6.6 Hz, 1H), 1.78 (h, *J* = 3.0 Hz, 4H), 1.10 (d, *J* = 6.7 Hz, 3H), 1.05 (d, *J* = 6.7 Hz, 3H).

^{13}C NMR (101 MHz, $CDCl_3$) δ 173.7, 147.6, 130.4, 128.4, 100.7, 99.8, 77.2, 69.8, 64.9, 46.5, 38.1, 34.8, 33.9.

The data is in accordance with the one reported in the literature.[140]

1-(1-(4-methoxyphenyl)oct-1-yn-3-yl)pyrrolidine (187)

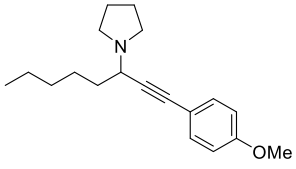

Following the general procedure: hexanal (0.1 g, 1.0 mmol), pyrrolidine (0.08 mL, 1.0 mmol), 4-ethynylanisole (0.13 mL, 1.0

mmol) and catalyst (0.5 mol%) were used as starting substrates, yielding 90% (0.26 g) of the desired compound as a yellow oil.

^{1}H NMR (400 MHz, $CDCl_3$) δ 7.37 – 7.32 (m, 2H), 6.83 – 6.78 (m, 2H), 3.79 (s, 3H), 3.65 (dd, *J* = 8.8, 5.9 Hz, 1H), 2.75 (qt, *J* = 4.3, 1.9 Hz, 2H), 2.68 (ddd, *J* = 6.6, 5.0, 2.3 Hz, 2H), 1.84 – 1.75 (m, 4H), 1.74 – 1.66 (m, 2H), 1.63 – 1.42 (m, 2H), 1.38 – 1.27 (m, 4H), 0.93 – 0.85 (m, 3H).

^{13}C NMR (101 MHz, $CDCl_3$) δ 159.3, 133.2, 115.8, 113.9, 86.8, 85.1, 55.3, 55.3, 49.8, 35.21, 31.8, 26.5, 23.6, 22.7, 14.2.

The data is in accordance with the one reported in the literature.[141]

1-(1,3-bis(4-methoxyphenyl)prop-2-yn-1-yl)pyrrolidine (188)

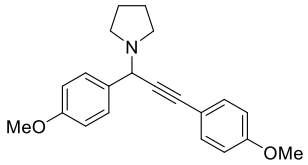

Following the general procedure: *p*-anisaldehyde (0.15 g, 1.1 mmol), pyrrolidine (0.09 mL, 1.1 mmol), 4-ethynylanisole (0.16 mL, 1.1 mmol) and catalyst (0.5 mol%) were used as starting substrates, yielding 92% (0.33 g) of the desired compound as a yellow oil.

^{1}H NMR (400 MHz, $CDCl_3$) δ 7.61 – 7.55 (m, 2H), 7.44 – 7.40 (m, 2H), 6.92 – 6.88 (m, 2H), 6.87 – 6.83 (m, 2H), 4.96 (s, 1H), 3.81 (s, 3H), 3.81 (s, 3H), 2.81 (s, 4H), 1.86 (td, *J* = 6.0, 3.5 Hz, 4H).

^{13}C NMR (101 MHz, $CDCl_3$) δ 159.8, 159.5, 133.7, 133.3, 129.8, 114.1, 114.0, 113.9, 87.9, 84.1, 58.8, 55.4, 55.4, 50.5, 23.7.

HRMS (ESI) m/z: Calcd for $C_{21}H_{24}NO_2^+$ = 322.1802; Found = 322.1804

IR (DRIFT): 3059, 2962, 2235, 1720, 1469, 1194, 981, 573 cm^{-1}.

1-(1-cyclohexyl-3-phenylprop-2-in-2-yl)piperidine (137)

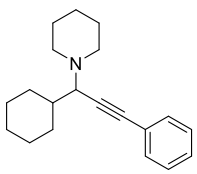

Following the general procedure: cyclohexanecarboxaldehyde (0.17 mL, 1.5 mmol), piperidine (0.13 mL, 1.5 mmol), phenylacetylene (0.21 mL, 1.5 mmol) and catalyst (0.5 mol%) were used as starting substrates, yielding 85% (0.36 g) of the desired compound as a transparent oil.

^{1}H NMR (300 MHz, $CDCl_3$) δ 7.47 – 7.49 (m, 2H), 7.30 – 7.32 (m, 3H), 3.14 (d, 1H, *J* = 9.9 Hz), 2.63 – 2.71 (m, 2H), 2.41 – 2.48 (m, 2H), 2.16 – 2.17 (m, 2H), 0.90 – 1.82 (m, 15H).

^{13}C NMR (151 MHz, $CDCl_3$) δ 131.8, 128.3, 127.7, 123.9, 87.8, 86.3, 64.5, 50.9, 39.7, 31.5, 30.5, 26.9, 26.4, 26.4, 26.2, 24.9.

The data is in accordance with the one reported in the literature.[129]

1-(3-(4-methoxyphenyl)-1-phenylprop-2-yn-1-yl)piperidine (179)

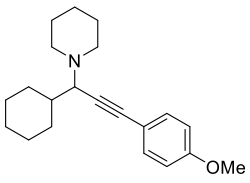

Following the general procedure: cyclohexanecarboxaldehyde (0.17 g, 1.5 mmol), piperidine (0.13 g, 1.5 mmol), and 4-ethynilanisole (0.19 g, 1.5 mmol) were used as starting substrates, yielding 86% (0.40 g) of the desired compound as a yellow crystalline solid.

^{1}H NMR (400 MHz, $CDCl_3$) δ 7.39 (d, *J* = 8.8 Hz, 2H), 6.83 (d, *J* = 8.8 Hz, 2H), 3.80 (s, 3H), 3.10 (d, *J* = 9.9 Hz, 1H), 2.70 – 2.59 (m, 2H), 2.46 – 2.36 (m, 2H), 2.17 – 2.01 (m, 2H), 1.83 – 1.74 (m, 2H), 1.67 – 1.53 (m, 5H), 1.50 – 1.41 (m, 2H), 1.34 – 1.16 (m, 4H), 1.09 – 0.88 (m, 2H).

^{13}C NMR (101 MHz, $CDCl_3$) δ 159.2, 133.1, 116.1, 113.9, 86.2, 86.0, 64.5, 55.3, 50.9, 39.7, 31.4, 30.6, 26.9, 26.4 (3C), 26.2, 24.9.

The data is in accordance with the one reported in the literature.[142]

1-(1-(2,4-dichlorophenyl)-3-phenylprop-2-yn-1-yl)piperidine (189)

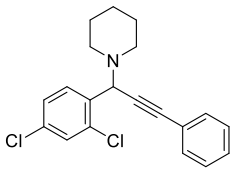

Following the general procedure: 2,4-dichlorobenzaldehyde (0.20 g, 1.1 mmol), piperidine (0.11 mL, 1.1 mmol), phenylacetylene (0.13 mL, 1.1 mmol) and catalyst (3 mol%) were used as starting substrates. After the work-up, the residue obtained was subjected to chromatographic column (Hexanes/EtOAc, 100/1) yielding 68% (0.27 g) of the desired compound as a yellow oil.

^{1}H NMR (400 MHz, $CDCl_3$) δ 7.68 (d, *J* = 8.3 Hz, 1H), 7.52 – 7.46 (m, 2H), 7.41 (d, *J* = 2.2 Hz, 1H), 7.33 (dt, *J* = 4.8, 1.7 Hz, 3H), 7.24 (d, *J* = 2.1 Hz, 1H), 5.02 (s, 1H), 2.57 (t, *J* = 5.4 Hz, 4H), 1.56 (tq, *J* = 12.8, 7.2, 6.7 Hz, 4H), 1.42 (p, *J* = 5.8 Hz, 2H).

^{13}C NMR (101 MHz, $CDCl_3$) δ 135.5, 135.4, 134.0, 131.9, 131.5, 129.7, 128.4, 128.4, 126.6, 123.1, 88.2, 85.3, 59.0, 50.9, 26.2, 24.5.

The data is in accordance with the one reported in the literature.[143]

1-(1-(2,5-dichlorophenyl)-3-phenylprop-2-yn-1-yl)piperidine (190)

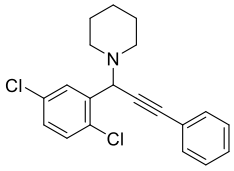

Following the general procedure: 2,5-dichlorobenzaldehyde (0.20 g, 1.7 mmol), piperidine (0.11 mL, 1.1 mmol), phenylacetylene (0.12 mL, 1.1 mmol) and catalyst (3 mol%) were used as starting substrates. After the work-up, the residue obtained was subjected to chromatographic column (Hexanes/EtOAc, 100/1) yielding 45% (0.18 g) of the desired compound as a yellow oil.

^{1}H NMR (400 MHz, $CDCl_3$) δ 7.72 (d, *J* = 2.6 Hz, 1H), 7.53 – 7.48 (m, 2H), 7.35 – 7.32 (m, 3H), 7.31 (s, 1H), 7.22 (dd, *J* = 8.5, 2.5 Hz, 1H), 5.03 (s, 1H), 2.59 (t, *J* = 5.5 Hz, 4H), 1.57 (tt, *J* = 11.1, 6.0 Hz, 4H), 1.44 (q, *J* = 5.7 Hz, 2H).

^{13}C NMR (101 MHz, $CDCl_3$) δ 138.43, 133.05, 132.36, 131.99, 130.99, 130.53, 128.94, 128.47, 122.99, 88.39, 84.92, 59.35, 50.93, 26.23, 24.52.

HRMS (ESI) m/z: Calcd for $C_{20}H_{20}Cl_2N^+$ = 344.0968; Found = 344.0965

IR (DRIFT): 3059, 2962, 2222, 1722, 1489, 1194, 980, 825, 690, 492 cm^{-1}.

1-(1-(2-bromophenyl)-3-phenylprop-2-yn-1-yl)piperidine (191)

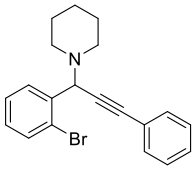

Following the general procedure: 2-bromobenzaldehyde (0.15 g, 0.8 mmol), piperidine (0.08 mL, 0.8 mmol), phenylacetylene (0.09 mL, 0.8 mmol) and catalyst (3 mol%) were used as starting substrates. After the work-up, the residue obtained was subjected to chromatographic column (Hexanes/EtOAc, 100/1) yielding 34% (0.1 g) of the desired compound as a yellow oil.

^{1}H NMR (400 MHz, $CDCl_3$) δ 7.77 (d, *J* = 7.8 Hz, 1H), 7.59 (d, *J* = 7.9 Hz, 1H), 7.54 – 7.48 (m, 2H), 7.37 – 7.28 (m, 4H), 7.16 (td, *J* = 7.7, 1.7 Hz, 1H), 5.05 (s, 1H), 2.62 (s, 4H), 1.57 (qt, *J* = 12.7, 6.3 Hz, 4H), 1.45 (q, *J* = 5.8 Hz, 2H).

^{13}C NMR (101 MHz, $CDCl_3$) δ 133.27, 131.91, 131.89, 130.80, 129.15, 128.40, 128.26, 126.91, 125.40, 123.27, 88.13, 85.79, 61.80, 50.77, 26.24, 24.59.

The data is in accordance with the one reported in the literature.[138]

1-(3-(4-methoxyphenyl)-1-phenylprop-2-yn-1-yl)piperidine (192)

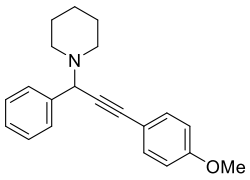

Following the general procedure: benzaldehyde (0.12 mL,1.2 mmol), piperidine (0.12 mL, 1.2 mmol), 4-ethynilanisole (0.15 mL, 1.2 mmol) and catalyst (0.5 mol%) were used as starting substrates, yielding 86% (0.31 g) of the desired compound as a yellow oil.

^{1}H NMR (400 MHz, $CDCl_3$) δ 7.66 (d, *J* = 6.8 Hz, 2H), 7.48 – 7.43 (m, 2H), 7.40 – 7.34 (m, 2H), 7.33 – 7.28 (m, 1H), 6.89 – 6.84 (m, 2H), 4.83 (s, 1H), 3.82 (s, 3H), 2.60 (s, 4H), 1.61 (dq, *J* = 12.9, 7.3, 6.1 Hz, 4H).

^{13}C NMR (101 MHz, $CDCl_3$) δ 159.6, 133.7, 133.3, 128.8, 128.2, 127.7, 114.1, 114.0, 88.0, 83.8, 62.5, 55.4, 50.8, 26.1, 24.4.

The data is in accordance with the one reported in the literature.[140]

1-(1-(2,4-dichlorophenyl)-3-(4-methoxyphenyl)prop-2-yn-1-yl)piperidine(193)

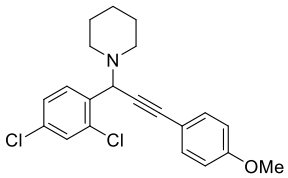

Following the general procedure: 2,4-dichlorobenzaldehyde (0.15 g, 0.9 mmol), piperidine (0.09 mL, 0.9 mmol), 4-ethynilanisole (0.11 mL, 0.9 mmol) and catalyst (3 mol%) were used as starting substrates After the work-up, the residue obtained was subjected to chromatographic column (Hexanes/EtOAc, 100/1) yielding 75% (0.24 g) of the desired compound as a yellow oil.

^{1}H NMR (400 MHz, $CDCl_3$) δ 7.67 (d, *J* = 8.3 Hz, 1H), 7.43 – 7.39 (m, 3H), 7.24 (dd, *J* = 8.5, 2.3 Hz, 1H), 6.85 (d, *J* = 8.8 Hz, 2H), 5.00 (s, 1H), 3.82 (s, 3H), 2.61 – 2.51 (m, 4H), 1.54 (tq, *J* = 12.9, 6.9 Hz, 4H), 1.42 (p, *J* = 5.9 Hz, 2H).

^{13}C NMR (101 MHz, $CDCl_3$) δ 159.7, 135.6, 135.4, 133.9, 133.3, 131.5, 129.6, 126.6, 115.2, 114.1, 87.9, 83.8, 59.0, 55.5, 26.2, 24.5.

HRMS (ESI) m/z: Calcd for $C_{21}H_{22}Cl_2NO^+$ = 374.1073; Found = 374.1067

IR (DRIFT): 3074, 2935, 2208, 1678, 1508, 1381, 1173, 924, 829, 594 cm^{-1}

1-(1-(4-methoxyphenyl)-3-phenylprop-2-yn-1-yl)piperidine (194)

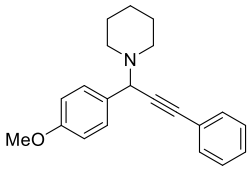

Following the general procedure: *p*-anisaldehyde (0.15 g, 1.1 mmol), piperidine (0.11 mL, 1.1 mmol), phenylacetylene (1.2 mL, 1.1 mmol) and catalyst (0.5 mol%) were used as starting substrates, yielding 65% (0.22 g) of the desired compound as a yellow oil.

^{1}H NMR (400 MHz, $CDCl_3$) δ 7.57 – 7.48 (m, 4H), 7.33 (td, *J* = 3.8, 1.9 Hz, 3H), 7.26 (d, *J* = 1.3 Hz, 1H), 6.93 – 6.86 (m, 2H), 4.75 (s, 1H), 3.82 (d, *J* = 1.4 Hz, 3H), 2.57 (q, *J* = 5.7 Hz, 4H), 1.59 (h, *J* = 6.8 Hz, 4H), 1.51 – 1.39 (m, 2H).

^{13}C NMR (101 MHz, $CDCl_3$) δ 159.1, 131.9, 129.8, 128.4, 128.1, 123.5, 113.5, 87.8, 86.5, 61.9, 55.4, 26.3, 24.6.

The data is in accordance with the one reported in the literature.[144]

1-(1-phenyloct-1-yn-3-yl)piperidine (195)

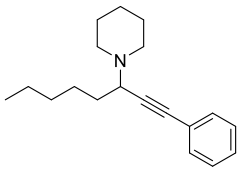

Following the general procedure: hexanal (0.1 g, 1.0 mmol), piperidine (0.10 mL, 1.0 mmol), 4-ethynylanisole (0.11 mL, 1.0 mmol) and catalyst (0.5 mol%) were used as starting substrates, yielding 95% (0.26 g) of the desired compound as a yellow oil.

^{1}H NMR (400 MHz, $CDCl_3$) δ 7.47 – 7.40 (m, 2H), 7.34 – 7.26 (m, 3H), 3.48 (dd, *J* = 9.2, 5.7 Hz, 1H), 2.69 (ddd, *J* = 11.0, 7.2, 3.7 Hz, 2H), 2.49 (td, *J* = 7.2, 3.7 Hz, 2H), 1.71 – 1.53 (m, 6H), 1.46 (dd, *J* = 7.9, 4.2 Hz, 2H), 1.39 – 1.30 (m, 4H), 0.96 – 0.86 (m, 3H).

^{13}C NMR (101 MHz, $CDCl_3$) δ 131.8, 128.3, 127.8, 123.8, 88.4, 85.7, 58.8, 50.7, 33.6, 31.8, 26.7, 26.3, 24.7, 22.7, 14.2.

The data is in accordance with the one reported in the literature.[145]

1-(4-methyl-1-phenylpent-1-yn-3-yl)piperidine (196)

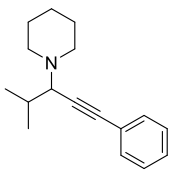

Following the general procedure: isobutyraldehyde (0.1 g, 1.4 mmol), piperidine (0.14 mL, 1.4 mmol), 4-ethynylanisole (0.15 mL, 1.4 mmol) and catalyst (0.5 mol%) were used as starting substrates, yielding 93% (0.31 g) of the desired compound as a yellow oil.

^{1}H NMR (400 MHz, $CDCl_3$) δ 7.48 – 7.42 (m, 2H), 7.33 – 7.26 (m, 3H), 2.99 (d, *J* = 9.8 Hz, 1H), 2.64 (m, 2H), 2.42 (m, 2H), 1.92 (dp, *J* = 9.9, 6.6 Hz, 1H), 1.68 – 1.52 (m, 4H), 1.45 (p, *J* = 5.9 Hz, 2H), 1.11 (d, *J* = 6.6 Hz, 3H), 1.02 (d, *J* = 6.6 Hz, 3H).

^{13}C NMR (101 MHz, $CDCl_3$) δ 131.8, 128.3, 127.7, 123.9, 88.0, 86.1, 65.8, 50.9, 30.5, 26.46, 24.9, 20.8, 20.0.

The data is in accordance with the one reported in the literature.[146]

4-(1-cyclohexyl-3-phenylprop-2-in-2-yl)morpholine (138)

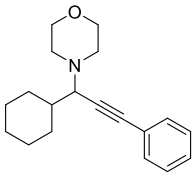

Following the general procedure: cyclohexanecarboxaldehyde (0.17 mL, 1.5 mmol), morpholine (0.13 mL, 1.5 mmol) phenylacetylene (0.21 mL, 1.5 mmol) and catalyst (0.5 mol%) were used as starting substrates, yielding 77% (0.32 g) of the desired compound as a white crystalline substance.

^{1}H NMR (400 MHz, $CDCl_3$) δ 7.44 (m, 2H), 7.30 (d, 2H, *J* = 5.4 Hz), 3.75 (m, 4H), 3.13 (d, 1H, *J* = 9.6 Hz), 2.70 (m, 2H), 2.52 (m, 2H), 2.11 (d, 1H, *J* = 12.6 Hz), 2.05 (d, 1H, *J* = 13.4 Hz), 1.77 (m, 2H), 1.69 (m, 1H), 1.60 (m, 1H), 1.25 (m, 3H), 1.01 (m, 2H).

^{13}C NMR (151 MHz, $CDCl_3$) δ 131.9, 128.3, 128.0, 123.6, 86.9, 86.8, 67.4, 64.1, 39.2, 31.1, 30.5, 27.1, 26.9, 26.3, 26.2.

The data is in accordance with the one reported in the literature.[129]

4-(1-cyclohexyl-3-(4-methoxyphenyl)prop-2-yn-1-yl)morpholine (178).

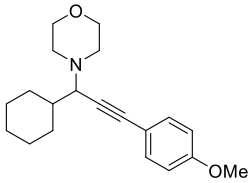

Following the general procedure: cyclohexanecarboxaldehyde (0.17 mL, 1.5 mmol), morpholine (0.13 mL, 1.5 mmol) 4-ethynilanisole (0.21 mL, 1.5 mmol) and catalyst (0.5 mol%) were used as starting substrates, yielding 94% (0.42 g) of the desired compound as a transparent oil.

^{1}H NMR (400 MHz, $CDCl_3$) δ 7.39 (d, *J* = 8.8 Hz, 2H), 6.84 (d, *J* = 8.8 Hz, 2H), 3.83 – 3.68 (m, 7H), 3.13 (d, *J* = 9.8 Hz, 1H), 2.79 – 2.65 (m, 2H), 2.57 – 2.46 (m, 2H), 2.17 – 1.99 (m, 2H), 1.83 – 1.55 (m, 4H), 1.30 – 0.93 (m, 5H).

^{13}C NMR (101 MHz, $CDCl_3$) δ 159.3, 133.1, 115.7, 113.9, 86.6, 85.1, 67.3, 64.1, 55.3, 50.0, 39.2, 31.1, 30.4, 26.8, 26.3, 26.1.

The data is in accordance with the one reported in the literature.[141]

4-(1-cyclohexyl-3-(2-methoxyphenyl)prop-2-yn-1-yl)morpholine (197)

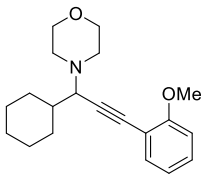

Following the general procedure: cyclohexanecarboxaldehyde (0.17 g, 1.5 mmol), morpholine (0.13 g, 1.5 mmol), and 2-methoxyphenylacetylene (0.2 g, 1.5 mmol) and catalyst (0.5 mol%) were used as starting substrates, yielding 63% (0.30 g) of the desired compound as a transparent oil.

^{1}H NMR (400 MHz, $CDCl_3$) δ 7.43 (dd, *J* = 7.6, 1.8 Hz, 1H), 7.32 – 7.23 (m, 1H), 6.96 – 6.84 (m, 2H), 3.89 (s, 3H), 3.84 – 3.61 (m, 4H), 3.21 (d, *J* = 9.8 Hz, 1H), 2.75 (s, 2H), 2.63 – 2.40 (m, 2H), 2.26 – 2.01 (m, 2H), 1.83 – 1.60 (m, 4H), 1.36 – 1.02 (m, 5H).

^{13}C NMR (101 MHz, $CDCl_3$) δ 160.2, 133.6, 129.3, 120.4, 112.8, 110.8, 91.2, 82.9, 67.4, 64.3, 55.9, 50.0, 39.3, 31.0, 30.5, 26.9, 26.3, 26.2.

HRMS (ESI): Calcd for $C_{20}H_{28}NO_2^+$: 314.2114; Found: 314.2109.

4-(3-(4-((tert-butyldimethylsilyl)oxy)phenyl)-1-cyclohexylprop-2-yn-1-yl)morpholine (198)

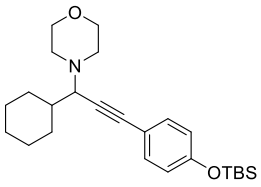

Following the general procedure: cyclohexanecarboxaldehyde (0.17 g, 1.5 mmol), morpholine (0.13 mg, 1.5 mmol), and tert-butyl(4-ethynylphenoxy)dimethylsilane (0.35 g, 1.5 mmol) and catalyst (0.5 mol%) were used as starting substrates, yielding 51% (0.32 g) of the desired compound as a transparent oil.

^{1}H NMR (400 MHz, $CDCl_3$) δ 7.33 (d, *J* = 8.6 Hz, 2H), 6.78 (d, *J* = 8.6 Hz, 2H), 3.84 – 3.68 (m, 4H), 3.13 (d, *J* = 9.8 Hz, 1H), 2.76 – 2.66 (m, 2H), 2.57 – 2.47 (m, 2H), 2.17 – 2.01 (m, 2H), 1.83 – 1.56 (m, 5H), 1.20-1.10 (s, 4H), 1.05-1.10 (s, 9H), 0.21 (s, 6H).

^{13}C NMR (101 MHz, $CDCl_3$) δ 155.7, 133.2, 120.2, 116.4, 86.7, 85.3, 67.4, 64.1, 39.3, 31.1, 30.5, 26.9, 26.3, 26.2, 25.8, 18.4, -4.3.

HRMS (ESI) m/z: Calcd for $C_{25}H_{40}NO_2Si^+$: 414.2822; Found: 414.2819.

1-(1-cyclohexyl-3-phenylprop-2-yn-1-yl)azepane (176)

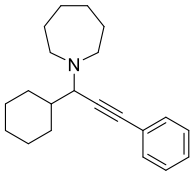

Following the general procedure: cyclohexanecarboxaldehyde (0.17 g, 1.5 mmol), azepane (0.15 g, 1.5 mmol), and phenylacetylene (0.15 g, 1.5 mmol) and catalyst (0.5 mol%) were used as starting substrates, yielding 82% (0.37 g) of the desired compound as a yellow oil.

^{1}H NMR (400 MHz, $CDCl_3$) δ 7.49 – 7.39 (m, 2H), 7.34 – 7.27 (m, 3H), 3.18 (d, *J* = 10.1 Hz, 1H), 2.88 – 2.76 (m, 2H), 2.65 – 2.54 (m, 2H), 2.25 – 2.06 (m, 2H), 1.83 – 1.57 (m, 11H), 1.58 – 1.46 (m, 1H), 1.35 – 1.15 (m, 3H), 1.07 – 0.86 (m, 2H).

^{13}C NMR (101 MHz, $CDCl_3$) δ 131.8, 128.3, 127.6, 124.1, 89.1, 85.0, 65.4, 52.8, 40.9, 31.3, 30.8, 29.4, 27.3, 27.0, 26.4, 26.2.

The data is in accordance with the one reported in the literature.[141]

1-(1-cyclohexyl-3-(4-methoxyphenyl)prop-2-yn-1-yl)azepane (177)

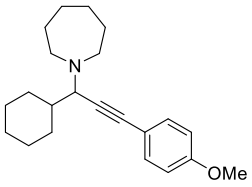

Following the general procedure: cyclohexanecarboxaldehyde (0.17 g, 1.5 mmol), azepane (0.15 g, 1.5 mmol), and 4-ethynilanisole (0.20 g, 1.5 mmol), yielding 76% (0.37 g) of the desired compound as a yellow crystalline substance.

^{1}H NMR (400 MHz, $CDCl_3$) δ 7.35 (d, *J* = 8.8 Hz, 2H), 6.81 (d, *J* = 8.8 Hz, 2H), 3.80 (s, 3H), 3.13 (d, *J* = 10.0 Hz, 1H), 2.83 – 2.72 (m, 2H), 2.60 – 2.50 (m, 2H), 2.20 – 2.04 (m, 2H), 1.77 – 1.56 (m, 11H), 1.54 – 1.44 (m, 1H), 1.31 – 1.12 (m, 3H), 1.04 – 0.83 (m, 2H).

^{13}C NMR (101 MHz, $CDCl_3$) δ 159.2, 133.2, 116.3, 113.9, 87.4, 84.7, 65.4, 55.4, 52.8, 41.0, 31.3, 30.8, 29.4, 27.3, 27.0, 26.4, 26.2.

The data is in accordance with the one reported in the literature.[141]

1-(1,3-diphenylprop-2-yn-1-yl)azepane (139)

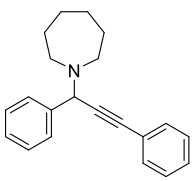

Following the general procedure: benzaldehyde (0.10 g, 0.9 mmol), azepane (0.11 ml, 0.9 mmol), and phenylacetylene (0.10 ml, 0.9 mmol), yielding 90% (0.25 g) of the desired compound as a transparent oil.

^{1}H NMR (400 MHz, $CDCl_3$) δ 7.75 – 7.70 (m, 2H), 7.56 – 7.50 (m, 2H), 7.39 – 7.28 (m, 6H), 4.95 (s, 1H), 2.76 (dd, *J* = 6.4, 4.0 Hz, 4H), 1.74 – 1.59 (m, 8H).

^{13}C NMR (101 MHz, $CDCl_3$) δ 131.9, 129.1, 128.4, 128.4, 128.1, 127.5, 123.5, 87.3, 86.8, 62.8, 52.8, 31.0, 29.0, 27.1.

The data is in accordance with the one reported in the literature.[147]

1-(1-(2,4-dichlorophenyl)-3-phenylprop-2-yn-1-yl)azepane (199)

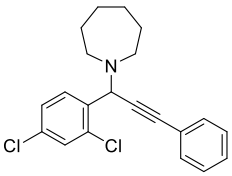

Following the general procedure: 2,4-dichlorobenzaldehyde (0.18 g, 1.0 mmol), azepane (0.11 ml, 1.0 mmol), and phenylacetylene (0.11 ml, 1.0 mmol), yielding 88% (0.31 g) of the desired compound as a yellow oil.

^{1}H NMR (400 MHz, $CDCl_3$) δ 7.71 (d, *J* = 8.3 Hz, 1H), 7.52 – 7.46 (m, 2H), 7.40 (d, *J* = 2.1 Hz, 1H), 7.33 (ddd, *J* = 4.5, 2.7, 1.4 Hz, 3H), 7.26 – 7.22 (m, 1H), 5.07 (s, 1H), 2.74 (ddd, *J* = 7.4, 4.8, 2.0 Hz, 4H), 1.69 – 1.43 (m, 8H).

^{13}C NMR (101 MHz, $CDCl_3$) δ 136.2, 135.7, 133.8, 131.9, 131.2, 129.7, 128.4, 128.4, 128.35, 126.5, 123.2, 87.5, 85.9, 59.3, 51.9, 31.0, 29.1, 27.2.

HRMS (ESI) m/z: Calcd for $C_{21}H_{22}Cl_2N^+$ = 358.1124; Found = 358.1130

IR (DRIFT): 3059, 2929, 2206, 1716, 1585, 1442, 1068, 773, 567 cm^{-1}.

1-(1-(2,4-dichlorophenyl)-3-(4-methoxyphenyl)prop-2-yn-1-yl)azepane (200)

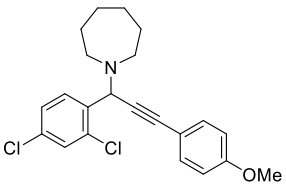

Following the general procedure: 2,4-dichlorobenzaldehyde (0.18 g, 1.0 mmol), azepane (0.11 ml, 1.0 mmol), and 4-ethynilanisole (0.13 g, 1.0 mmol), yielding 88% (0.34 g) of the desired compound as a yellow oil.

^{1}H NMR (400 MHz, $CDCl_3$) δ 7.71 (d, *J* = 8.3 Hz, 1H), 7.43 – 7.38 (m, 3H), 7.23 (dd, *J* = 8.3, 2.2 Hz, 1H), 6.87 – 6.84 (m, 2H), 5.05 (s, 1H), 3.82 (s, 3H), 2.73 (m, 4H), 1.68 – 1.40 (m, 8H).

^{13}C NMR (101 MHz, $CDCl_3$) δ 159.68, 135.70, 133.77, 133.71, 133.31, 131.24, 129.70, 126.49, 115.28, 114.06, 87.34, 84.31, 59.28, 55.44, 51.88, 31.05, 29.11, 27.23.

HRMS (ESI) m/z: Calcd for $C_{22}H_{24}Cl_2NO^+$ = 388.1230; Found = 388.1229

IR (DRIFT): 3037, 2929, 2208, 1604, 1508, 1325, 1070, 806, 741, 498 cm^{-1}.

6.6. KA^2 coupling reaction

General procedure: To a pressure vial, containing the catalyst (2.5 mol%) and 4 Å sieves, were loaded the ketone (1 eq.), amine (1 eq.), and acetylene (1 eq.). The reaction was stirred for 4 hours at 110 ºC in neat conditions. Afterwards, the mixture was dissolved in EtOAc (10 mL) and filtered to remove the catalyst. The crude mixture was purified by column chromatography.

1-(1-(phenylethynyl)cyclohexyl)pyrrolidine (150)

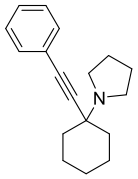

Following the general protocol: cyclohexanone (1.05 ml, 10.2 mmol), pyrrolidine (0.84 ml, 10.2 mmol), phenylacetylene (1.12 ml, 10.2 mmol) and catalyst (167 mg, 0.25mmol). Purification through column chromatography (100/1 to 1/1, Hexanes/EtOAc) yielded the title compound (2.50 g, 9.87 mmol) as an orange oil.

^{1}H NMR (400 MHz, $CDCl_3$) δ 7.46 – 7.42 (m, 2H), 7.31 – 7.27 (m, 3H), 2.80 (td, *J* = 5.7, 4.5, 2.7 Hz, 4H), 2.04 (dd, *J* = 11.1, 3.4 Hz, 2H), 1.83 – 1.76 (m, 4H), 1.73 – 1.61 (m, 6H), 1.53 (td, *J* = 11.7, 4.9 Hz, 2H).

^{13}C NMR (101 MHz, $CDCl_3$) δ 131.7, 128.2, 127.6, 123.7, 90.4, 86.1, 59.3, 47.1, 37.9, 25.7, 23.6, 23.1.

The results are in accordance with the literature.[103]

1-(1-((4-methoxyphenyl)ethynyl)cyclohexyl)pyrrolidine (151)

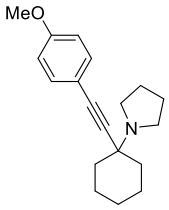

Following the general protocol: cyclohexanone (0.16 ml, 1.53 mmol), pyrrolidine (0.13 ml, 1.53 mmol), 4-ethynylanisole (202 mg, 1.53 mmol) and catalyst (21.0 mg, 0.04 mmol). Purification through column chromatography (100/1 to 1/1, Hexanes/EtOAc) yielded the title compound (406 mg, 1.43 mmol) as a yellow oil.

^{1}H NMR (400 MHz, DMSO) δ 7.32 (d, *J* = 8.8 Hz, 2H), 6.90 (d, *J* = 8.8 Hz, 2H), 3.75 (s, 3H), 2.65 (td, *J* = 5.4, 4.3, 2.5 Hz, 4H), 1.90 – 1.81 (m, 2H), 1.71 – 1.65 (m, 4H), 1.64 – 1.43 (m, 7H), 1.26 (d, *J* = 11.6 Hz, 1H).

^{13}C NMR (101 MHz, DMSO) δ 158.9, 132.8, 114.8, 114.1, 89.0, 84.9, 58.1, 55.2, 46.4, 37.3, 25.2, 23.2, 22.2.

The results are in accordance with the literature.[103]

1-(1-((4-(trifluoromethyl)phenyl)ethynyl)cyclohexyl)pyrrolidine

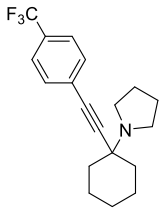

Following the general protocol: cyclohexanone (0.16 ml, 1.53 mmol), pyrrolidine (0.13 ml, 1.53 mmol), 4-(trifluoromethyl)phenylacetylene (0.25 ml, 1.53 mmol) and catalyst (21.0 mg, 0.04 mmol). Purification through column chromatography (100/1 to 1/1, Hexanes/EtOAc) yielded the title compound (427 mg, 1.33 mmol) as a yellow oil.

^{1}H NMR (400 MHz, DMSO) δ 7.71 (d, *J* = 8.8 Hz, 2H), 7.61 (dt, *J* = 7.7, 0.9 Hz, 2H), 2.68 (td, *J* = 5.2, 4.4, 2.3 Hz, 4H), 1.90 (dd, *J* = 9.8, 5.8 Hz, 2H), 1.75 – 1.67 (m, 4H), 1.67 – 1.45 (m, 7H), 1.28 (d, *J* = 10.0 Hz, 1H).

^{13}C NMR (101 MHz, DMSO) δ 132.2, 125.5, 125.5, 125.4, 125.4, 94.1, 84.0, 58.3, 46.4, 37.1, 25.1, 23.2, 22.1.

The results are in accordance with the literature.[102]

1-(1-((2-methoxynaphthalen-1-yl)ethynyl)cyclohexyl)pyrrolidine (153)

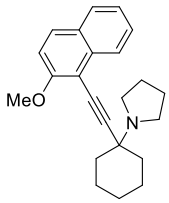

Following the general protocol: cyclohexanone (0.11 ml, 1.02 mmol), pyrrolidine (0.09 ml, 1.02 mmol), 1-ethynyl-2-methoxynaphthalene (185 mg, 1.02 mmol) and catalyst (14.1 mg, 0.03 mmol). Purification through column chromatography (100/1 to 1/1, Hexanes/EtOAc) yielded the title compound (199 mg, 0.60 mmol) as a yellow oil.

^{1}H NMR (400 MHz, $CDCl_3$) δ 8.26 (dd, *J* = 8.6, 1.2 Hz, 1H), 7.77 (dd, *J* = 8.8, 2.4 Hz, 2H), 7.53 (ddd, *J* = 8.3, 6.8, 1.3 Hz, 1H), 7.40 – 7.33 (m, 1H), 7.24 (d, *J* = 9.1 Hz, 1H), 3.99 (s, 3H), 3.05 – 2.89 (m, 4H), 2.18 (dt, *J* = 12.5, 2.7 Hz, 2H), 1.91 – 1.59 (m, 12H).

^{13}C NMR (101 MHz, $CDCl_3$) δ 159.2, 134.7, 129.4, 128.7, 128.2, 127.2, 125.4, 124.2, 113.3, 107.2, 100.2, 80.3, 60.7, 60.5, 56.9, 47.5, 38.1, 25.9, 23.8, 23.4.

HRMS (ESI) m/z: Calcd for $C_{23}H_{28}NO^+$ = 334.2166; Found = 334.2165

IR (DRIFT): 3074, 2906, 2208, 1597, 1442, 1053, 754, 542 cm^{-1}.

2-methyl-4-(1-(pyrrolidin-1-yl)cyclohexyl)but-3-yn-2-ol (154)

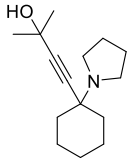

Following the general protocol: cyclohexanone (0.11 ml, 1.02 mmol), pyrrolidine (0.09 ml, 1.02 mmol), 2-methylbut-3-yn-2-ol (0.10 ml, 1.02 mmol) and catalyst (14.1 mg, 0.03 mmol). Purification through column chromatography (100/1 to 1/1, Hexanes/EtOAc) yielded the title compound (235 mg, 1.00 mmol) as an orange oil.

^{1}H NMR (400 MHz, $CDCl_3$) δ 2.66 – 2.54 (m, 4H), 2.29 – 2.18 (m, 1H), 1.82 – 1.76 (m, 2H), 1.69 – 1.64 (m, 4H), 1.52 (d, *J* = 4.7 Hz, 4H), 1.44 (s, 6H), 1.41 – 1.27 (m, 3H), 1.15 – 1.04 (m, 1H).

^{13}C NMR (101 MHz, $CDCl_3$) δ 91.3, 81.9, 64.9, 46.8, 37.7, 32.2, 25.6, 23.4, 22.9.

The results are in accordance with the literature.[103]

1-(2-methyl-4-phenylbut-3-yn-2-yl)pyrrolidine (155)

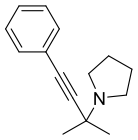

Following the general protocol: acetone (0.13 ml, 1.72 mmol), pyrrolidine (0.14 ml, 1.72 mmol), phenylacetylene (0.19 ml, 1.72 mmol) and catalyst (23.8 mg, 0.04 mmol). Purification through column chromatography (100/1 to 1/1, Hexanes/EtOAc) yielded the title compound (328 mg, 1.54 mmol) as a colourless oil.

^{1}H NMR (400 MHz, $CDCl_3$) δ 7.43 – 7.39 (m, 2H), 7.31 – 7.27 (m, 3H), 2.89 – 2.80 (m, 4H), 1.87 – 1.81 (m, 4H), 1.52 (s, 6H).

^{13}C NMR (101 MHz, $CDCl_3$) δ 131.9, 128.3, 128.0, 123.4, 91.1, 84.3, 48.5, 29.6, 23.9.

The results are in accordance with the literature.[148]

1-(4-(4-methoxyphenyl)-2-methylbut-3-yn-2-yl)pyrrolidine (156)

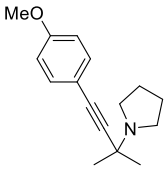

Following the general protocol: acetone (0.10 ml, 1.29 mmol), pyrrolidine (0.11 ml, 1.29 mmol), 4-ethynylanisole (0.19 ml, 1.72 mmol) and catalyst (17.8 mg, 0.03 mmol). Purification through column chromatography (100/1 to 1/1, Hexanes/EtOAc) yielded the title compound (219 mg, 0.90 mmol) as a colourless oil.

^{1}H NMR (400 MHz, $CDCl_3$) δ 7.34 (d, *J* = 8.8 Hz, 2H), 6.80 (d, *J* = 8.8 Hz, 2H), 3.78 (s, 3H), 2.85 – 2.73 (m, 4H), 1.84 – 1.76 (m, 4H), 1.47 (s, 6H).

^{13}C NMR (101 MHz, CDCl3) δ 159.3, 133.2, 115.7, 113.9, 89.8, 83.7, 55.4, 54.4, 48.3, 29.8, 23.9.

HRMS (ESI) m/z: Calcd for $C_{16}H_{22}NO^+$ = 244.1696; Found = 244.1701

IR (DRIFT): 3076, 2951, 2218, 1770, 1606, 1508, 1281, 1032, 831, 544 cm^{-1}.

1-(2-methyl-4-(4-(trifluoromethyl)phenyl)but-3-yn-2-yl)pyrrolidine (157)

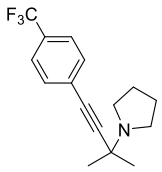

Following the general protocol: acetone (0.08 ml, 1.03 mmol), pyrrolidine (0.09 ml, 1.03 mmol), 4-(trifluoromethyl)phenylacetylene (0.17 ml, 1.03 mmol) and catalyst (14.3 mg, 0.03 mmol). Purification through column chromatography (100/1 to 1/1, Hexanes/EtOAc) yielded the title compound (254 mg, 0.90 mmol) as a colourless oil.

^{1}H NMR (400 MHz, $CDCl_3$) δ 7.55 – 7.49 (m, 4H), 2.84 (td, *J* = 5.4, 4.4, 2.5 Hz, 4H), 1.87 – 1.79 (m, 4H), 1.52 (s, 6H).

^{13}C NMR (101 MHz, $CDCl_3$) δ 132.1, 125.35, 125.31, 125.28, 125.24, 93.7, 83.3, 54.9, 48.5, 29.4, 23.9.

HRMS (ESI) m/z: Calcd for $C_{16}H_{19}F_3N^+$ = 282.1465; Found = 282.1458

IR (DRIFT): 3047, 2972, 2224, 1614, 1406, 1325, 843, 598 cm^{-1}.

1-(2-methyl-4-phenylbut-3-yn-2-yl)piperidine (158)

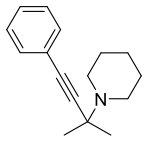

Following the general protocol: acetone (0.10 ml, 1.29 mmol), piperidine (0.13 ml, 1.29 mmol), phenylacetylene (0.14 ml, 1.29 mmol) and catalyst (17.8 mg, 0.03 mmol). Purification through column chromatography (100/1 to 1/1, Hexanes/EtOAc) yielded the title compound (145 mg, 0.64 mmol) as a yellow oil.

^{1}H NMR (400 MHz, $CDCl_3$) δ 7.42 (dd, *J* = 6.6, 3.0 Hz, 2H), 7.29 (q, *J* = 3.1, 2.6 Hz, 3H), 2.73 (s, 4H), 1.69 (p, *J* = 5.6 Hz, 4H), 1.52 (s, 6H), 1.46 (t, *J* = 5.8 Hz, 2H).

^{13}C NMR (101 MHz, $CDCl_3$) δ 131.8, 128.3, 128.0, 123.4, 91.1, 84.3, 60.5, 48.2, 27.9, 26.2, 24.3.

HRMS (ESI) m/z: Calcd for $C_{16}H_{22}N^+$ = 228.1747; Found = 228.1746

IR (DRIFT): 3080, 2978, 2224, 1641, 1489, 1144, 897, 690, 486 cm^{-1}.

1-((1r,3r,5r,7r)-2-(phenylethynyl)adamantan-2-yl)pyrrolidine (159)

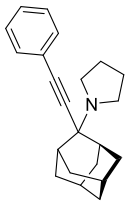

Following the general protocol: adamantanone (150 mg, 1.00 mmol), pyrrolidine (0.08 ml, 1.00 mmol), phenylacetylene (0.11 ml, 1.00 mmol) and catalyst (13.8 mg, 0.02 mmol). Purification through column chromatography (100/1 to 1/1, Hexanes/EtOAc) yielded the title compound (289 mg, 0.95 mmol) as a brownish oil.

^{1}H NMR (400 MHz, $CDCl_3$) δ 7.47 – 7.41 (m, 2H), 7.32 – 7.26 (m, 3H), 2.68 (d, *J* = 45.0 Hz, 4H), 2.35 – 2.21 (m, 4H), 2.01 (t, *J* = 3.2 Hz, 2H), 1.86 (t, *J* = 3.2 Hz, 1H), 1.76 (ddt, *J* = 21.4, 6.9, 3.3 Hz, 9H), 1.51 (dt, *J* = 10.1, 2.6 Hz, 2H).

^{13}C NMR (101 MHz, $CDCl_3$) δ 131.8, 128.3, 127.6, 124.1, 91.8, 86.2, 63.9, 46.0, 38.2, 35.8, 35.1, 31.4, 27.4, 27.0, 24.1.

HRMS (ESI) m/z: Calcd for $C_{22}H_{28}N^+$ = 306.2217; Found = 306.2214

IR (DRIFT): 3082, 2906, 2669, 2208, 1597, 1354, 1130, 754, 542 cm^{-1}.

1-((1r,3r,5r,7r)-2-((4-methoxyphenyl)ethynyl)adamantan-2-yl)pyrrolidine (160)

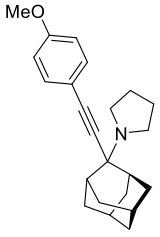

Following the general protocol: adamantanone (150 mg, 1.00 mmol), pyrrolidine (0.08 ml, 1.00 mmol), 4-ethynylanisole (132 mg, 1.00 mmol) and catalyst (13.8 mg, 0.02 mmol). Purification through column chromatography (100/1 to 1/1, Hexanes/EtOAc) yielded the title compound (301 mg, 0.90 mmol) as a brownish oil.

^{1}H NMR (400 MHz, $CDCl_3$) δ 7.36 (d, *J* = 8.7 Hz, 2H), 6.82 (d, *J* = 8.8 Hz, 2H), 3.80 (s, 3H), 2.68 (s, 4H), 2.31 – 2.18 (m, 4H), 1.97 (t, *J* = 3.1 Hz, 2H), 1.88 – 1.82 (m, 1H), 1.80 – 1.68 (m, 9H), 1.48 (dt, *J* = 12.3, 3.0 Hz, 2H).

^{13}C NMR (101 MHz, $CDCl_3$) δ 159.1, 133.1, 116.5, 113.9, 90.3, 85.7, 63.6, 55.4, 45.8, 38.2, 35.9, 35.1, 31.5, 27.4, 27.1, 24.1.

HRMS (ESI) m/z: Calcd for $C_{23}H_{30}NO^+$ = 336.2322; Found = 336.2320

IR (ATR): 3074, 2947, 2669, 2054, 1890, 1604, 1173, 833, 642, 540 cm^{-1}

1-((1r,3r,5r,7r)-2-((4-(trifluoromethyl)phenyl)ethynyl)adamantan-2-yl)pyrrolidine (161)

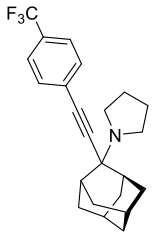

Following the general protocol: adamantanone (150 mg, 1.00 mmol), pyrrolidine (0.08 ml, 1.00 mmol), 4-(trifluoromethyl)phenylacetylene (0.16 ml, 1.00 mmol) and catalyst (13.8 mg, 0.02 mmol). Purification through column chromatography (100/1 to 1/1, Hexanes/EtOAc) yielded the title compound (314 mg, 0.84 mmol) as a yellow oil.

^{1}H NMR (400 MHz, $CDCl_3$) δ 7.56 – 7.49 (m, 4H), 3.06 – 2.43 (m, 4H), 2.32 – 2.19 (m, 4H), 2.01 (t, *J* = 3.1 Hz, 2H), 1.86 (d, *J* = 3.1 Hz, 1H), 1.82 – 1.69 (m, 9H), 1.54 – 1.46 (m, 2H).

^{13}C NMR (101 MHz, $CDCl_3$) δ 132.1, 125.3, 125.2, 125.2, 125.2, 94.9, 85.1, 63.9, 46.0, 38.1, 35.8, 35.1, 31.4, 27.3, 26.9, 24.4.

HRMS (ESI) m/z: Calcd for $C_{23}H_{26}F_3N^+$ = 374.2091; Found = 374.2086

IR (DRIFT): 3057, 2929, 2644, 2214, 1913, 1670, 1254, 958, 737, 428 cm^{-1}.

1-((1r,3r,5r,7r)-2-(phenylethynyl)adamantan-2-yl)piperidine (162)

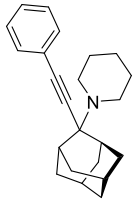

Following the general protocol: adamantanone (150 mg, 1.00 mmol), piperidine (0.10 ml, 1.00 mmol), phenylacetylene (0.11 ml, 1.00 mmol) and catalyst (13.8 mg, 0.02 mmol). Purification through column chromatography (100/1 to 1/1, Hexanes/EtOAc) yielded the title compound (212 mg, 0.66 mmol) as a colourless oil.

^{1}H NMR (400 MHz, $CDCl_3$) δ 7.44 (dd, *J* = 7.5, 2.1 Hz, 2H), 7.32 – 7.24 (m, 3H), 2.25 – 2.18 (m, 4H), 2.13 – 2.00 (m, 4H), 1.87 – 1.66 (m, 8H), 1.54 (t, *J* = 13.2 Hz, 2H), 1.42 (dd, *J* = 12.3, 3.2 Hz, 2H), 1.19 (d, *J* = 58.6 Hz, 2H).

^{13}C NMR (101 MHz, $CDCl_3$) δ 131.7, 128.2, 127.4, 124.2, 91.4, 86.2, 62.8, 47.0, 45.8, 39.3, 37.9, 36.3, 35.0, 33.5, 30.9, 27.5, 27.0, 26.9, 25.1.

HRMS (ESI) m/z: Calcd for $C_{23}H_{30}N^+$ = 320.2373; Found = 320.2373

IR (DRIFT): 3078, 2974, 2655, 2212, 1597, 1493, 1099, 860, 690 cm^{-1}.

1-(1-(phenylethynyl)cyclobutyl)pyrrolidine (163)

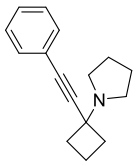

Following the general protocol: cyclobutanone (0.11 ml, 1.43 mmol), pyrrolidine (0.12 ml, 1.43 mmol), phenylacetylene (0.16 ml, 1.43 mmol) and catalyst (19.7 mg, 0.04 mmol). Purification through column chromatography (100/1 to 1/1, Hexanes/EtOAc) yielded the title compound (232 mg, 1.03 mmol) as a yellow oil.

^{1}H NMR (400 MHz, $CDCl_3$) δ 7.47 – 7.38 (m, 2H), 7.27 (dd, *J* = 5.1, 2.1 Hz, 3H), 2.70 – 2.58 (m, 4H), 2.34 – 2.23 (m, 4H), 2.09 (dq, *J* = 11.3, 8.5 Hz, 1H), 1.92 (ddd, *J* = 9.6, 7.2, 4.8 Hz, 1H), 1.81 (dq, *J* = 6.8, 2.9 Hz, 4H).

^{13}C NMR (101 MHz, $CDCl_3$) δ 131.8, 128.3, 127.8, 123.5, 90.8, 84.9, 58.0, 47.3, 34.5, 23.8, 14.9.

HRMS (ESI) m/z: Calcd for $C_{16}H_{20}N^+$ = 226.1591; Found = 226.1595

IR (DRIFT): 3060, 2967, 2219, 1682, 1599, 1384, 1171, 831, 507 cm^{-1}.

1-(1-((4-methoxyphenyl)ethynyl)cyclobutyl)pyrrolidine (164)

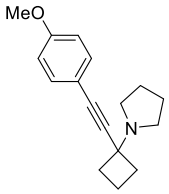

Following the general protocol: cyclobutanone (0.11 ml, 1.43 mmol), pyrrolidine (0.12 ml, 1.43 mmol), 4-ethynylanisole (189 mg, 1.43 mmol) and catalyst (19.7 mg, 0.04 mmol). Purification through column chromatography (100/1 to 1/1, Hexanes/EtOAc) yielded the title compound (296mg, 1.16 mmol) as a yellow oil.

^{1}H NMR (400 MHz, $CDCl_3$) δ 7.33 (d, *J* = 8.8 Hz, 2H), 6.78 (d, *J* = 8.8 Hz, 2H), 3.75 (s, 3H), 2.64 – 2.57 (m, 4H), 2.31 – 2.22 (m, 4H), 2.09 – 2.02 (m, 1H), 1.92 – 1.88 (m, 1H), 1.80 – 1.75 (m, 4H).

^{13}C NMR (101 MHz, $CDCl_3$) δ 159.23, 133.10, 115.72, 113.83, 89.35, 84.46, 57.91, 55.26, 47.17, 34.55, 23.78, 14.88.

HRMS (ESI) m/z: Calcd for: $C_{17}H_{22}NO^+$ = 256.1696; Found = 256.1696

IR (DRIFT): 3014, 2951, 2218, 1770, 1606, 1464, 1248, 1032, 831, 544 cm^{-1}.

1-(1-((4-(trifluoromethyl)phenyl)ethynyl)cyclobutyl)pyrrolidine (165)

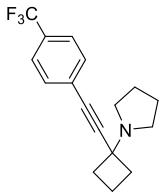

Following the general protocol: cyclobutanone (0.11 ml, 1.43 mmol), pyrrolidine (0.12 ml, 1.43 mmol), 4-(trifluoromethyl)phenylacetylene (0.23 ml, 1.43 mmol) and catalyst (19.7 mg, 0.04 mmol). Purification through column chromatography (100/1 to 1/1, Hexanes/EtOAc) yielded the title compound (314 mg, 1.07 mmol) as a yellow oil.

^{1}H NMR (400 MHz, $CDCl_3$) δ 7.58 – 7.50 (m, 4H), 2.69 – 2.57 (m, 4H), 2.38 – 2.22 (m, 4H), 2.13 – 2.04 (m, 1H), 1.95 – 1.90 (m, 1H), 1.84 – 1.77 (m, 4H).

^{13}C NMR (101 MHz, $CDCl_3$) δ 132.1, 125.3, 125.3, 125.2, 125.2, 94.1, 83.7, 58.0, 47.36, 34.45, 23.87, 14.9.

HRMS (ESI) m/z: Calcd for $C_{17}H_{19}F_3N^+$ = 294.1465; Found = 294.1466

IR (DRIFT): 3057, 2951, 2218, 1774, 1689, 1446, 1105, 843, 567 cm^{-1}.

1-(1-(phenylethynyl)cyclohexyl)piperidine (166)

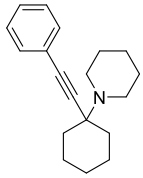

Following the general protocol: cyclohexanone (0.11 ml, 1.02 mmol), piperidine (0.10 ml, 1.02 mmol), phenylacetylene (0.11 ml, 1.02 mmol) and catalyst (12.6 mg, 0.03 mmol). Purification through column chromatography (100/1 to 1/1, Hexanes/EtOAc) yielded the title compound (239 mg, 0.89 mmol) as a colourless oil.

^{1}H NMR (400 MHz, DMSO) δ 7.44 – 7.36 (m, 2H), 7.36 – 7.30 (m, 3H), 2.57 (t, *J* = 5.3 Hz, 4H), 1.91 (dd, *J* = 11.1, 6.2 Hz, 2H), 1.66 – 1.26 (m, 14H).

^{13}C NMR (101 MHz, DMSO) δ 131.33, 128.48, 127.97, 122.89, 90.74, 85.26, 58.17, 46.63, 35.28, 26.19, 25.25, 24.42, 22.08.

The results are in accordance with the literature.[103]

4-(1-(phenylethynyl)cyclohexyl)morpholine (167)

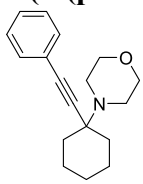

Following the general protocol: cyclohexanone (0.11 ml, 1.02 mmol), morpholine (0.09 ml, 1.02 mmol), phenylacetylene (0.11 ml, 1.02 mmol) and catalyst (14.1 mg, 0.03 mmol). Purification through column chromatography

(100/1 to 1/1, Hexanes/EtOAc) yielded the title compound (173 mg, 0.64 mmol) as a colourless oil.

^{1}H NMR (400 MHz, $CDCl_3$) δ 7.44 (dd, *J* = 6.6, 3.0 Hz, 2H), 7.29 (p, *J* = 3.6 Hz, 3H), 3.88 – 3.71 (m, 4H), 2.78 (s, 4H), 2.12 – 1.99 (m, 2H), 1.74 (dq, *J* = 10.6, 5.5, 4.4 Hz, 2H), 1.60 (ddd, *J* = 22.9, 10.8, 6.4 Hz, 5H), 1.30 – 1.25 (m, 1H).

^{13}C NMR (101 MHz, $CDCl_3$) δ 131.8, 128.3, 128.1, 123.3, 89.1, 86.9, 67.3, 58.9, 44.8, 35.4, 25.3, 24.5.

The results are in accordance with the literature.[103]

N,N-dibutyl-1-(phenylethynyl)cyclohexan-1-amine (168)

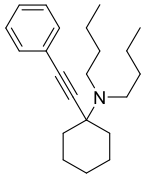

Following the general protocol: cyclohexanone (0.11 ml, 1.02 mmol), dibutylamine (0.17 ml, 1.02 mmol), phenylacetylene (0.11 ml, 1.02 mmol) and catalyst (14.1 mg, 0.03 mmol). Purification through column chromatography (100/1 to 25/1, Hexanes/EtOAc) yielded the title compound (78 mg, 0.25 mmol) as a colourless oil.

^{1}H NMR (400 MHz, $CDCl_3$) δ 7.42 (dd, *J* = 5.2, 2.4 Hz, 2H), 7.32 – 7.27 (m, 3H), 2.65 (s, 4H), 2.17 – 1.92 (m, 2H), 1.83 – 1.28 (m, 12H), 0.98 – 0.86 (m, 6H).

HRMS (ESI) m/z: Calcd for $C_{22}H_{34}N^+$ = 312.2686; Found = 312.2687

The results are in accordance with the literature.[149]

N-benzyl-N-methyl-1-(phenylethynyl)cyclohexan-1-amine (169)

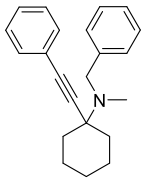

Following the general protocol: cyclohexanone (0.11 ml, 1.02 mmol), *n*-methyl-1-phenylmethanamine (0.13 ml, 1.02 mmol), phenylacetylene (0.11 ml, 1.02 mmol) and catalyst (14.1 mg, 0.03 mmol). Purification through column chromatography (100/1 to 25/1, Hexanes/EtOAc) yielded the title compound (167 mg, 0.55 mmol) as a yellow oil.

^{1}H NMR (400 MHz, $CDCl_3$) δ 7.54 – 7.50 (m, 2H), 7.44 – 7.40 (m, 2H), 7.37 – 7.32 (m, 5H), 7.27 – 7.23 (m, 1H), 3.72 (s, 2H), 2.25 (s, 3H), 2.14 (dd, *J* = 9.9, 5.6 Hz, 2H), 1.90 – 1.58 (m, 8H).

^{13}C NMR (101 MHz, $CDCl_3$) δ 141.2, 131.9, 128.9, 128.8, 128.4, 128.3, 128.3, 127.8, 126.66, 123.9, 90.9, 85.7, 59.3, 55.8, 36.8, 35.4, 25.9, 22.9.

The results are in accordance with the literature.[102]

(8R,9S,13S,14S)-13-methyl-17-(phenylethynyl)-17-(pyrrolidin-1-yl)-7,8,9,11,12,13,14,15,16,17-decahydro-6H-cyclopenta[a]phenanthren-3-ol (170)

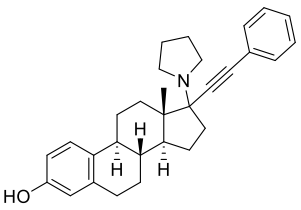

Following the general protocol: estrone (150 mg, 0.55 mmol), pyrrolidine (0.09 ml, 1.11 mmol), phenylacetylene (0.06 ml, 0.55. mmol) and cataqlyst (7.7 mg, 0.01 mmol). Purification through column chromatography (100/1 to 1/1, DCM/EtOAc) yielded the title compound (153 mg, 0.36 mmol) as a yellow solid.

^{1}H NMR (400 MHz, $CDCl_3$) δ 7.49 – 7.41 (m, 2H), 7.30 (dq, *J* = 7.0, 3.1, 2.4 Hz, 3H), 7.15 (dd, *J* = 8.6, 1.0 Hz, 1H), 6.63 (dd, *J* = 8.4, 2.8 Hz, 1H), 6.56 (d, *J* = 2.7 Hz, 1H), 2.90 – 2.70 (m, 6H), 2.35 – 2.19 (m, 2H), 2.16 – 1.84 (m, 6H), 1.77 (d, *J* = 6.3 Hz, 4H), 1.58 – 1.28 (m, 5H), 0.95 (s, 3H).

^{13}C NMR (101 MHz, $CDCl_3$) δ 153.6, 138.3, 132.6, 131.8, 129.7, 128.4, 127.8, 126.6, 123.9, 115.5, 112.9, 91.0, 86.9, 72.2, 51.2, 49.4, 48.3, 43.6, 39.5, 38.4, 35.3, 29.9, 27.6, 26.9, 23.7, 23.4, 13.4.

HRMS (ESI) m/z: Calcd for $C_{30}H_{36}NO^+$ = 426.2792; Found = 426.2786

IR (DRIFT): 3305, 3076, 2931, 2214, 1705, 1610, 1489, 1178, 868, 690, 528 cm^{-1}.

1-(1-ethynylcyclohexyl)pyrrolidine (175)

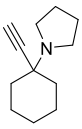

Method 1: To a pressure vial containing 2-methyl-4-(1-(pyrrolidin-1-yl)cyclohexyl)but-3-yn-2-ol (100mg, 0.42 mmol) and sodium hydride (20.4 mg, 0.51 mmol) was added 1 ml of toluene. The reaction mixture was stirred at 100 °C for 1 hour. Upon completion, 5 ml of EtOAc was added. Filtration and evaporation of the solvent yielded 98% of the desired compound (74 mg, 0.42 mmol) as a brown oil. No further purification was required.

Method 2: To a pressure vial, containing the catalyst (2.5 mol%) and 4 Å sieves, were loaded the cyclohexanone (500mg, 5.09 mmol), pyrrolidine (0.42 ml, 5.09 mmol), and 2-methylbut-3-

yn-2-ol (0.50 ml, 5.09 mmol). The reaction was stirred for 4 hours at 110 ºC in neat conditions. Afterwards, the reaction mixture was cooled down to room temperature and 5 ml of toluene was added followed by sodium hydride (146 mg, 6.12 mmol). The mixture was stirred at 100 ^{o}C for 1 hour. Upon completion, filtration and evaporation of the solvent yielded 94% of the desired compound (849 mg, 4.79 mmol) as a brown oil.

^{1}H NMR (400 MHz, $CDCl_3$) δ 2.63 (d, *J* = 6.2 Hz, 4H), 2.20 (s, 1H), 1.88 – 1.81 (m, 2H), 1.69 (dd, *J* = 10.6, 3.0 Hz, 4H), 1.62 – 1.36 (m, 8H).

^{13}C NMR (101 MHz, $CDCl_3$) δ 84.4, 73.0, 58.6, 46.8, 37.7, 25.6, 23.4, 22.7.

The results are in accordance with the literature.[103]

7. List of abbreviations

Å	Ångström
Ac	acetyl
Alk	alkyl
Ar	aryl
ATR	attenuated total reflection
B	byte
Bn	benzyl
Bu	butyl
Bz	benzoyl
cat.	catalytic
Calcd	calculated
DCC	*N,N'*-Dicyclohexylcarbodiimide
DCE	1,2-dichloroethane
DCM	dichloromethane
DFT	density functional theory
DMAP	4-dimethylaminopyridine
DMF	dimethylformamide
DMSO	dimethyl sulfoxide
DNA	Deoxyribonucleic acid
EDC	1-Ethyl-3-(3-dimethylaminopropyl)carbodiimide
ee	enantiomeric excess
eq.	equivalent
Et	ethyl
Et_2O	diethyl ether
EtOAc	ethyl acetate
EtOH	ethanol
ESI	electrospray ionization
HD	hard drives
HOMO	highest occupied molecular orbital
HRMS	high-resolution mass spectrometry

IR	infrared spectrometry
LUMO	lowest unoccupied molecular orbital
kB	kilobyte
MB	megabyte
m	meta
Me	methyl
MeCN	acetonitrile
MeOH	methanol
MIC	minimum inhibitory concentration
MW	microwave
n.d.	not determined
NHC	*N*-heterocyclic carbenes
NMR	nuclear magnetic resonance
o-	ortho
p-	para
Ph	phenyl
n-Pr	propyl
i-Pr	isopropyl
r.t.	room temperature
R_f	retention factor (in chromatography)
SSD	solid-state drives
TBS	tert-butyldimethylsilyl
tert-	tertiary
THF	tetrahydrofuran
TLC	thin-layer chromatography
TM	transition metal
TMS	trimethylsilyl
ZB	zettabyte

8. Bibliography

1. Butler, W. M., Enemark, J. H., Parks, J. & Balch, A. L. Chelative addition of hydrazines to coordinated isocyanides. Structure of Chugaev's red salt. *Inorg. Chem.* **12**, 451–457 (1973).
2. Öfele, K. 1,3-Dimethyl-4-imidazolinyliden-(2)-pentacarbonylchrom ein neuer übergangsmetall-carben-komplex. *J. Organomet. Chem.* **12**, P42–P43 (1968).
3. Wanzlick, H. W. Aspects of Nucleophilic Carbene Chemistry. *Angew. Chemie Int. Ed. English* **1**, 75–80 (1962).
4. Sch önherr, H. -J & Wanzlick, H. -W. Chemie nucleophiler Carbene, XX HX-Abspaltung aus 1.3-Diphenyl-imidazoliumsalzen. Quecksilbersalz-Carben-Komplexe. *Chem. Ber.* **103**, 1037–1046 (1970).
5. Lachmann, B., Steinmaus, H. & Wanzlick, H.-W. Chemie nucleophiler carbene—XXI. *Tetrahedron* **27**, 4085–4090 (1971).
6. Arduengo, A. J., Harlow, R. L. & Kline, M. A stable crystalline carbene. *J. Am. Chem. Soc.* **113**, 361–363 (1991).
7. Dröge, T. & Glorius, F. The Measure of All Rings—N-Heterocyclic Carbenes. *Angew. Chemie Int. Ed.* **49**, 6940–6952 (2010).
8. Bourissou, D., Guerret, O., Gabbaï, F. P. & Bertrand, G. Stable Carbenes. *Chem. Rev.* **100**, 39–92 (2000).
9. Krahulic, K. E., Enright, G. D., Parvez, M. & Roesler, R. A Stable N-Heterocyclic Carbene with a Diboron Backbone. *J. Am. Chem. Soc.* **127**, 4142–4143 (2005).
10. Biju, A. T., Hirano, K., Fröhlich, R. & Glorius, F. Switching the electron-donor properties of N-heterocyclic carbenes by a facile deprotonation strategy. *Chem. - An Asian J.* **4**, 1786–1789 (2009).
11. Benhamou, L. *et al.* Facile Derivatization of a "Chemo-active" NHC Incorporating an Enolate Backbone and Relevant Tuning of Its Electronic Properties. *Organometallics* **29**, 2616–2630 (2010).
12. Iglesias, M. *et al.* Novel Expanded Ring N-Heterocyclic Carbenes: Free Carbenes, Silver Complexes, And Structures. *Organometallics* **27**, 3279–3289 (2008).

13. Fischer, E. O. & Maasböl, A. On the Existence of a Tungsten Carbonyl Carbene Complex. *Angew. Chemie Int. Ed. English* **3**, 580–581 (1964).

14. Raubenheimer, H. G. Fischer carbene complexes remain favourite targets, and vehicles for new discoveries. *Dalt. Trans.* **43**, 16959–16973 (2014).

15. Schrock, R. R. *et al.* Synthesis of Molybdenum Imido Alkylidene Complexes and Some Reactions Involving Acyclic Olefins. *J. Am. Chem. Soc.* **112**, 3875–3886 (1990).

16. Vyboishchikov, S. F. & Frenking, G. Structure and Bonding of Low-Valent (Fischer-Type) and High-Valent (Schrock-Type) Transition Metal Carbene Complexes. *Chem. - A Eur. J.* **4**, 1428–1438 (1998).

17. Neshat, A., Mastrorilli, P. & Mobarakeh, A. M. Recent advances in catalysis involving bidentate n-heterocyclic carbene ligands. *Molecules* **27**, (2022).

18. Schaper, L., Hock, S. J., Herrmann, W. A. & Kühn, F. E. Synthesis and Application of Water-Soluble NHC Transition-Metal Complexes. *Angew. Chemie Int. Ed.* **52**, 270–289 (2013).

19. Peris, E. Smart N-Heterocyclic Carbene Ligands in Catalysis. *Chem. Rev.* **118**, 9988–10031 (2018).

20. Liang, X. *et al.* Recent advances in the medical use of silver complex. *Eur. J. Med. Chem.* **157**, 62–80 (2018).

21. Hindi, K. M., Panzner, M. J., Tessier, C. A., Cannon, C. L. file:///C:/Users/Admin/Desktop/Literature/ibáñez-et-a.-2020-n-heterocyclic-carbenes-a-door-open-to-supramolecular-organometallic-chemistry. pd. & Youngs, W. J. The Medicinal Applications of Imidazolium Carbene−Metal Complexes. *Chem. Rev.* **109**, 3859–3884 (2009).

22. Ibáñez, S., Poyatos, M. & Peris, E. N-Heterocyclic Carbenes: A Door Open to Supramolecular Organometallic Chemistry. *Acc. Chem. Res.* **53**, 1401–1413 (2020).

23. Benhamou, L., Chardon, E., Lavigne, G., Bellemin-Laponnaz, S. & César, V. Synthetic Routes to N-Heterocyclic Carbene Precursors. *Chem. Rev.* **111**, 2705–2733 (2011).

24. Praetorius, J. M. & Crudden, C. M. N-Heterocyclic carbene complexes of rhodium: structure, stability and reactivity. *Dalt. Trans.* **9226**, 4079 (2008).

25. Tolman, C. A. Steric effects of phosphorus ligands in organometallic chemistry and

homogeneous catalysis. *Chem. Rev.* **77**, 313–348 (1977).

26. Dorta, R. *et al.* Steric and Electronic Properties of N-Heterocyclic Carbenes (NHC): A Detailed Study on Their Interaction with Ni(CO) 4. *J. Am. Chem. Soc.* **127**, 2485–2495 (2005).

27. Chianese, A. R., Li, X., Janzen, M. C., Faller, J. W. & Crabtree, R. H. Rhodium and iridium complexes of N-heterocyclic carbenes via transmetalation: Structure and dynamics. *Organometallics* **22**, 1663–1667 (2003).

28. Hillier, A. C. *et al.* A Combined Experimental and Theoretical Study Examining the Binding of N -Heterocyclic Carbenes (NHC) to the Cp*RuCl (Cp* = η 5 -C 5 Me 5) Moiety: Insight into Stereoelectronic Differences between Unsaturated and Saturated NHC Ligands. *Organometallics* **22**, 4322–4326 (2003).

29. Viciu, M. S. *et al.* Synthetic and Structural Studies of (NHC)Pd(allyl)Cl Complexes (NHC = N -heterocyclic carbene). *Organometallics* **23**, 1629–1635 (2004).

30. Díez-González, S. & Nolan, S. P. Stereoelectronic parameters associated with N-heterocyclic carbene (NHC) ligands: A quest for understanding. *Coord. Chem. Rev.* **251**, 874–883 (2007).

31. Arduengo, A. J., Dias, H. V. R., Calabrese, J. C. & Davidson, F. Homoleptic carbene-silver(I) and carbene-copper(I) complexes. *Organometallics* **12**, 3405–3409 (1993).

32. LIN, I. J. B. & VASAM, C. S. SILVER(I) N-HETEROCYCLIC CARBENES. *Comments Inorg. Chem.* **25**, 75–129 (2004).

33. Chen, P.-W. & Tao, Y.-W. Crystal structure of 7-hydroxy-5-methoxy-4,6-dimethylisobenzofuran-1(3 H)-one, C 11 H 12 O 4. *Zeitschrift für Krist. - New Cryst. Struct.* **234**, 423–424 (2019).

34. Caballero, A. *et al.* Corrigendum to : "1,1′-(Pyridine-2,6-diyl)bis(3-benzyl-2,3-dihydro-1H-imidazol-2-ylidene), a new multidentate N-heterocyclic biscarbene and its silver(I) complex derivative". *J. Organomet. Chem.* **627**, 263–264 (2001).

35. Guerret, O. *et al.* systems, we first performed ab initio calculations. 6 The parent compound 1 is a true minimum on the potential surface, although as expected higher in energy than the triazole isomers 2-4 and. *Science (80-.).* **65**, 6668–6669 (1997).

36. Guerret, O., Solé, S., Gornitzka, H., Trinquier, G. & Bertrand, G. 1,2,4-Triazolium-5-

ylidene and 1,2,4-triazol-3,5-diylidene as new ligands for transition metals. *J. Organomet. Chem.* **600**, 112–117 (2000).

37. Wang, H. M. J. & Lin, I. J. B. Facile synthesis of silver(I)-carbene complexes. Useful carbene transfer agents. *Organometallics* **17**, 972–975 (1998).

38. Hayes, J. M., Viciano, M., Peris, E., Ujaque, G. & Lledós, A. Mechanism of Formation of Silver N -Heterocyclic Carbenes Using Silver Oxide: A Theoretical Study. *Organometallics* **26**, 6170–6183 (2007).

39. de Frémont, P. *et al.* Synthesis of Well-Defined N -Heterocyclic Carbene Silver(I) Complexes. *Organometallics* **24**, 6301–6309 (2005).

40. Garrison, J. C. & Youngs, W. J. Ag(I) N-Heterocyclic Carbene Complexes: Synthesis, Structure, and Application. *Chem. Rev.* **105**, 3978–4008 (2005).

41. Magill, A. M. *et al.* Palladium(II) complexes containing mono-, bi- and tridentate carbene ligands. Synthesis, characterisation and application as catalysts in C□C coupling reactions. *J. Organomet. Chem.* **617**–**618**, 546–560 (2001).

42. César, V., Bellemin-Laponnaz, S. & Gade, L. H. Direct Coupling of Oxazolines and N-Heterocyclic Carbenes: A Modular Approach to a New Class of C−N Donor Ligands for Homogeneous Catalysis. *Organometallics* **21**, 5204–5208 (2002).

43. Ramnial, T. *et al.* A monomeric imidazol-2-ylidene-silver(I) chloride complex: Synthesis, structure, and solid state 109Ag and 13C CP/MAS NMR characterization. *Inorg. Chem.* **42**, 1391–1393 (2003).

44. Lee, C. K. *et al.* Silver(I) N-Heterocyclic Carbenes with Long N-Alkyl Chains. *Organometallics* **25**, 3768–3775 (2006).

45. Wang, J.-W., Song, H.-B., Li, Q.-S., Xu, F.-B. & Zhang, Z.-Z. Macrocyclic dinuclear gold(I) and silver(I) NHCs complexes. *Inorganica Chim. Acta* **358**, 3653–3658 (2005).

46. Kascatan-Nebioglu, A., Panzner, M. J., Garrison, J. C., Tessier, C. A. & Youngs, W. J. Synthesis and Structural Characterization of N -Heterocyclic Carbene Complexes of Silver(I) and Rhodium(I) from Caffeine. *Organometallics* **23**, 1928–1931 (2004).

47. Sakamoto, R. *et al.* Synthesis, characterization, and structure–activity relationship of the antimicrobial activities of dinuclear N-heterocyclic carbene (NHC)-silver(I) complexes. *J. Inorg. Biochem.* **163**, 110–117 (2016).

48. Tate, B. K., Jordan, A. J., Bacsa, J. & Sadighi, J. P. Stable Mono- and Dinuclear Organosilver Complexes. *Organometallics* **36**, 964–974 (2017).

49. Jakob, C. H. G. *et al.* Anticancer and antibacterial properties of trinuclear Cu(I), Ag(I) and Au(I) macrocyclic NHC/urea complexes. *J. Organomet. Chem.* **932**, 121643 (2021).

50. Fatima, T. *et al.* Tri N-Heterocyclic Carbene Trinuclear Silver(I) complexes: Synthesis and In Vitro cytotoxicity studies. *J. Mol. Struct.* **1222**, 128890 (2020).

51. Weiss, D. T. *et al.* Application of Open Chain Tetraimidazolium Salts as Precursors for the Synthesis of Silver Tetra(NHC) Complexes. *Inorg. Chem.* **54**, 415–417 (2015).

52. Schulte to Brinke, C., Pape, T. & Hahn, F. E. Synthesis of polynuclear Ag(i) and Au(i) complexes from macrocyclic tetraimidazolium salts. *Dalt. Trans.* **42**, 7330 (2013).

53. Hahn, F. E., Radloff, C., Pape, T. & Hepp, A. Synthesis of Silver(I) and Gold(I) Complexes with Cyclic Tetra- and Hexacarbene Ligands. *Chem. – A Eur. J.* **14**, 10900–10904 (2008).

54. Haque, R. A. *et al.* Ag(I)-N-heterocyclic carbene complexes of N-allyl substituted imidazol-2-ylidenes with ortho-, meta- and para-xylyl spacers: Synthesis, crystal structures and in vitro anticancer studies. *Inorg. Chem. Commun.* **22**, 113–119 (2012).

55. Gutiérrez-Blanco, A. *et al.* Synthesis and Characterization of Poly-NHC-Derived Silver(I) Assemblies and Their Transformation into Poly-Imidazolium Macrocycles. *Eur. J. Inorg. Chem.* **2021**, 2442–2451 (2021).

56. Garrison, J. C. & Youngs, W. J. Ag(I) N-heterocyclic carbene complexes: Synthesis, structure, and application. *Chem. Rev.* **105**, 3978–4008 (2005).

57. Saif, M. J. & Flower, K. R. A general method for the preparation of N-heterocyclic carbene–silver(I) complexes in water. *Transit. Met. Chem.* **38**, 113–118 (2013).

58. Coleman, K. S., Chamberlayne, H. T., Turberville, S., Green, M. L. H. & Cowley, A. R. Silver(<scp>i</scp>) complex of a new imino-N-heterocyclic carbene and ligand transfer to palladium(<scp>ii</scp>) and rhodium(<scp>i</scp>). *Dalt. Trans.* **3**, 2917–2922 (2003).

59. Mata, J. A. *et al.* Reactivity Differences in the Syntheses of Chelating N-Heterocyclic Carbene Complexes of Rhodium Are Ascribed to Ligand Anisotropy. *Organometallics* **23**, 1253–1263 (2004).

60. Asay, M., Quezada-Miriel, M., Ochoa-Sanfelice, J. R. & Martinez-Otero, D. 2,6-Lutidine-linked bis-saturated NHC pincer ligands, silver complexes and transmetallation. *J. Organomet. Chem.* **859**, 10–17 (2018).

61. Werner, A. & Vilmos, A. Beitrag zur Konstitution anorganischer Verbindungen. XVII. Mitteilung. Über Oxalatodiäthylendiaminkobaltisalze. *Zeitschrift für Anorg. Chemie* **21**, 145–158 (1899).

62. Werner, A. Zur Kenntnis des asymmetrischen Kobaltatoms. I. *Berichte der Dtsch. Chem. Gesellschaft* **44**, 1887–1898 (1911).

63. Ganzmann, C. & Gladysz, J. A. Phase Transfer of Enantiopure Werner Cations into Organic Solvents: An Overlooked Family of Chiral Hydrogen Bond Donors for Enantioselective Catalysis. *Chem. - A Eur. J.* **14**, 5397–5400 (2008).

64. Chavarot, M. *et al.* 'Chiral-at-metal' octahedral ruthenium(II) complexes with achiral ligands: A new type of enantioselective catalyst. *Inorg. Chem.* **42**, 4810–4816 (2003).

65. Hamelin, O., Rimboud, M., Pécaut, J. & Fontecave, M. Chiral-at-metal ruthenium complex as a metalloligand for asymmetric catalysis. *Inorg. Chem.* **46**, 5354–5360 (2007).

66. Chen, L.-A. *et al.* Asymmetric Catalysis with an Inert Chiral-at-Metal Iridium Complex. *J. Am. Chem. Soc.* **135**, 10598–10601 (2013).

67. Schulte, T. R. *et al.* Chiral-at-Metal Phosphorescent Square-Planar Pt(II)-Complexes from an Achiral Organometallic Ligand. *J. Am. Chem. Soc.* **139**, 6863–6866 (2017).

68. Smith, L. Historical Perspectives on Water Purification. in *Chemistry and Water* 421–468 (Elsevier, 2017). doi:10.1016/B978-0-12-809330-6.00012-X.

69. Hoang, T. P. N., Ghori, M. U. & Conway, B. R. Topical Antiseptic Formulations for Skin and Soft Tissue Infections. *Pharmaceutics* **13**, 558 (2021).

70. Dunn, P. M. Dr Carl Crede (1819-1892) and the prevention of ophthalmia neonatorum. *Arch. Dis. Child. - Fetal Neonatal Ed.* **83**, 158F – 159 (2000).

71. White, R. J. An historical overview of the use of silver in wound management. *Br. J. Nurs.* **10**, S3–S8 (2001).

72. MOYER, C. A. Treatment of Large Human Burns With 0.5% Silver Nitrate Solution. *Arch. Surg.* **90**, 812 (1965).

73. Fox, C. L. Silver Sulfadiazine—A New Topical Therapy for Pseudomonas in Burns. *Arch. Surg.* **96**, 184 (1968).

74. Konop, M., Damps, T., Misicka, A. & Rudnicka, L. Certain Aspects of Silver and Silver Nanoparticles in Wound Care: A Minireview. *J. Nanomater.* **2016**, 1–10 (2016).

75. Sim, W., Barnard, R., Blaskovich, M. A. T. & Ziora, Z. Antimicrobial Silver in Medicinal and Consumer Applications: A Patent Review of the Past Decade (2007–2017). *Antibiotics* **7**, 93 (2018).

76. Mijnendonckx, K., Leys, N., Mahillon, J., Silver, S. & Van Houdt, R. Antimicrobial silver: uses, toxicity and potential for resistance. *BioMetals* **26**, 609–621 (2013).

77. Durán, N. *et al.* Silver nanoparticles: A new view on mechanistic aspects on antimicrobial activity. *Nanomedicine Nanotechnology, Biol. Med.* **12**, 789–799 (2016).

78. Gupta, A., Maynes, M. & Silver, S. Effects of Halides on Plasmid-Mediated Silver Resistance in Escherichia coli. *Appl. Environ. Microbiol.* **64**, 5042–5045 (1998).

79. Silver, S. Bacterial silver resistance: Molecular biology and uses and misuses of silver compounds. *FEMS Microbiol. Rev.* **27**, 341–353 (2003).

80. Pirnay, J.-P. *et al.* Molecular Epidemiology of Pseudomonas aeruginosa Colonization in a Burn Unit: Persistence of a Multidrug-Resistant Clone and a Silver Sulfadiazine-Resistant Clone. *J. Clin. Microbiol.* **41**, 1192–1202 (2003).

81. Kascatan-Nebioglu, A., Panzner, M. J., Tessier, C. A., Cannon, C. L. & Youngs, W. J. N-Heterocyclic carbene–silver complexes: A new class of antibiotics. *Coord. Chem. Rev.* **251**, 884–895 (2007).

82. Melaiye, A. *et al.* Formation of Water-Soluble Pincer Silver(I)−Carbene Complexes: A Novel Antimicrobial Agent. *J. Med. Chem.* **47**, 973–977 (2004).

83. Melaiye, A. *et al.* Silver(I)−Imidazole Cyclophane gem -Diol Complexes Encapsulated by Electrospun Tecophilic Nanofibers: Formation of Nanosilver Particles and Antimicrobial Activity. *J. Am. Chem. Soc.* **127**, 2285–2291 (2005).

84. Nayak, S. & Gaonkar, S. L. Coinage Metal N- Heterocyclic Carbene Complexes: Recent Synthetic Strategies and Medicinal Applications. *ChemMedChem* **16**, 1360–1390 (2021).

85. Roland, S. *et al.* Investigation of a series of silver-N-Heterocyclic carbenes as

antibacterial agents: Activity, synergistic effects, and cytotoxicity. *Chem. - A Eur. J.* **17**, 1442–1446 (2011).

86. Haque, R. A., Haziz, U. F. M., Abdullah, A. A. A., Shaheeda, N. & Razali, M. R. New non-functionalized and nitrile-functionalized benzimidazolium salts and their silver(I) complexes: Synthesis, crystal structures and antibacterial studies. *Polyhedron* **109**, 208–217 (2016).

87. Napoli, M. *et al.* Silver(I) N-heterocyclic carbene complexes: Synthesis, characterization and antibacterial activity. *J. Organomet. Chem.* **725**, 46–53 (2013).

88. Crist, D. R., Hsieh, Z. H., Quicksall, C. O. & Sun, M. K. Silver(I) interactions with ketones. Site of complexation with acetophenones and effectiveness as a Lewis acid catalyst. *J. Org. Chem.* **49**, 2478–2483 (1984).

89. Li, M., Wu, W. & Jiang, H. Recent Advances in Silver-Catalyzed Transformations of Electronically Unbiased Alkenes and Alkynes. *ChemCatChem* **12**, 5034–5050 (2020).

90. Álvarez-Corral, M., Muñoz-Dorado, M. & Rodríguez-García, I. Silver-Mediated Synthesis of Heterocycles. *Chem. Rev.* **108**, 3174–3198 (2008).

91. Li, L. *et al.* Silver-Catalyzed Oxidative C(sp 3)−P Bond Formation through C−C and P−H Bond Cleavage. *Angew. Chemie* **129**, 10675–10680 (2017).

92. Xu, P., Guo, S., Wang, L. & Tang, P. Silver-catalyzed oxidative activation of benzylic C-H bonds for the synthesis of difluoromethylated arenes. *Angew. Chemie - Int. Ed.* **53**, 5955–5958 (2014).

93. Lauder, K., Toscani, A., Scalacci, N. & Castagnolo, D. Synthesis and Reactivity of Propargylamines in Organic Chemistry. *Chem. Rev.* **117**, 14091–14200 (2017).

94. Magueur, G., Crousse, B. & Bonnet-Delpon, D. Direct access to CF3-propargyl amines and conversion to difluoromethyl imines. *Tetrahedron Lett.* **46**, 2219–2221 (2005).

95. Aubrecht, K. B., Winemiller, M. D. & Collum, D. B. BF 3 -Mediated Addition of Lithium Phenylacetylide to an Imine: Correlations of Structures and Reactivities. BF 3 ·R 3 N Derivatives as Substitutes for BF 3 ·Et 2 O. *J. Am. Chem. Soc.* **122**, 11084–11089 (2000).

96. McNally, J. J., Youngman, M. A. & Dax, S. L. Mannich reactions of resin-bound substrates: 2. A versatile three-component solid-phase organic synthesis methodology.

Tetrahedron Lett. **39**, 967–970 (1998).

97. Dyatkin, A. B. & Rivero, R. A. The solid phase synthesis of complex propargylamines using the combination of sonogashira and mannich reactions. *Tetrahedron Lett.* **39**, 3647–3650 (1998).

98. Li, P., Wang, L., Zhang, Y. & Wang, M. Highly efficient three-component (aldehyde–alkyne–amine) coupling reactions catalyzed by a reusable PS-supported NHC–Ag(I) under solvent-free reaction conditions. *Tetrahedron Lett.* **49**, 6650–6654 (2008).

99. Li, Y., Chen, X., Song, Y., Fang, L. & Zou, G. Well-defined N-heterocyclic carbene silver halides of 1-cyclohexyl-3- arylmethylimidazolylidenes: Synthesis, structure and catalysis in A 3-reaction of aldehydes, amines and alkynes. *Dalt. Trans.* **40**, 2046–2052 (2011).

100. Chen, M. T., Landers, B. & Navarro, O. Well-defined (N-heterocyclic carbene)-Ag(i) complexes as catalysts for A 3 reactions. *Org. Biomol. Chem.* **10**, 2206–2208 (2012).

101. Pereshivko, O. P., Peshkov, V. A. & Van der Eycken, E. V. Unprecedented Cu(I)-Catalyzed Microwave-Assisted Three-Component Coupling of a Ketone, an Alkyne, and a Primary Amine. *Org. Lett.* **12**, 2638–2641 (2010).

102. Chalkidis, S. G. & Vougioukalakis, G. C. KA2 Coupling, Catalyzed by Well-Defined NHC-Coordinated Copper(I): Straightforward and Efficient Construction of α-Tertiary Propargylamines**. *European J. Org. Chem.* **26**, (2023).

103. Schlimpen, F. *et al.* α-Tertiary Propargylamine Synthesis via KA2-Type Coupling Reactions under Solvent-Free CuI-Zeolite Catalysis. *J. Org. Chem.* **86**, 16593–16613 (2021).

104. Gulati, U., Rajesh, U. C. & Rawat, D. S. CuO/Fe2O3NPs: robust and magnetically recoverable nanocatalyst for decarboxylative A3 and KA2 coupling reactions under neat conditions. *Tetrahedron Lett.* **57**, 4468–4472 (2016).

105. Hosseini-Sarvari, M. & Moeini, F. Nano copper(I) oxide-zinc oxide catalyzed coupling of aldehydes or ketones, secondary amines, and terminal alkynes in solvent-free conditions. *New J. Chem.* **38**, 624–635 (2014).

106. Fan, J., Yang, Y., Tao, C. & Li, M. Cadmium-Doped and Pincer Ligand-Modified Gold Nanocluster for Catalytic KA 2 Reaction . *Angew. Chemie* **135**, (2023).

107. Tzouras, N. V., Neofotistos, S. P. & Vougioukalakis, G. C. Zn-Catalyzed Multicomponent KA2 Coupling: One-Pot Assembly of Propargylamines Bearing Tetrasubstituted Carbon Centers. *ACS Omega* **4**, 10279–10292 (2019).

108. Reinsel, D., Gantz, J. & Rydning, J. The Digitization of the World - From Edge to Core. *Fram. Int. Data Corp.* US44413318 (2018).

109. Ayres, R. U., Méndez, G. V. & Peiró, L. T. Recycling Rare Metals. *Handb. Recycl. State-of-the-art Pract. Anal. Sci.* 27–38 (2014) doi:10.1016/B978-0-12-396459-5.00004-0.

110. Zhirnov, V., Zadegan, R. M., Sandhu, G. S., Church, G. M. & Hughes, W. L. Nucleic acid memory. *Nat. Mater.* **15**, 366–370 (2016).

111. Wang, S., Mao, X., Wang, F., Zuo, X. & Fan, C. Data Storage Using DNA. *Adv. Mater.* **36**, 1–23 (2024).

112. Doricchi, A. *et al.* Emerging Approaches to DNA Data Storage: Challenges and Prospects. *ACS Nano* **16**, 17552–17571 (2022).

113. Cafferty, B. J. *et al.* Storage of Information Using Small Organic Molecules. *ACS Cent. Sci.* **5**, 911–916 (2019).

114. Nagarkar, A. A. *et al.* Storing and Reading Information in Mixtures of Fluorescent Molecules. *ACS Cent. Sci.* **7**, 1728–1735 (2021).

115. Bohn, P., Weisel, M. P., Wolfs, J. & Meier, M. A. R. Molecular data storage with zero synthetic effort and simple read-out. *Sci. Rep.* **12**, 13878 (2022).

116. Baker, M. V. *et al.* Cationic, linear Au(I) N-heterocyclic carbene complexes: Synthesis, structure and anti-mitochondrial activity. *Dalt. Trans.* **6**, 3708–3715 (2006).

117. Tan, K. V., Dutton, J. L., Skelton, B. W., Wilson, D. J. D. & Barnard, P. J. Nickel(II) and Palladium(II) Complexes with Chelating N-Heterocyclic Carbene Amidate Ligands: Interplay between Normal and Abnormal Coordination Modes. *Organometallics* **32**, 1913–1923 (2013).

118. Chiu, P. L., Lai, C.-L., Chang, C.-F., Hu, C.-H. & Lee, H. M. Synthesis, Structural Characterization, Computational Study, and Catalytic Activity of Metal Complexes Based on Tetradentate Pyridine/ N -Heterocyclic Carbene Ligand. *Organometallics* **24**, 6169–6178 (2005).

119. Sharma, S. K., Upreti, S. & Gupta, R. Effect of ligand architecture on the structure and

properties of square-planar nickel(II) complexes of amide-based macrocycles. *Eur. J. Inorg. Chem.* 3247–3259 (2007) doi:10.1002/ejic.200700122.

120. Ségaud, N., Johnson, C., Farre, A. & Albrecht, M. Exploring the stability of the NHC–metal bond using thiones as probes. *Chem. Commun.* **57**, 10600–10603 (2021).

121. Iwasaki, T. *et al.* Nickel-catalyzed coupling reaction of alkyl halides with aryl Grignard reagents in the presence of 1,3-butadiene: Mechanistic studies of four-component coupling and competing cross-coupling reactions. *Chem. Sci.* **9**, 2195–2211 (2018).

122. Giannerini, M., Fañanás-Mastral, M. & Feringa, B. L. Direct catalytic cross-coupling of organolithium compounds. *Nat. Chem.* **5**, 667–672 (2013).

123. Gundogdu, O., Altundas, R. & Kara, Y. Preparation of arylmagnesium/lithium from aryl bromides and their coupling and substitution reactions in tetrahydrofuran. *Appl. Organomet. Chem.* **31**, 1–4 (2017).

124. Safaei-Ghomi, J., Zahedi, S. & Basharnavaz, H. Synthesis and Characterization of Ionic Liquid Supported on Fe3O4 Nanoparticles and a DFT Study of 1,3-Dipolar Cycloaddition for the Synthesis of Isoxazolidines in the Presence of Ionic Liquid-Fe3O4. *Polycycl. Aromat. Compd.* **40**, 574–584 (2020).

125. Cavassin, E. D. *et al.* Comparison of methods to detect the in vitro activity of silver nanoparticles (AgNP) against multidrug resistant bacteria. *J. Nanobiotechnology* **13**, 1–16 (2015).

126. Jalal, M. *et al.* Biosynthesis of silver nanoparticles from oropharyngeal candida glabrata isolates and their antimicrobial activity against clinical strains of bacteria and fungi. *Nanomaterials* **8**, (2018).

127. Orsini, A., Vitérisi, A., Bodlenner, A., Weibel, J. M. & Pale, P. A chemoselective deprotection of trimethylsilyl acetylenes catalyzed by silver salts. *Tetrahedron Lett.* **46**, 2259–2262 (2005).

128. dCode. https://www.dcode.fr/binary-image.

129. Mateus, M., Kiss, A., Císařová, I., Karpiński, T. M. & Rycek, L. Synthesis of silver complexes with chelating bidentate N -heterocyclic ligands, their application in catalytic A 3 coupling, and as antimicrobial agents. *Appl. Organomet. Chem.* **37**, 675–687 (2023).

130. Tan, K. V., Dutton, J. L., Skelton, B. W., Wilson, D. J. D. & Barnard, P. J. Nickel(II)

and palladium(II) complexes with chelating N-heterocyclic carbene amidate ligands: Interplay between normal and abnormal coordination modes. *Organometallics* **32**, 1913–1923 (2013).

131. Ye, W., Xu, J., Tan, C.-T. & Tan, C.-H. 1,5,7-Triazabicyclo[4.4.0]dec-5-ene (TBD) catalyzed Michael reactions. *Tetrahedron Lett.* **46**, 6875–6878 (2005).

132. Polt, R. *et al.* Optically active 4- and 5-coordinate transition metal complexes of bifurcated dipeptide Schiff bases. *Inorg. Chem.* **42**, 566–574 (2003).

133. Mohammadian, R., Kamyar, N., Kaffashian, A., Amini, M. M. & Shaabani, A. Synthesis of Defect-Engineered Homochiral Metal-Organic Frameworks Using L-Amino Acids: A Comprehensive Study of Chiral Catalyst Performance in CO2 Fixation Reaction. *ChemistrySelect* **5**, 10346–10354 (2020).

134. Adamczak, A., Ożarowski, M. & Karpiński, T. M. Antibacterial Activity of Some Flavonoids and Organic Acids Widely Distributed in Plants. *J. Clin. Med.* **9**, 109 (2019).

135. Adamczak, A., Ożarowski, M. & Karpiński, T. M. Curcumin, a Natural Antimicrobial Agent with Strain-Specific Activity. *Pharmaceuticals* **13**, 153 (2020).

136. Boucher, M. M., Furigay, M. H., Quach, P. K. & Brindle, C. S. Liquid-Liquid Extraction Protocol for the Removal of Aldehydes and Highly Reactive Ketones from Mixtures. *Org. Process Res. Dev.* **21**, 1394–1403 (2017).

137. Shabbir, S., Lee, Y. & Rhee, H. Au(III) catalyst supported on a thermoresponsive hydrogel and its application to the A-3 coupling reaction in water. *J. Catal.* **322**, 104–108 (2015).

138. Cui, J. *et al.* Silver-Mediated Organic Transformations of Propargylamines to Enones, α-Thioketones, and Isochromans. *ChemistrySelect* **4**, 1476–1482 (2019).

139. Jeganathan, M., Dhakshinamoorthy, A. & Pitchumani, K. One-pot synthesis of propargylamines using Ag(I)-exchanged K10 montmorillonite clay as reusable catalyst in water. *ACS Sustain. Chem. Eng.* **2**, 781–787 (2014).

140. Brambilla, E. *et al.* Silver-catalysed A3-coupling reactions in phenylacetic acid/alkylamine N-oxide eutectic mixture under dielectric heating: An alternative approach to propargylamines. *Appl. Organomet. Chem.* 1–10 (2022) doi:10.1002/aoc.6669.

141. Sampani, S. I. *et al.* Shedding light on the use of Cu(ii)-salen complexes in the A3 coupling reaction. *Dalt. Trans.* **49**, 289–299 (2020).

142. Salam, N. *et al.* Synthesis of silver-graphene nanocomposite and its catalytic application for the one-pot three-component coupling reaction and one-pot synthesis of 1,4-disubstituted 1,2,3-triazoles in water. *RSC Adv.* **4**, 10001–10012 (2014).

143. Neshat, A. *et al.* Heterocyclic thiolates and phosphine ligands in copper-catalyzed synthesis of propargylamines in water. *Appl. Organomet. Chem.* **35**, 1–12 (2021).

144. Liu, Z., Yuan, D. & Su, Y. A Novel and Versatile Copper-Nanomagnetic Catalyst for Synthesis of Propargylamines and Diaryl Sulfides. *Catal. Letters* **153**, 698–712 (2023).

145. Yan, S., Pan, S., Osako, T. & Uozumi, Y. Solvent-Free A3 and KA2 Coupling Reactions with mol ppm Level Loadings of a Polymer-Supported Copper(II)-Bipyridine Complex for Green Synthesis of Propargylamines. *ACS Sustain. Chem. Eng.* **7**, 9097–9102 (2019).

146. Zhu, N. X. *et al.* Synthesis, structure and multifunctional catalytic properties of a Cu(i)-coordination polymer with outer-hanging CuBr2. *RSC Adv.* **6**, 108645–108653 (2016).

147. Yi, R. *et al.* Expeditious and highly efficient synthesis of propargylamines using a Pd-Cu nanowires catalyst under solvent-free conditions. *Appl. Organomet. Chem.* **33**, 1–7 (2019).

148. Udaykumar, B. & Periasamy, M. Synthesis of Propargylamines via Michael Addition Using Methyl Vinyl Ketone Derivatives, 1-Alkynes, and Secondary Amines Catalyzed by Copper (I) Halides. *ACS Omega* **4**, 21587–21595 (2019).

149. Perumgani, P. C., Keesara, S., Parvathaneni, S. & Mandapati, M. R. Polystyrene supported: N -phenylpiperazine-Cu(II) complex: An efficient and reusable catalyst for KA2-coupling reactions under solvent-free conditions. *New J. Chem.* **40**, 5113–5120 (2016).

9. Author's publications

Thesis-Related Publications:

(1) Mateus, M.; Rycek, L. Silver Complex Bearing N-Heterocyclic Carbene Bidentate Chelating Ligand as an Efficient Catalyst in Solvent-Free KA^2 Coupling. *ChemPlusChem.* **2024**, submitted.

(2) Mateus, M.; Kiss, A.; Císařová, I.; Karpiński, T. M.; Rycek, L. Synthesis of Silver Complexes with Chelating Bidentate N -heterocyclic Ligands, Their Application in Catalytic A 3 Coupling, and as Antimicrobial Agents. *Appl. Organomet. Chem.* **2023**, *37* (4), 675–687.

Additional Publications:

(3) Kunák, D.; Mateus, M.; Rycek, L. Synthesis and Structure Confirmation of Selagibenzophenone C. *European J. Org. Chem.* **2022**, *2022* (11).

(4) Lapinskaite, R.; Malatinec, Š.; Mateus, M.; Rycek, L. Cross-Coupling as a Key Step in the Synthesis and Structure Revision of the Natural Products Selagibenzophenones A and B. *Catalysts* **2021**, *11* (6), 708.

(5) Rycek, L.; Mateus, M.; Beytlerová, N.; Kotora, M. Catalytic Cyclotrimerization Pathway for Synthesis of Selaginpulvilins C and D: Scope and Limitations. *Org. Lett.* **2021**, *23* (12), 4511–4515.